TRANSPORTATION RESEARCH RECORD
567

Traffic Flow Theory and Applications

10 reports prepared for the 54th Annual Meeting of the Transportation Research Board

TRB
TRANSPORTATION RESEARCH BOARD
NATIONAL RESEARCH COUNCIL
Washington, D. C., 1976

Transportation Research Record 567
Price $8.00
Edited for TRB by Marjorie Moore

Subject areas
53 traffic control and operations
54 traffic flow

The project that is the subject of this report was approved by the Governing Board of the National Research Council, whose members are drawn from the councils of the National Academy of Sciences, the National Academy of Engineering, and the Institute of Medicine. The members of the committee responsible for the report were chosen for their special competence and with regard for appropriate balance.

This report has been reviewed by a group other than the authors according to procedures approved by a Report Review Committee consisting of members of the National Academy of Sciences, the National Academy of Engineering, and the Institute of Medicine.

The views expressed in this report are those of the authors and do not necessarily reflect the view of the committee, the Transportation Research Board, the National Academy of Sciences, or the sponsors of the project.

LIBRARY OF CONGRESS CATALOGING IN PUBLICATION DATA

National Research Council. Transportation Research Board.
Traffic flow theory and applications.

(Transportation research record; 567)
1. Traffic flow—Congresses. I. Title. II. Series.
TE7.H5 no. 567 [HE336.T7] 380.5'08s
ISBN 0-309-02480-3 [387.3'1] 76-14433

CONTENTS

FURTHER EVALUATION OF SINGLE- AND TWO-REGIME TRAFFIC FLOW MODELS

Avishai Ceder* and Adolf D. May, Institute of Transportation and Traffic Engineering, University of California, Berkeley

Because many road facilities operate under high-density conditions, it is important to consider more accurate interrelationships among the basic traffic flow variables. Previous papers by May and Keller concerned with the evaluation of traffic flow models have examined the macroscopic relationships derived from the generalized car-following model designed by Gazis, Herman, and Rothery. Their results form the basis for consideration of other data sets that could be subjected to similar evaluation procedures. This paper presents an investigation of single-regime traffic flow models in which 32 sets of speed-concentration measurements were used. Those 32 data sets are also used to investigate two-regime traffic flow models. Then 13 new sets of data are evaluated based on predictions from the investigations of the single- and two-regime models. Procedures developed by May and Keller are used as a guide to investigate single-regime traffic flow models in an m, ℓ matrix format in order to study the variability of those exponents of the sensitivity component that belong to the generalized car-following equation. The deficiencies of the various models are identified, and the need to investigate two-regime models is stressed. Two-regime traffic flow models are investigated in an m, ℓ matrix format that is derived from the generalized car-following equation. Both the single- and two-regime models show consistency in the m, ℓ matrix, which makes it possible to predict the results of a new data set. The results of the additional 13 sets of data confirm the predictions. The overall analysis of the 45 data sets emphasizes the most appropriate m, ℓ values for the single- and two-regime approaches, particularly those concerned with traffic flow models for freeway lanes.

•THE NEED to consider more accurate interrelationships among the basic traffic flow variables has become imperative as the number of road facilities operating at near-capacity has increased. Development of flow control and ramp-metering techniques and design of new roadways must be based on the relationships among speed, flow, and concentration, particularly under high-concentration conditions.

In recent years a number of steady-state flow equations for the interrelationships among traffic flow variables have been suggested.

Previous papers (1, 2) show that the microscopic and macroscopic theories of traffic flow can be reduced to the equation of the general car-following model formulated by Gazis, Herman, and Rothery (3):

$$\ddot{X}_{n+1}(t+T) = \alpha \frac{[\dot{X}_{n+1}(t+T)]^m}{[X_n(t) - X_{n+1}(t)]^\ell} [\dot{X}_n(t) - \dot{X}_{n+1}(t)] \quad (1)$$

*When the research was performed, Mr. Ceder was on leave from the Road Safety Center, Technion, Haifa, Israel.

Publication of this paper sponsored by Committee on Traffic Flow Theory and Characteristics.

where the single and double dots represent speed and acceleration (deceleration) and

X_n, X_{n+1} = positions of the leading car and the following car, respectively,
T = time lag of response to stimulus, and
m, ℓ, and α = constant parameters.

The steady-state flow formulation of this equation can be obtained by integrating the above equation; it is given by Gazis et al. as

$$f_n(u) = cf_\ell(s) + c' \tag{2}$$

where

u = steady-state speed of the traffic stream,
s = constant average spacing, and
c' and c = some appropriate constants consistent with physical restrictions.

By selecting proper combinations of the exponents m and ℓ in equations 1 and 2, known microscopic and macroscopic traffic flow models can be obtained.

In previous papers (1, 2), an evaluation process was used to determine appropriate values of m and ℓ; it was applied to two sets of typical data—namely, freeway and tunnel data.

Evaluations of the m and ℓ coordinates in a matrix format for the single-regime models were rather surprising inasmuch as the selected m and ℓ coordinates for the freeway data were quite similar to those found in the tunnel data (1). However, the two-regime models indicate differences between the selected freeway and tunnel models in the free-flow regime, although identical results were found in the congested regime (2). These results form the basis for consideration of other data sets that can be evaluated with similar procedures.

This paper presents an investigation of single- and two-regime traffic flow models based on equations 1 and 2 and an evaluation of new sets of data based on the predictions made.

First, flow relationship equations are determined for the single-regime models and for parameters such as free-flow speed, optimum speed, optimum concentration, maximum flow, and jam concentration for each set of data and for each m, ℓ combination. The results are summarized in a two-dimensional matrix.

Second, two-regime traffic flow models concerned with free-flow and congested-flow regimes are investigated by using an evaluation process similar to that used for single-regime models.

After the characteristics of the single- and two-regime traffic flow models are identified, new sets of data are evaluated by using the same evaluation procedure used for the single- and two-regime models.

DATA SELECTION

Before we proceed into the three major parts of this work, a brief description of the actual traffic data is given.

To ensure appropriate speed-concentration relationships requires that traffic flow variables be sampled over the range of all possible concentrations. The two groups of data sets evaluated in this paper are based on data collected during a fixed time period. The first group of 32 data sets, based on speed-concentration measurements, was collected at the following locations:

1. Eisenhower Expressway, Chicago;
2. Holland Tunnel, New York;

3. Hollywood Freeway, Los Angeles (10 data sets, five locations for 2 days each);
4. Pasadena Freeway, Los Angeles (eight data sets, four locations for 2 days each);
5. Penn-Lincoln Parkway, Pittsburgh (six data sets, three locations for 2 days each);
6. U.S. highway in Virginia (two data sets, one for median lane and one for shoulder lane); and
7. Munich-Salzburg Autobahn, Germany (four data sets, one for median lane and one for shoulder lane and for both directions).

These 32 data sets were based on samples taken at 1-min time intervals, and mean speeds and mean concentrations are calculated for each interval.

A procedure similar to that developed by Drake et al. (4) was used to systematically reduce data points on the 32 data sets. That is, the number of measurements falling in the most sparse 5-vehicle-per-mile concentration range was determined, and a like number of measurements were randomly sampled from each of the other 5-vehicle-per-mile ranges. This statistical procedure provides uniform distribution of the data points over the available concentration range.

The second group of 13 data sets is based on data collected on the 42-mile (68-km) Los Angeles Freeway surveillance and control system. This second group of data sets was collected on the Santa Monica Freeway at 11 stations (SM-12 to SM-22) along 5 miles (8 km) of a four- and five-lane directional freeway. In addition, two data sets were obtained from a collector-distributor road and an on-ramp within the 5-mile freeway section. Data were collected on the same day for all stations during the morning peak and were based on 5-min roadway occupancy and volume measurements. According to Athol (5), there is a linear relationship between occupancy and concentration in which three times the occupancy can be associated with the concentration value. As will be seen in equation 3, the relationship between speed and concentration depends on normalized concentration, and therefore the exact linear transformation from occupancy to concentration is not of major importance. However, for consideration of absolute values of concentration and speed in the second group of data sets, the linear transformation should be taken into account.

A systematic procedure for uniformity of data points over the concentration range was performed on the second group of data sets. This procedure was similar to that used with the first data sets, but, instead of reducing the number of data points, it increased the number of observations by weighting them. In each 5-vehicle-per-mile range, the number of observations was increased up to the number of observations falling in the densest 5-vehicle-per-mile concentration range. In addition, in each range, equal consideration has been given to individual data points. This procedure makes it possible to have approximately 100 data points in each set as was used in the first group of data sets. It is worth mentioning here that data collected during a fixed time period represent the traffic flow variables during that period. However, from the comparison of 1-min and 5-min samples, it appears that no difference in the magnitudes of the traffic flow characteristics between the two samples is evident. This latter point will be shown later. Thus, the traffic flow models can be evaluated (at least with the data in this paper) with 5-min samples as well as with 1-min samples.

SINGLE-REGIME MODELS

The objective is to select single-regime models for 32 speed-concentration data sets that satisfy preselected statistical and traffic flow criteria. The evaluation procedure was initially developed in earlier papers (1, 2) and will be briefly summarized here.

In the evaluation procedure, an m, ℓ matrix is used in which the various microscopic and macroscopic theories of traffic flow can be positioned. Each m and ℓ combination represents a specific model that can be expressed mathematically by equations 1 and 2. The selected model is one that satisfies preselected statistical and traffic flow criteria.

For the single-regime model, only models with an x-intercept (jam concentration) and a y-intercept (free-flow speed) were considered. This limited the investigation of

the m, ℓ matrix to the region where $m < 1$ and $\ell > 1$. Further, it was required that in equation 1 the speed function and the spacing function of the sensitivity component remain in the numerator and denominator respectively. This limited the investigation of the m, ℓ matrix to the region where $m \geq 0$ and $\ell \geq 0$. The combination of these two requirements restricted the investigation of the m, ℓ matrix to the region where $0 \leq m \leq 1$ and $\ell > 1$. An upper limit was placed on ℓ such that $\ell \leq 3.1$ because this limit on ℓ covers all the previous macroscopic models, as will be shown later. For this range of m and ℓ values, the following macroscopic equation can be derived from equation 1:

$$u^{1-m} = u_f^{1-m}\left[1 - \left(\frac{k}{k_j}\right)^{\ell-1}\right] \tag{3}$$

where

u, u_f = steady-state and free-flow speeds and
k, k_j = concentration and jam concentration.

In addition, the constant α of equation 1 can be determined for the restricted m, ℓ region as

$$\alpha = \frac{\ell - 1}{1 - m} \times \frac{u_f^{1-m}}{k_j^{\ell-1}} \tag{4}$$

m and ℓ as a Function of the Traffic Flow Characteristics

From equations 1 and 2 we see that m and ℓ are the basis for evaluating driver behavior at both the microscopic and macroscopic levels. When the above-mentioned requirements for m and ℓ values are considered, a dependency of m and ℓ on traffic flow characteristics can be obtained. Such a dependency will include k_j, u_f, and optimum parameters u_o, k_o of speed and concentration respectively.

Equation 3 has the following form at maximum flow:

$$\left(\frac{u_o}{u_f}\right)^{1-m} = 1 - \left(\frac{k_o}{k_j}\right)^{\ell-1} \tag{5}$$

Rearrangement of equation 5 gives

$$m = 1 - \frac{\ell n\left[1 - \left(\frac{k_o}{k_j}\right)^{\ell-1}\right]}{\ell n\left(\frac{u_o}{u_f}\right)} \tag{6}$$

The steady-state flow equation is $q = u \times k$, where q is the flow, and for optimum conditions (maximum flow) $dq/dk = 0$.

When the optimum parameters are substituted in the optimum condition [after the first derivative with respect to k in the equation $q = f(k)$], the following equation is obtained:

$$\left(\frac{k_o}{k_j}\right)^{\ell - m} = \frac{1 - m}{\ell - m} \tag{7}$$

Substituting equation 6 into equation 7 gives

$$\left(\frac{k_o}{k_j}\right)^{\ell - 1} \left\{ \frac{(\ell - 1)\ell n\left(\frac{u_o}{u_f}\right)}{\ell n\left[1 - \left(\frac{k_o}{k_j}\right)^{\ell - 1}\right]} + 1 \right\} = 1 \tag{8}$$

The nonlinear fluctuations of ℓ can be estimated from equation 8 as a function of u_f, k_j, u_o, and k_o, and thereafter the fluctuations of m can be determined from equation 6.

Evaluation Procedure and Results

For the single-regime model, four criteria were used to select the best model: mean deviation, jam concentration, free-flow speed, and maximum flow. A model was accepted if all of the following preselected criteria were met: (a) the mean deviation within 10 percent of the minimum mean deviation; (b) the jam concentration between 185 and 250 vehicles per mile; (c) the free-flow speed within an 8-mph (13-km/h) acceptable range; and (d) the maximum flow within a 300-vehicle-per-hour acceptable range. The acceptable ranges in free-flow speed and maximum flow were estimated from each data set and differed from one data set to another.

The results of this investigation of single-regime models using the 32 data sets are given in Table 1. The results are discussed for (a) models considering minimum mean deviation only, (b) models considering all criteria, and (c) models considering previously identified macroscopic models.

The models having the smallest mean deviation for each of the 32 data sets are given in Table 1. Almost all of these models lie along the m = 0.8 or 0.9 axis with ℓ values between 1.6 and 3.0. However, no models are acceptable when the traffic flow criteria are also considered. The most consistent undesirable characteristic of these minimum mean deviation models is the extremely large values for jam concentration (Figure 1).

The selected models considering all criteria are also given in Table 1. The models selected for 24 of the 32 data sets meet all criteria. Seven of the selected models do not meet the maximum flow criterion, and two do not meet the free-flow speed criterion. These selected models are shown on the m, ℓ matrix in Figure 2. The selected models generally follow a diagonal line extending from m = 0, ℓ = 2 (Greenshields' model, 7) to m = 1, ℓ = 3 (Drake, Schoefer, and May's model, 4). To emphasize the zone of the results in the m, ℓ matrix, an envelope line marking the area that contains all selected models is drawn (Figure 2). One interesting thing shown in Figure 2 is that the selected m, ℓ combinations for freeway shoulder lanes and the tunnel lane tend to be located along the upper right edge of this envelope area; i.e., there is a tendency toward relatively lower ℓ and higher m values.

The Greenberg (6), Greenshields (7), Underwood (8), and Drake et al. (4) macroscopic models are shown in the m, ℓ matrix in Figure 2 in relation to the selected models. None appears to be superior to the other macroscopic integer models. It should be noted that the Greenshields model (7) results in a linear speed-concentration relationship and usually exhibits the undesirable characteristic of an extremely low jam concentration. The Greenberg model (6) results in a concave-shaped speed-concentration relationship and does not have a y-intercept (free-flow speed of infinity). The Underwood model (8) results in a concave-shaped speed-concentration relationship and usually exhibits the undesirable characteristic of an extremely high free-flow speed

Table 1. Selected models for single regime.

Location	Data Points	k Range	Minimum Deviation Model						Selected Model					
			m	ℓ	MD	k_j	u_f	q_m	m	ℓ	MD	k_j	u_f	q_m
1. Eisenhower at Harlem	118	14 to 118	0.9	2.5	4.29	375[a]	56[a]	1,732[a]	0.8	2.8	4.50	220	50	1,810
2. Holland Tunnel	118	6 to 113	0.9	2.2	2.65	539[a]	45	1,284[a]	0.6	2.1	2.65	211	45	1,307
3. Hollywood at Sunset	98	15 to 127	0.6	1.8	6.08	250	68[a]	1,570[a]	0.5	1.8	6.08	211	66[a]	1,594[a]
4. Hollywood at Sunset	97	15 to 150	0.9	2.3	3.70	462[a]	59[a]	1,709	0.7	2.5	4.05	211	52	1,810
5. Hollywood at Hollywood	90	22 to 136	0.9	2.3	4.03	547[a]	54[a]	1,860[a]	0.7	2.8	4.41	220	44	1,969[a]
6. Hollywood at Hollywood	88	13 to 123	0.9	2.8	3.38	350[a]	51[a]	2,040[a]	0.8	3.0	3.43	231	49	2,104
7. Hollywood at Bronson	73	16 to 141	0.8	2.1	3.69	403[a]	54[a]	1,721[a]	0.7	2.5	3.91	241	45	1,795
8. Hollywood at Bronson	78	29 to 118	0.8	2.4	5.27	274[a]	64[a]	2,021	0.8	2.9	5.35	223	52	2,062
9. Hollywood at Fifield	78	18 to 117	0.1	1.1	3.40	423[a]	193[a]	2,211[a]	0.2	1.8	3.57	231	50	2,018
10. Hollywood at Fifield	82	9 to 114	0.8	3.0	4.42	240	42[a]	1,885	0.7	2.6	4.44	230	45	1,857
11. Hollywood at Franklin	75	12 to 106	0.2	2.4	3.70	152[a]	47	1,977	0.6	2.7	3.70	194	46	1,965
12. Hollywood at Franklin	78	18 to 111	0.9	2.5	4.77	431[a]	53	1,872	0.7	2.4	4.77	235	53	1,888
13. Pasadena at College East	61	15 to 138	0.8	1.6	4.40	1,210[a]	77[a]	2,191	0.1	1.9	4.82	203	56[a]	2,235
14. Pasadena at College East	58	14 to 121	0.9	2.6	2.85	409[a]	55	2,085[a]	0.7	2.5	2.90	232	55	3,100[a]
15. Pasadena at Castelar West	51	14 to 144	0.9	2.1	2.75	874[a]	50[a]	1,899	0.4	2.0	2.90	237	48	1,968
16. Pasadena at Castelar West	46	16 to 125	0.9	2.7	1.58	431[a]	79[a]	2,062	0.6	2.5	1.61	225	47	2,078
17. Pasadena at Castelar East	31	16 to 199	0.9	2.1	1.97	707[a]	57[a]	1,775	0.6	2.1	2.02	237	55	1,791
18. Pasadena at Castelar East	40	13 to 112	0.9	2.0	3.07	1,144[a]	52	2,095	0.3	1.8	3.09	248	54	2,088
19. Pasadena at Bishop West	41	16 to 96	0.9	2.5	1.91	539[a]	42	1,856	0.6	2.4	1.92	243	42	1,854
20. Pasadena at Bishop West	66	15 to 101	0.9	2.6	2.36	467[a]	44	1,924	0.6	2.4	2.37	233	45	1,927
21. Penn-Lincoln at Laurel	77	7 to 149	0.9	2.8	5.28	376[a]	45	1,919[a]	0.6	2.6	5.34	206	46	1,956[a]
22. Penn-Lincoln at Laurel	69	7 to 128	0.9	2.7	5.09	399[a]	49	2,002	0.7	2.5	5.11	243	50	2,002
23. Penn-Lincoln at Braddock	82	15 to 100	0.8	1.9	5.68	401[a]	66[a]	1,515[a]	0.7	2.4	5.88	206	52	1,608
24. Penn-Lincoln at Braddock	75	12 to 106	0.9	2.2	4.17	602[a]	60[a]	1,920	0.7	2.3	4.21	250	57	1,965[a]
25. Penn-Lincoln at tunnel	74	21 to 116	0.9	2.0	3.71	999[a]	48[a]	1,668	0.4	2.0	3.76	221	44	1,685
26. Penn-Lincoln at tunnel	51	20 to 112	0.2	2.1	2.50	166[a]	43	1,663	0.5	2.3	2.50	201	42	1,654
27. Virginia in lane 1	111	11 to 110	0.9	2.1	3.60	551[a]	69	1,656	0.7	2.0	3.63	249	70	1,670
28. Virginia in lane 2	105	11 to 105	0.9	2.4	5.47	369[a]	76	2,047[a]	0.8	2.4	5.51	237	75	2,069[a]
29. Munich-Salzburg in lane 1[b]	93	3 to 68	0.9	2.6	5.49	251[a]	61	1,427	0.9	2.7	5.51	231	60	1,436
30. Munich-Salzburg in lane 2[b]	98	1 to 60	0.7	2.9	6.81	101[a]	75	1,629	0.9	2.7	6.97	195	78	1,572[a]
31. Munich-Salzburg in lane 1[c]	91	1 to 67	0.4	1.8	4.67	170[a]	66	1,545	0.5	1.8	4.67	204	67	1,563
32. Munich-Salzburg in lane 2[c]	119	1 to 67	0.1	1.7	5.90	134[a]	76	1,833	0.5	1.8	5.93	211	76	1,838

[a]Does not meet criterion. [b]Northbound. [c]Southbound.

Figure 1. Characteristics of single-regime models.

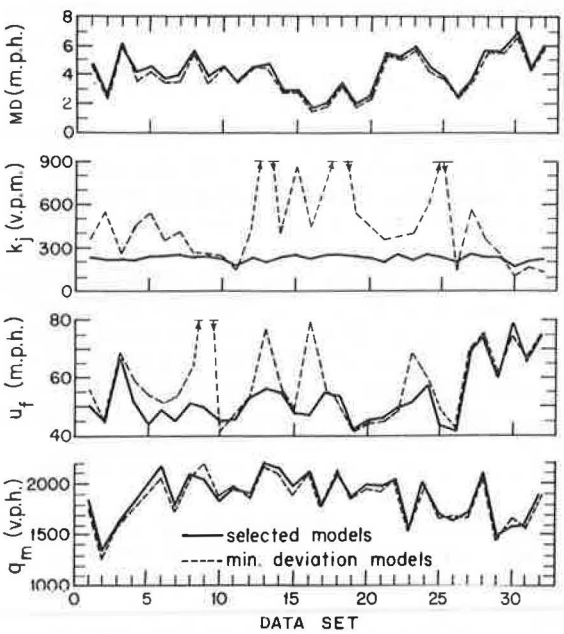

Figure 2. Location of selected single-regime models (32 data sets).

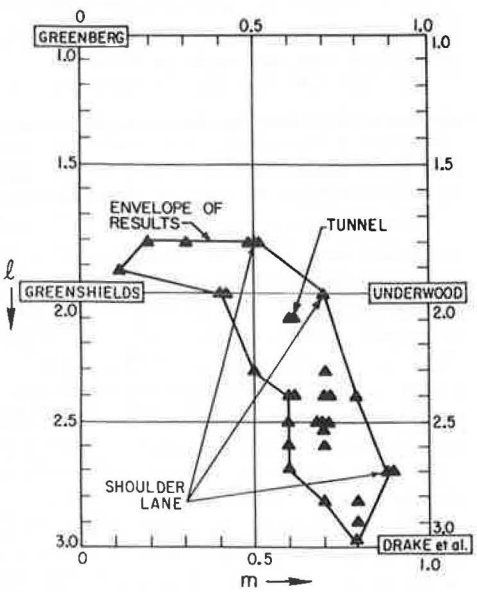

and does not have an x-intercept (jam concentration of infinity). The Drake et al. (4) model results in a concave-shaped speed-concentration relationship in the low concentration range and a convex-shaped relationship in the high concentration range. It has the undesirable characteristic of not having an x-intercept (jam concentration of infinity). Consequently, the advantage of the noninteger m, ℓ models is to minimize or eliminate the undesirable features of the integer m, ℓ models.

TWO-REGIME MODELS

The initial work on single-regime models was extended to an investigation of two-regime models to obtain improved representation of the data sets, particularly at near-capacity levels of flow. Edie (9) first proposed the two-regime approach, and the inspection of the 32 sets of speed-concentration measurements supported such an approach.

The procedures used in the two-regime model evaluation were identical to those used in the single-regime model evaluation with two exceptions. For the congested-flow regime, only data points with concentration values of more than 50 vehicles per mile were included, and the free-flow speed and maximum flow criteria were removed. For the free-flow regime, only data points with concentration values of less than 60 vehicles per mile were included, and the jam concentration criterion was removed. The selection of 50 to 60 vehicles per mile as the possible discontinuity range between the congested-flow and free-flow regimes was based on the inspection of the speed-concentration data sets.

Congested-Flow Regime

The two criteria used in selecting the congested-flow regime models were mean deviation and jam concentration. A model was accepted if its mean deviation was within 10 percent of the minimum mean deviation and if its jam concentration was between 185 and 250 vehicles per mile. The best selected model has the smallest mean deviation of several models (m, ℓ combinations) that meet the jam concentration criterion. The boundaries of the m, ℓ combinations investigated were $0 \leq m < 1$ and $0 \leq \ell \leq 3.1$. The boundaries are based on previous investigations to determine the proper range for m and ℓ. The extended region (over the region of the single-regime models) in the m, ℓ matrix for the congested-flow regime is $0 \leq m < 1$ and $0 \leq \ell < 1$. This region has the undesirable characteristic of not having a y-intercept (free-flow speed of infinity), which is not of major importance for congested-flow models. However, this extended region requires a different macroscopic equation than equation 3, which can be determined from equation 2 as

$$u^{1-m} = \alpha \frac{1 - m}{1 - \ell} \left(k^{\ell - 1} - k_j^{\ell - 1} \right) \tag{9}$$

As mentioned earlier, only data points with concentration values of more than 50 vehicles per mile were included in this analysis.

The results of this investigation of the congested-flow regime using the 32 data sets are given in Table 2. These results are discussed for (a) models considering minimum mean deviation only, (b) models considering all criteria, and (c) initial ($m = \ell = 0$) and extended ($m = 0$, $\ell = 1$) car-following models.

The models having the smallest mean deviation for each of the 32 data sets are given in Table 2. Almost all of these models lie either along the $m = 0$ axis with ℓ values between 0 and 1 or along the $\ell = 0$ axis with m values between 0 and 1. Eight of the models are represented by $m = 0$, $\ell = 0.9$, which is very close to the extended car-following model or Greenberg's model (6) ($m = 0$, $\ell = 1$). However, only eight of the

Table 2. Selected models for two-regime measurements (congested flow).

Location	Data Points	k Range	Minimum Deviation Model				Selected Model				Model With m = 0, ℓ = 0		Model With m = 0, ℓ = 1	
			m	ℓ	MD	k_j	m	ℓ	MD	k_j	MD	k_j	MD	k_j
1	72	50 to 118	0.4	0.0	3.28	348[a]	0.0	0.2	3.31	229	3.29	402[a]	3.42	161[a]
2	63	50 to 113	0.8	0.0	1.88	169[a]	0.0	0.4	1.96	231	1.92	413[a]	2.04	170[a]
3	72	50 to 127	0.7	0.0	5.88	166[a]	0.0	0.2	5.98	232	5.94	276[a]	6.15	175[a]
4	62	50 to 150	0.0	0.6	2.14	207	0.0	0.6	2.14	207	2.18	329[a]	2.16	188
5	73	50 to 136	0.0	0.9	3.53	212	0.0	0.9	3.53	212	3.67	993[a]	3.53	212
6	51	50 to 123	0.1	0.0	2.48	357[a]	0.0	0.1	2.49	245	2.48	269[a]	2.66	167[a]
7	57	50 to 141	0.1	0.5	3.36	333[a]	0.0	0.7	3.63	242	3.36	770[a]	3.64	209
8	61	50 to 118	0.2	0.0	5.46	474[a]	0.0	0.0	5.47	227	5.47	227	5.62	147[a]
9	63	50 to 117	0.0	0.9	3.42	466[a]	0.1	0.2	3.46	221	3.46	124[a]	3.42	369[a]
10	55	50 to 114	0.3	0.9	3.58	257[a]	0.2	0.8	3.58	234	3.61	421[a]	3.61	171[a]
11	55	50 to 106	0.0	0.9	3.95	229	0.0	0.9	3.95	229	4.10	536[a]	3.96	209
12	57	50 to 111	0.0	0.4	4.62	256[a]	0.0	0.5	4.62	234	4.63	618[a]	4.64	176[a]
13	44	50 to 138	0.9	0.0	4.29	100[a]	0.0	0.1	4.39	244	4.37	160[a]	4.57	422[a]
14	33	50 to 121	0.4	0.0	2.83	253[a]	0.0	0.3	2.94	242	3.87	368[a]	3.10	174[a]
15	35	50 to 144	0.3	0.0	1.98	186	0.3	0.0	1.98	186	2.01	7,802[a]	2.39	241
16	29	50 to 125	0.0	0.9	1.68	214	0.0	0.9	1.68	214	1.95	962[a]	1.68	204
17	20	50 to 99	0.0	0.9	1.55	256[a]	0.8	0.7	1.67	190	1.67	355[a]	1.56	256[a]
18	26	50 to 112	0.9	0.0	2.68	114[a]	0.3	0.2	2.74	186	2.74	257[a]	2.91	272[a]
19	26	50 to 96	0.2	0.8	1.61	863[a]	0.5	0.5	1.62	222	1.62	124[a]	1.62	396[a]
20	41	50 to 101	0.0	0.1	2.62	4,513[a]	0.8	0.7	2.62	225	2.26	517[a]	2.65	221
21	45	50 to 149	0.0	0.2	5.15	239	0.0	0.2	5.15	239	5.15	289[a]	5.29	175[a]
22	39	50 to 128	0.1	0.9	6.03	207	0.1	0.9	6.03	207	6.10	434[a]	6.04	180[a]
23	53	50 to 100	0.1	0.0	4.47	104[a]	0.2	0.3	4.47	201	4.47	109[a]	4.49	380[a]
24	46	50 to 106	0.4	0.0	4.01	1,168[a]	0.8	0.7	4.03	204	4.02	527[a]	4.06	255[a]
25	53	50 to 116	0.4	0.0	3.89	142[a]	0.0	0.0	3.89	227	3.89	227	3.96	312[a]
26	33	50 to 112	0.0	0.9	2.59	254[a]	0.2	0.1	2.79	234	2.59	327[a]	2.49	229
27	59	50 to 110	0.1	0.9	2.55	238	0.1	0.9	2.55	238	2.58	4,269[a]	2.55	193
28	56	50 to 105	0.2	0.3	3.54	384[a]	0.0	0.2	3.54	249	3.54	342[a]	3.59	160[a]
29	6	50 to 68	0.9	0.0	2.44	168[a]	0.1	0.0	3.09	234	3.10	179[a]	3.21	121[a]
30	8	50 to 60	0.0	0.9	3.45	174[a]	0.0	0.8	3.45	188	3.45	498[a]	3.45	160[a]
31	6	50 to 67	0.0	0.9	1.52	178[a]	0.1	0.9	1.52	203	1.54	921[a]	1.52	165[a]
32	17	50 to 67	0.0	0.0	7.03	156[a]	0.2	0.2	7.04	197	7.03	156[a]	7.04	276

[a]Does not meet criterion.

Figure 3. Characteristics of congested-flow regime models.

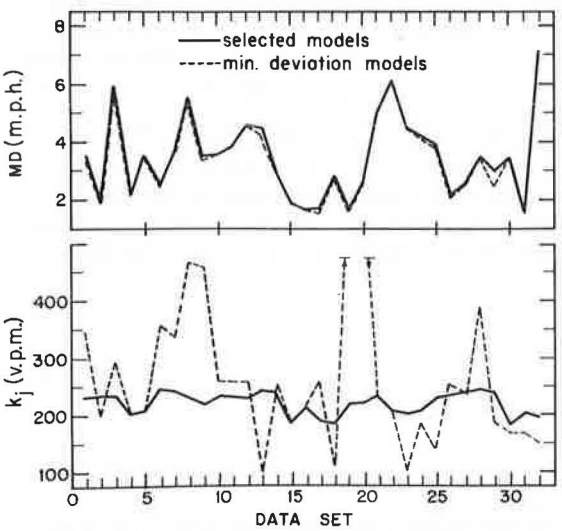

Figure 4. Location of selected two-regime models (32 data sets).

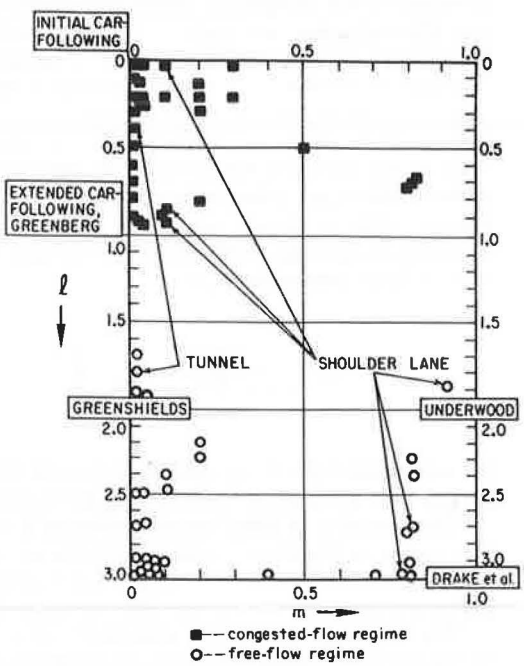

models are acceptable when the jam concentration and the mean deviation criteria are considered.

The selected models considering all criteria are also given in Table 2. The models selected for all 32 data sets meet both the mean deviation and jam concentration criteria. Figure 3 shows the two characteristics of the congested-flow models of both the selected and minimum deviations models. This figure and Table 2 indicate that neither m and ℓ values nor the mean deviation is sensitive to changes in the jam concentration values. This effect can be anticipated from equations 8 and 6 for changes in m and ℓ. On the other hand, the lack of data points under extremely high concentration conditions may explain the nonsensitivity property of the mean deviation with respect to the jam concentration.

The selected models are shown on the m, ℓ matrix in Figure 4. Almost all of these models lie along the m = 0 axis with ℓ values between 0 and 1. This is the region of the m, ℓ matrix that lies between the initial (m = 0, ℓ = 0) and the extended (m = 0, ℓ = 1) car-following models. These two models as they relate to the data set results are discussed below.

The mean deviation and jam concentration for the initial and the extended car-following models for each of the 32 data sets are also given in Table 2. Although the resulting mean deviations are all within 10 percent of the minimum mean deviation, the models are generally not acceptable because the jam concentrations lie outside the specified range. Although the initial car-following model generally has smaller mean deviations, the extended car-following model fulfills the jam concentration criteria in most cases. These results give significant support to the earlier work on car-following theory (3, 9).

Free-Flow Regime

The three criteria used in selecting the free-flow regime models were mean deviation, free-flow speed, and maximum flow. A model was accepted if the mean deviation was within 10 percent of the minimum mean deviation, if the free-flow speed was within an 8-mph (13-km/h) acceptable range, and if the maximum flow was within a 300-vehicle-per-hour acceptable range. The acceptable ranges in free-flow speed and maximum flow were estimated from each data set and differed from one data set to another. The boundaries of the m, ℓ combinations investigated were $0 \leq m < 1$ and $0 \leq \ell < 3.1$. As mentioned earlier, only data points with concentration values of less than 60 vehicles per mile were included in this analysis.

The results of this investigation of the free-flow regime using the 32 data sets are given in Table 3. These results are discussed for (a) models considering minimum mean deviation only, (b) models considering all criteria, and (c) models considering other previously identified macroscopic models.

Although half of the models having the minimum mean deviation for each of the 32 data sets lie in the vicinity of m = 0 and ℓ = 3, the remaining models are scattered in the matrix from m = 0 to m = 0.9 and from ℓ = 1.1 to ℓ = 3.1. However, 15 of the models are acceptable when the minimum mean deviation and the free-flow speed and maximum flow criteria are considered.

The selected models considering all criteria are also given in Table 3. By selecting models that slightly increase the minimum mean deviation, the free-flow speed criterion is fulfilled for all selected models and 23 models fulfill the maximum flow criteria. These selected models are graphically represented on the m, ℓ matrix shown in Figure 4. These models lie either along the m = 0 axis with ℓ values between 1.7 and 3.1 or along the m = 0.8 axis with ℓ values between 1.9 and 3.1. An interesting point about Figure 4 is that the m and ℓ free-flow regime models associated with measurements taken in tunnel and shoulder lanes are somewhat scattered away from most of the freeway m, ℓ combinations. On the other hand, that is not the case in the congested-flow models in which the m, ℓ combinations of tunnel and shoulder lanes are among the other freeway m, ℓ combinations. The free-flow regime model characteristics are shown in Figure 5 for both the selected and minimum deviation models. In addition, Figure 5

Table 3. Selected models for two-regime measurements (free flow).

Location	Data Points	k Range	Minimum Deviation Model					Selected Model				
			m	ℓ	MD	u_f	q_m	m	ℓ	MD	u_f	q_m
1	57	14 to 60	0.0	3.1	4.26	52	1,792[a]	0.0	2.7	4.43	54	1,802
2	66	6 to 60	0.0	1.8	3.01	47	1,324	0.0	1.8	3.01	47	1,324
3	31	15 to 20	0.0	3.1	6.70	48	1,672[a]	0.0	2.5	6.75	51	1,684[a]
4	38	15 to 60	0.0	3.1	4.11	53	1,752	0.0	3.1	4.11	53	1,752
5	24	22 to 60	0.0	3.1	6.67	48	1,860[a]	0.0	2.5	6.73	51	1,919[a]
6	42	13 to 60	0.0	3.1	3.44	48	2,297	0.0	3.1	3.44	48	2,297
7	17	16 to 60	0.0	3.1	3.23	47	1,575[a]	0.0	2.9	3.34	48	1,580[a]
8	26	29 to 60	0.6	1.1	3.24	232[a]	9,633[a]	0.0	3.1	3.30	49	2,551
9	19	18 to 60	0.4	1.1	3.16	321[a]	2,084[a]	0.8	2.3	3.30	50	1,570[a]
10	40	9 to 60	0.0	2.0	5.04	45	2,373[a]	0.0	2.0	5.04	45	2,373[a]
11	35	12 to 60	0.8	2.7	3.63	46	1,939	0.8	2.7	3.63	46	1,939
12	37	18 to 60	0.0	3.1	5.46	49	1,844	0.0	3.1	5.46	49	1,844
13	19	15 to 60	0.7	3.0	1.42	49	2,282[a]	0.4	3.0	1.42	49	2,246
14	30	14 to 60	0.6	3.1	1.60	52	2,188[a]	0.7	3.0	1.60	52	2,217
15	21	14 to 60	0.8	3.1	2.84	43	1,830	0.8	3.1	2.84	43	1,830
16	22	16 to 60	0.8	2.4	1.54	48	2,194	0.8	2.4	1.54	48	2,194
17	15	22 to 60	0.0	3.1	2.29	48	1,644[a]	0.2	2.2	2.44	55	1,649[a]
18	19	13 to 60	0.0	1.3	3.12	72[a]	3,122[a]	0.0	1.9	3.16	50	2,134
19	19	16 to 60	0.0	3.1	2.00	40	1,661[a]	0.0	2.7	2.09	41	1,707
20	31	15 to 60	0.1	2.4	1.78	45	1,912	0.1	2.4	1.78	45	1,912
21	38	7 to 60	0.0	3.1	4.61	43	2,526[a]	0.0	3.1	4.61	43	2,526[a]
22	36	7 to 60	0.0	1.4	6.10	58[a]	6,330[a]	0.8	3.1	6.28	47	2,267[a]
23	31	15 to 60	0.0	3.0	5.98	50	1,702	0.0	3.0	5.98	50	1,702
24	32	12 to 60	0.0	3.1	3.94	53	1,862	0.0	3.1	3.94	53	1,862
25	30	21 to 60	0.0	3.1	3.22	39	1,501	0.0	3.1	3.22	39	1,501
26	26	20 to 60	0.0	3.1	2.38	39	1,533[a]	0.2	2.3	2.49	42	1,601
27	82	11 to 60	0.8	3.0	3.54	59[a]	1,617	0.8	2.9	3.54	60	1,610
28	71	11 to 60	0.2	3.1	5.44	71	2,115[a]	0.0	3.1	5.45	70	2,132
29	91	3 to 60	0.8	2.7	5.47	61	1,400	0.8	2.7	5.47	61	1,400
30	97	1 to 60	0.1	2.5	6.80	77	1,646	0.1	2.5	6.80	77	1,646
31	89	1 to 60	0.9	1.9	4.71	66	1,617	0.9	1.9	4.71	66	1,617
32	114	1 to 60	0.0	1.7	5.74	76	1,823	0.0	1.7	5.74	76	1,823

[a]Does not meet criterion.

Figure 5. Characteristics of free-flow regime models.

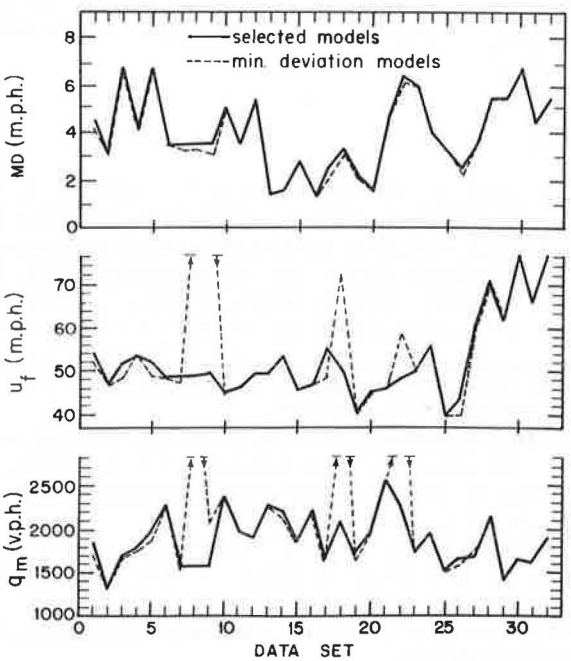

Table 4. Selected models for single regime (13 data sets).

Station Number	Data Points	k Range	Minimum Deviation Model						Selected Model					
			m	ℓ	MD	k_j	u_f	q_m	m	ℓ	MD	k_j	u_f	q_m
SM-12	86	3 to 132	0.9	2.7	3.55	337[a]	58	2,032	0.7	2.4	3.76	234	59	2,095
SM-13	87	6 to 99	0.8	2.7	3.57	226	61	2,091	0.8	2.7	3.57	226	61	2,091
SM-14	101	3 to 135	0.9	2.6	3.56	395[a]	57	2,104	0.7	2.5	3.65	227	57	2,141
SM-15	83	6 to 114	0.9	2.6	2.60	362[a]	60	2,013	0.8	2.6	2.68	245	60	2,037
SM-16	110	3 to 129	0.9	2.4	3.44	411[a]	63	1,888[a]	0.7	2.3	3.57	220	63	1,924
SM-17	97	6 to 156	0.9	2.3	2.94	488[a]	65	1,994	0.7	2.3	3.21	241	62	2,084
SM-18	92	3 to 108	0.9	2.5	2.89	389[a]	57	1,846[a]	0.7	2.6	3.18	196	55	1,916
SM-19	93	3 to 105	0.9	2.7	3.03	329[a]	61	2,072	0.8	2.6	3.06	238	62	2,070
SM-20	96	6 to 99	0.9	2.9	3.34	297[a]	55	2,010	0.7	2.7	3.40	189	56	2,009
SM-21	96	3 to 108	0.9	2.3	2.37	506[a]	62	1,963	0.6	2.1	2.46	223	64	1,975
SM-22	87	3 to 78	0.9	2.5	2.93	362[a]	61	1,830[a]	0.8	2.5	2.94	235	61	1,836[a]
LaBrea (on-ramp)	108	9 to 144	0.1	1.6	2.01	264[a]	53	2,153	0.0	1.6	2.02	241	52	2,152
Venice (CD-on)	91	3 to 189	0.9	1.7	3.20	1,687[a]	57[a]	1,303	0.9	1.8	3.26	1,313[a]	51	1,333

[a]Does not meet criterion.

shows that the acceptable values of the parameters u_f and q_m can be obtained by only slightly increasing the mean deviation.

The Greenberg (6), Greenshields (7), Underwood (8), and Drake et al. (4) models are shown on the m, ℓ matrix in Figure 4 in relation to the selected models. None of these macroscopic models appears to be appropriate for the various data sets. There is no justification for expecting the free-flow regime data sets to be represented by microscopic (car-following) theories. However, it is interesting to note that the selected free-flow models have the characteristic of a large ℓ value and a small m value. This causes the sensitivity component of the car-following equation to be numerically small, which would be expected in situations where vehicles are not in a car-following mode.

EXTENDED DATA

As has been mentioned earlier, the second group of data sets consists of 13 sets of data 11 of which were taken from freeway stations and two from on-ramp and collector-distributor road within the freeway section. This second group of data sets is based on 5-min time interval samples and is averaged across the total directional roadway.

Based on the the research on single- and two-regime models, an attempt was made to predict the results of m, ℓ combinations for both the minimum mean deviation models and selected models. These predictions and their verifications are discussed for (a) models considering single-regime approach, (b) models considering congested-flow regime only, and (c) models considering free-flow regime only.

Single-Regime Models

The single-regime model characteristics of the first group of data sets are shown in Figures 1, 2, and 3 and given in Table 1. When the m, ℓ combinations of the selected models are considered, it appears that the m and ℓ values of most of the data sets are within the region of $0.5 \leq m < 1$ and $2 \leq \ell \leq 3$ and tend to fall within the envelope of results shown in Figure 2 and extending from $m = 0$, $\ell = 2$ to $m = 1$, $\ell = 3$. Furthermore, all the m, ℓ combinations associated with models of non-inner freeway lanes are located along the upper right edge of the envelope area. Therefore, this envelope of results will be the basis for predicting the m, ℓ combinations of other data sets for freeway lanes.

The results of the investigation of single-regime models using the second data sets are given in Table 4. In addition, the m, ℓ combinations of these data sets are shown in Figure 6 for the selected models. It should be noted that the evaluation procedure and preselected criteria were used in the same way for both groups of data sets.

Consequently, from the new selected m, ℓ combinations the above prediction is indeed verified by the second group of data sets. This conclusion is shown in Figure 6 where the selected m, ℓ of the freeway models are within the predicted envelope area in the m, ℓ matrix.

Congested-Flow Models

The congested-flow regime model characteristics for the first group of data sets are shown in Figures 3 and 4 and given in Table 2. From Figure 4 and Table 2 it appears that the m and ℓ values of most of the data sets are within the region of $0 \leq m \leq 0.5$ and $0 \leq \ell \leq 1$ and the m values tend to approach zero. This observation is the basis for predicting m, ℓ combinations for other freeway data sets.

The results of the investigation of congested-flow regime models using the second group of data sets are given in Table 5. In addition, the selected m, ℓ combinations of these data sets were located in the m, ℓ matrix shown in Figure 7. Comparison of Figures 4 and 7 emphasizes the identical tendency of m to approach zero, but ℓ of the second data set has a slight tendency toward values greater than 1.0.

Figure 6. Location of selected single-regime models (13 data sets).

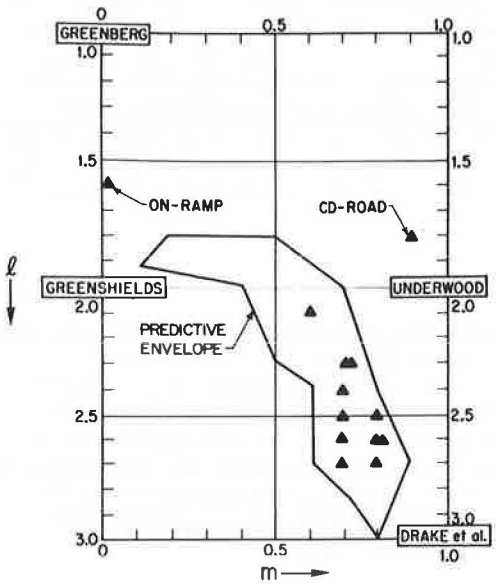

Figure 7. Location of selected two-regime models (13 data sets).

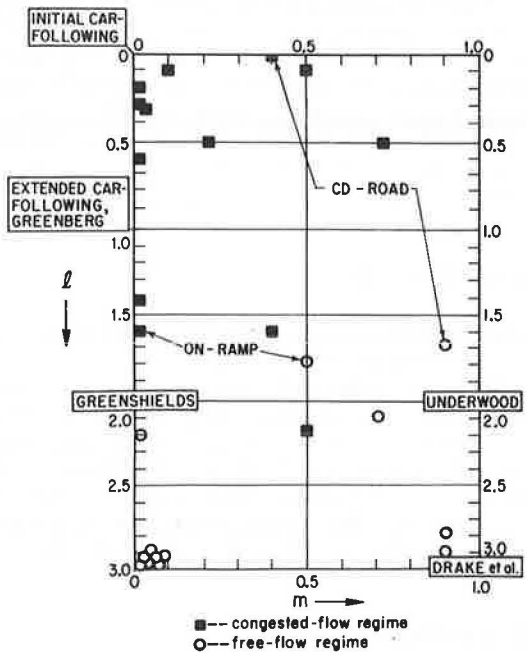

Table 5. Selected models for congested regime (13 data sets).

Station Number	Data Points	k Range	Minimum Deviation Model m	ℓ	MD	k_j	Selected Model m	ℓ	MD	k_j
SM-12	28	50 to 132	0.0	1.4	0.61	190	0.0	1.4	0.61	190
SM-13	35	50 to 99	0.6	0.1	1.92	112[a]	0.5	0.1	1.97	247
SM-14	47	50 to 135	0.9	1.8	2.26	926[a]	0.0	0.6	2.27	205
SM-15	44	50 to 114	0.2	0.2	1.02	399[a]	0.0	0.2	1.04	229
SM-16	56	50 to 129	0.9	1.6	0.89	1,209[a]	0.2	0.5	0.90	248
SM-17	43	50 to 156	0.3	0.1	0.95	605[a]	0.1	0.1	1.04	275[a]
SM-18	52	50 to 108	0.0	1.6	1.21	158[a]	0.5	2.2	1.21	199
SM-19	45	50 to 105	0.7	0.5	1.77	629[a]	0.0	0.3	1.81	245
SM-20	56	50 to 99	0.0	0.2	2.78	259[a]	0.0	0.3	2.78	233
SM-21	51	50 to 108	0.0	0.1	1.32	533[a]	0.7	0.5	1.33	248
SM-22	42	50 to 78	0.0	0.9	1.26	159[a]	0.4	1.6	1.28	181
LaBrea (on-ramp)	60	50 to 144	0.0	1.4	1.91	270[a]	0.0	1.6	1.91	247
Venice (CD-on)	52	50 to 189	0.0	0.1	1.28	535[a]	0.4	0.0	1.39	228

[a]Does not meet criterion.

Table 6. Selected models for free-flow regime (13 data sets).

Station Number	Data Points	k Range	Minimum Deviation Model m	ℓ	MD	u_f	q_m	Selected Model m	ℓ	MD	u_f	q_m
SM-12	58	3 to 60	0.9	2.8	3.88	58	2,072	0.9	2.8	3.88	58	2,072
SM-13	61	6 to 60	0.0	3.1	3.68	60	2,007	0.0	3.1	3.68	60	2,007
SM-14	64	3 to 60	0.0	3.1	3.63	56	2,055	0.0	3.1	3.63	56	2,055
SM-15	47	6 to 60	0.0	3.1	2.66	57	2,021	0.0	3.1	2.66	57	2,021
SM-16	62	3 to 60	0.0	3.1	3.25	60	1,879	0.0	3.1	3.25	60	1,879
SM-17	58	6 to 60	0.9	3.0	2.60	61	2,090	0.9	3.0	2.60	61	2,090
SM-18	56	3 to 60	0.0	3.1	2.74	56	1,731[a]	0.0	3.1	2.74	56	1,731[a]
SM-19	52	3 to 60	0.0	3.1	2.97	60	2,032	0.0	3.1	2.97	60	2,032
SM-20	50	6 to 60	0.0	3.1	3.77	54	1,986	0.0	3.0	3.77	54	1,986
SM-21	56	3 to 60	0.0	2.4	2.64	61	1,871[a]	0.0	2.2	2.69	63	1,908
SM-22	55	3 to 60	0.8	2.6	3.60	61	1,790[a]	0.7	2.1	3.81	65	1,903
LaBrea (on-ramp)	60	9 to 60	0.0	1.3	2.19	66[a]	2,998[a]	0.5	1.8	2.22	49	2,190
Venice (CD-on)	43	3 to 60	0.9	1.7	4.58	55	1,453	0.9	1.7	4.58	55	1,453

[a]Does not meet criterion.

Figure 8. Typical single- and two-regime models.

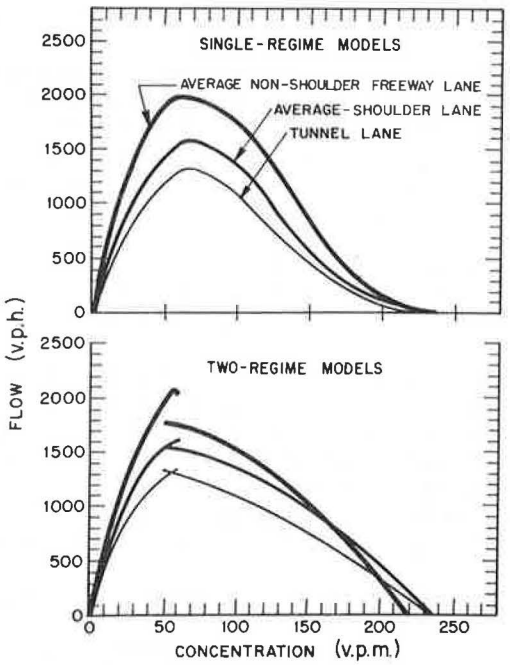

Free-Flow Regime Models

The free-flow regime model characteristics from the first group of data sets are shown in Figures 4 and 5 and given in Table 3. From Figure 4 and Table 3 it appears that the m and ℓ values of most of the data sets are within the region of $0 \leq m \leq 1$ and $2.5 \leq \ell \leq 3.0$ and tend to be centered around $m = 0$, $\ell = 3.0$. This tendency will be the basis for predicting m and ℓ values for other freeway data sets.

The results of the investigation of free-flow regime models using the second data sets are given in Table 6. In addition, the selected m, ℓ combinations are on the matrix shown in Figure 7. As can be seen from Figure 7, the above prediction is verified in which seven of 11 m, ℓ combinations (of freeway lanes data) are centered around $m = 0$, $\ell = 3.0$.

To visualize the differences among the various models with respect to type of road facility, three groups of models were identified for nonshoulder freeway lanes, shoulder freeway lanes, and a tunnel lane. These average models are shown in Figure 8 for the flow-concentration relationship. The average m, ℓ values for the nonshoulder freeway lanes are $m = 0.6$, $\ell = 2.4$; $m = 0.2$, $\ell = 0.5$; and $m = 0.2$, $\ell = 2.9$ for the single regime, congested-flow regime, and free-flow regime respectively. The average m, ℓ values for the shoulder lanes are $m = 0.7$, $\ell = 2.2$; $m = 0.1$, $\ell = 0.6$; and $m = 0.8$, $\ell = 2.5$ for the single, congested-flow, and free-flow regimes respectively. The m, ℓ combinations for the tunnel data are given in Tables 1, 2, and 3 (data set 2).

The consideration of road facilities other than nonshoulder freeway lanes is focused on tunnel, shoulder lanes, on-ramp, and CD road data sets. In single-regime models, although it is possible to distinguish between m, ℓ values for on-ramp and CD road data, it is unlikely that this distinction can be made for tunnel and shoulder lane data. In the congested-flow models no distinction can be made for the various data sets. This is as expected because under high concentration conditions traffic behavior is similar on all types of road facilities. In the free-flow models, m, ℓ combinations of tunnel, shoulder lane, on-ramp, and CD road are scattered away from most of the m, ℓ freeway models. It is reasonable to assume that different driver behavior is reflected under low concentration conditions on different types of road facilities (e.g., in a tunnel there are lower speeds and more cautious driving than on an open freeway lane).

CONCLUSIONS

This paper has evaluated macroscopic and microscopic models to determine which of them best represented observed sets of speed-concentration measurements. Single- and two-regime models of a free flow and congested flow were investigated. A total of 45 sets of measurements were analyzed; the results of the first 32 data sets were used to predict the results of the 13 remaining data sets.

In regard to single-regime models the more significant findings were as follows:

1. The mean deviation of the selected models varied from 1.6 to 7.0 mph (2.6 to 11.3 km/h) with a mean value of 3.8 mph (6.1 km/h);
2. The traffic flow criteria for the selected models were satisfied in 35 of the 45 data sets;
3. All previously proposed m, ℓ integer models had significant deficiencies in regard to acceptable traffic flow parameter values and mean deviations;
4. The area of the m, ℓ matrix in which the selected models are located is shown in Figures 2 and 6, and for inner freeway lanes the selected models tended toward m and ℓ of 0.6 and 2.4 respectively; and
5. The major disadvantage of the single-regime approach was that the selected models did not represent the data sets at near-capacity conditions.

The most significant findings with congested-flow two-regime models were that

1. The mean deviation of the selected models varies from 0.6 to 7.0 mph (1 to 11 km/h) with a mean value of 2.9 mph (4.7 km/h);
2. The jam concentration criterion for the selected models was satisfied in 44 of the 45 data sets;
3. Two previously proposed m, ℓ integer models ($m = 0$, $\ell = 1$) were marginally satisfactory but did not have the minimum mean deviations, and the jam concentration values were generally high;
4. The area of the m, ℓ matrix in which the selected models are located is shown in Figures 4 and 7, and the selected models tended toward m values approaching 0 and ℓ values between 0 and 1; and
5. The two-regime approach did result in more models satisfying the jam concentration criterion but only a slight reduction in the mean deviation.

The most significant findings with the free-flow two-regime models are given below.

1. The mean deviation of the selected models varied from 1.4 to 6.8 mph (2.3 to 10.9 km/h) with a mean value of 3.7 mph (6.0 km/h).
2. The traffic flow parameter criteria for the selected models were satisfied in 35 of the 45 data sets.
3. The area of the m, ℓ matrix in which the selected models are located is shown in Figures 4 and 7. The selected models are scattered over the lower portion of the m, ℓ matrix; however, the largest cluster of selected models occurs at $m = 0$ and $\ell = 3$.
4. With the two-regime approach no more models satisfied the maximum flow criterion and there was no significant reduction in the mean deviation.

In summary,

1. Previously proposed macroscopic models did not accurately represent the speed-concentration data sets;
2. The use of noninteger m, ℓ macroscopic models for single-regime analysis provided a significant improvement in accuracy and more realistic traffic parameter values but had the weakness of not well representing the data sets at near-capacity conditions;
3. The use of noninteger m, ℓ macroscopic models combined with two-regime analysis did support the visual appearance of the two-regime phenomenon in the data sets

but provided only slightly better representation of the data sets; and

4. For further improvement in selecting macroscopic models to represent speed-concentration sets of measurements a different generalized model should be developed that incorporates the two-regime approach.

ACKNOWLEDGMENTS

The authors wish to express their appreciation to the Division of Highways at Los Angeles, District 7, for supplying the data sets.

REFERENCES

1. A. D. May, Jr., and H. E. M. Keller. Non-Integer Car-Following Models. Highway Research Record 199, 1967, pp. 19-32.
2. A. D. May, Jr., and H. E. M. Keller. Evaluation of Single- and Two-Regime Traffic Flow Models. Proc., Fourth International Symposium on the Theory of Traffic Flow, Karlsruhe, 1968.
3. D. C. Gazis, R. Herman, and R. W. Rothery. Nonlinear Follow-the-Leader Models of Traffic Flow. Operations Research, Vol. 9, No. 4, 1960, pp. 545-567.
4. J. S. Drake, J. L. Schoefer, and A. D. May, Jr. A Statistical Analysis of Speed Density Hypotheses. Proc., Third International Symposium on the Theory of Traffic Flow, Elsevier, New York, 1967.
5. P. Athol. Interdependence of Certain Operational Characteristics Within a Moving Traffic Stream. Highway Research Record 72, 1965, pp. 58-87.
6. H. Greenberg. An Analysis of Traffic Flow. Operations Research, Vol. 7, No. 4, 1959, pp. 499-505.
7. B. D. Greenshields. A Study in Highway Capacity. HRB Proc., Vol. 14, 1934, pp. 448-477.
8. R. T. Underwood. Speed, Volume and Density Relationships. Quality and Density of Traffic Flow, Yale Bureau of Traffic, 1961, pp. 66-76.
9. L. C. Edie. Car-Following and Steady-State Theory for Non-Congested Traffic. Operations Research, Vol. 9, No. 1, 1961, pp. 66-76.

A DETERMINISTIC TRAFFIC FLOW MODEL FOR THE TWO-REGIME APPROACH

Avishai Ceder,* Institute of Transportation and Traffic Engineering,
University of California, Berkeley

In recent years it has been shown that the relationship between flow and concentration is probably not continuous under maximum flow conditions. A previous paper (2) concerned with the evaluation of traffic flow models examined the steady-state equations derived from the generalized car-following model designed by Gazis, Herman, and Rothery. These macroscopic relationships were subjected to 45 data sets, in which most of the data were from freeway lanes, for both single- and two-regime models. From the results of these data sets, the deficiencies of the various models using the two-regime approach were identified and the need for investigating a new two-regime approach was stressed. This paper discusses the development of a new model at both the microscopic and macroscopic levels. The steady-state equation derived from the new model is analytically evaluated by using 45 data sets. The model, based on a new car-following sensitivity component, shows that the free-flow regime and the congested-flow regime are fairly well adapted to convexity and concavity properties respectively in a speed-concentration relationship. By using the analysis of driver performance as a sensitivity measurement, model parameters are defined and evaluated. In addition, the two flow regimes are incorporated by means of breakpoint evaluation procedures. In the light of two-regime phenomena the new steady-state formulation may be superior to the steady-state equations derived from the generalized car-following model, particularly in simplicity and clarity.

•EDIE (1) was the first to point out the possibility of discontinuity in the flow-concentration curve under maximum flow conditions. He proposed two separate models. These models, which describe macroscopic relationships, are based on the convertibility models developed from the microscopic car-following model.

Because more and more road facilities are operating at near-capacity level, the importance of considering this discontinuity phenomenon is apparent. Furthermore, in a description of traffic behavior, this phenomenon will make the limitations more severe for hydrodynamic applications.

A previous paper (2) concerned with the evaluation of traffic flow models examined the macroscopic relationships derived from the generalized car-following model formulated by Gazis, Herman, and Rothery (3) as

$$\ddot{X}_{n+1}(t+T) = \alpha \frac{[\dot{X}_{n+1}(t+T)]^{a}}{[X_n(t) - X_{n+1}(t)]^{\ell}} [\dot{X}_n(t) - \dot{X}_{n+1}(t)] \quad (1)$$

where the single and double dots represent speed and acceleration (deceleration) and

*When this paper was written, Mr. Ceder was on leave from the Road Safety Center, Technion, Haifa, Israel.

Publication of this paper sponsored by Committee on Traffic Flow Theory and Characteristics.

X_n, X_{n+1} = positions of the leading car and the following car,
T = time lag of response to stimulus, and
m, ℓ, and α = some constant parameters.

Forty-five sets of speed-concentration measurements (2) were used to show the most appropriate speed-concentration relationships based on steady-state flow formulation obtained by integrating equation 1. These relationships were investigated in an m, ℓ matrix format to study the variability of those exponents of the sensitivity component that belong to equation 1. The results were summarized in a two-dimensional m, ℓ matrix for both single- and two-regime traffic flow models. By investigating single-regime models, other microscopic and macroscopic theories that can be reduced to the form of equation 1 can be evaluated. On the other hand, investigation of two-regime models stimulates speculation about the simplicity and clarity of the generalized car-following model for the two-regime approach.

The purpose of this paper is to develop and evaluate a simpler and more reliable traffic flow model than the generalized car-following model for two-regime traffic behavior.

This paper discusses the development of a new model at both the microscopic and macroscopic levels and presents on analytical evaluation of the new model by using actual traffic flow data.

The 45 data sets used in a previous work (2) are also the basis for the quantitative analysis performed in this paper. These data sets are described in detail elsewhere (2). The data sets can be separated into two groups: the first 32 data sets based on 1-min time interval samples and the remaining 13 sets based on 5-min samples. In both groups, the mean speed and mean concentration are calculated for each interval.

The sources of the first 32 data sets are given in Table 1. The remaining 13 data sets were taken on the Santa Monica Freeway, 11 (SM-12 to SM-22) on freeway lanes and two from a CD road and an on-ramp. The data selection procedure and other details concerning the data are described elsewhere (2).

The use of large amounts of actual data emphasizes the possibility that the new model could be applicable not only to traffic flow theory but also to planning new road facilities, road improvements, and freeway control projects.

After the deficiencies of two-regime traffic flow models based on equation 1 were identified, a new model was developed. Based on analysis of driver performance, this model shows how one can take into consideration the discontinuity phenomenon under peak flow conditions from gross aspects of traffic flow.

MODEL DEVELOPMENT

Previous studies in car-following (1, 3, 4) note the following stimulus-response relationship:

$$\begin{pmatrix}\text{driver's}\\ \text{response}\end{pmatrix}_{t+T} = \begin{pmatrix}\text{sensitivity}\\ \text{factors}\end{pmatrix}_t \times \begin{pmatrix}\text{given}\\ \text{stimulus}\end{pmatrix}_t \qquad (2)$$

Although attempts to improve the car-following theory have been made, two parts of this equation have not been modified. The first part of this relationship is the response of the following vehicle at time (t + T) in terms of deceleration (or acceleration). This response is proportional to the second part, the stimulus. A given stimulus is described in terms of relative speed (between the pair of vehicles under consideration) at time t.

The third part of equation 2, the sensitivity component, has undergone several stages of refinement. It has had the following functions: constant factor, inversely proportional to spacing (headway distance), inversely proportional to spacing squared and proportional to the absolute speed of the following vehicle, and the generalized expression as shown in equation 1.

Because there are some difficulties in the generalized car-following model (equation 1), an attempt will be made to develop a new sensitivity component. The deficiencies of equation 1 are particularly emphasized for the two-regime approach and are summarized below.

1. It has a rather complicated sensitivity function, namely,

$$\frac{\alpha[\dot{X}_{n+1}(t+T)]^m}{[X_n(t) - X_{n+1}(t)]^\ell}$$

where α, ℓ, m are arbitrary and are not subject to independent measurements (excluding particular m, ℓ combinations) for the two-regime models.

2. When equation 1 is converted to steady-state flow equations, the boundary parameters, free-flow speed and jam concentration, are not always defined for the entire m, ℓ plane.

3. Nine steady-state flow equations can be derived from equation 1 for the entire m, ℓ plane, which increases the complexity of such macroscopic relationships.

4. It is difficult and perhaps impossible to make stability evaluation of the nonlinear model shown in equation 1 (excluding the case where $m = \ell = 0$).

Herman and Potts (4) suggested that driver response to a given stimulus varies inversely with spacing and that there is a sensitivity function α_o/s, where s is the spacing between vehicles and α_o is a constant. Edie (1) proposed the introduction of the absolute vehicle speed into the sensitivity function and the square of the spacing $(\alpha \times u_{n+1})/s^2$, where u_{n+1} is the absolute speed of the following vehicle and α is a constant. Later, these two sensitivity functions were examined by Rothery et al. (5), who found that these two sensitivity components during the car-following mode improved the results obtained from the linear model, which has a constant sensitivity function. However, they indicated that there was no significant difference between the two functions that makes either of these sensitivity components superior to the other.

In addition, Pipe and Wojcik (6) used perceptual factors (rate of change of visual angle) to derive a car-following model. They demonstrated a sensitivity function of the form α/s^2. Finally, the previous paper (2) investigated two-regime models based on equation 1 and indicated that the m value (the speed exponent belonging to equation 1) tends to be closer to 0 than to 1 in both regimes. Therefore, the search for a simple model was narrowed to those situations where the sensitivity function is only inversely proportional to the spacing in various degrees. In addition, the following criteria for the new sensitivity component were considered:

1. It should be capable of describing real-world traffic data; and
2. The steady-state flow equations derived from the car-following model should minimize the deficiencies of equation 1 stated and, therefore, should (a) be reasonably simple, (b) provide a complete definition of all traffic flow parameters (free-flow speed, jam concentration, and optimum parameters), and (c) describe differences between the free-flow regime and congested-flow regime on the basis of average car-following behavior.

These criteria led to the decision that a sensitivity function be a combination of a weighting factor and a reciprocal spacing function. In addition, macroscopic models frequently included the normalized concentration component (k/k_j) within the speed-concentration relationship (2). Based on the assumption of steady-state flow, this normalized concentration becomes equivalent to the ratio between jam spacing and spacing. This ratio is used in the proposed sensitivity function as a power of a crucial weighting factor.

Consequently, the following sensitivity function is proposed:

$$\alpha \times \frac{A^{-s_j/s}}{s^2} \tag{3}$$

where

s and s_j = spacing and jam spacing and
A = nondimensional weighting factor.

MODEL SENSITIVITY

The microscopic form of the proposed model, which assumes that the (n + 1)th vehicle will react in a stable way to any motion of the lead nth vehicle, is

$$a_{n+1}(t + T) = \alpha \times \frac{A^{-\frac{s_j}{s(t)}}}{s^2(t)} [u_n(t) - u_{n+1}(t)] \tag{4}$$

where

a_{n+1} = deceleration or acceleration response at time t + T,
u_n, u_{n+1} = speeds of the leading and following vehicles at time t,
T = time lag of response to stimulus, and
α = a constant dependent on A and s_j.

The sensitivity term (equation 3) may not immediately indicate that the deceleration response increases inversely with spacing, which is required from a logical standpoint. Therefore, the following mathematical derivation is presented.

For convenience, a progressive ratio between the response and concentration is maintained (assuming a steady-state traffic stream) instead of an inverse ratio between the response and spacing. Thus, from equation 4, the required constraint will be

$$\frac{k^2}{A^{k/k_j}} < \frac{(k + \Delta k)^2}{A^{(k+\Delta k)/k_j}} \tag{5}$$

for $k = \frac{1}{s}$, $k_j = \frac{1}{s_j}$, $0 \le k \le k_j$, $0 \le \Delta k \le k_j - k$, or

$$A < \left(1 + \frac{\Delta k}{k}\right)^{2k_j/\Delta k}$$

By using boundary conditions, the maximum value of A in equation 5 for all k and Δk is

$$\text{Max } A = \lim_{\substack{\Delta k \to 0 \\ k \to k_j}} \left(1 + \frac{\Delta k}{k}\right)^{2k_j/\Delta k} = \lim_{\Delta k \to 0} \left[\left(1 + \frac{1}{k_j/\Delta k}\right)^{k_j/\Delta k}\right]^2 = e^2$$

Therefore, the range of A values that will maintain the deceleration response inversely with spacing is

$$0 < A < e^2 \tag{6}$$

If the time lag between response and stimulus and the variations in behavior from one driver to another are neglected, a steady-state equation can be derived from equation 4 since it is a perfect differential in t.

Thus, converting the symbols of equation 4 gives

$$\frac{du}{dt} = \frac{\alpha}{s^2} A^{-s_j/s} \frac{ds}{dt}$$

and integrating gives

$$u = \frac{\alpha k_j}{\ell n A} A^{-k/k_j} + c$$

where $k = 1/s$ and $k_j = 1/s_j$.

From boundary condition, i.e.,

$u \to 0$, $k \to k_j$ = jam concentration,

$k \to 0$, $u \to u_f$ = free-flow speed,

the following macroscopic model can be obtained [note that $\alpha = u_f A \times \ell n A / k_j (A - 1)$].

$$u = \frac{u_f}{A - 1}\left(A^{1-k/k_j} - 1\right) \tag{7}$$

for $A \neq 1.0$. Note that, in the case of $A = 1.0$, equation 4 becomes the same as the Pipe and Wojcik car-following model (6), which, in turn, is convertible to the Greenshields model (7) in steady-state flow. Therefore, an extension of the proposed model is

$$u = u_f\left(1 - \frac{k}{k_j}\right) \tag{8}$$

for $A = 1.0$.

Using the steady-state flow equation, $q = uk$, where q is the flow in vehicles per hour per lane, u is the speed in mph (km/h), and k is the concentration in vehicles per mile (per km) per lane, one can arrive at an equation satisfying optimum conditions, i.e., for $dq/dk = 0$, as follows:

$$A^{(k_o/k_j)-1} + \frac{k_o}{k_j} \ell n A = 1$$

for $A \neq 1.0$ and

$$k_o = \frac{k_j}{2} \tag{9}$$

for $A = 1.0$. Furthermore,

$$q_{max} = u_o k_o$$

where u_o is obtained from equation 7 or 8 by substituting k_o for k.

By drawing families of speed-concentration curves as functions of the weighting factor A and holding u_f and k_j constant with reasonable values, one can determine that for $0 < A < 1.0$ convex curves result, but, for $A > 1.0$, the curves are concave. As A goes to 1.0 from both sides, the concave and convex functions converge to a linear function and vice versa. Mathematically speaking,

$$u(k)''_k < 0 \quad \text{and} \quad u(k)'_k < 0$$

for $0 < A < 1.0$ and

$$u(k)''_k > 0 \quad \text{and} \quad u(k)'_k < 0 \tag{10}$$

for $A > 1.0$, where the prime and double prime represent the first and second derivatives with respect to k.

Based on analysis of driver performance the correlation between microscopic and macroscopic traffic behavior will now be examined with respect to the sensitivity component in equation 3.

According to Michaels (8), one can have an approximate relationship between spacing and the minimum absolute relative speed (min. $|\dot{s}|$) that can be detected for a given spacing. This relationship is shown in the upper right part of Figure 1. It is based on the mean value for the absolute threshold to angular velocity ($d\theta/dt = 6 \times 10^{-4}$ rad/sec) and on the car-following model, which is based on the rate of change of visual angle as derived by Pipe and Wojcik (6).

The minimum absolute relative speed curve (Figure 1) includes the following points:

1. Small spacing, $s_{1,4}$, and small relative speed, $\left(\frac{ds}{dt}\right)_{1,2}$;
2. Large spacing, $s_{2,3}$, and small relative speed, $\left(\frac{ds}{dt}\right)_{1,2}$;
3. Large spacing, $s_{2,3}$, and large relative speed, $\left(\frac{ds}{dt}\right)_{3,4}$; and
4. Small spacing, $s_{1,4}$, and large relative speed, $\left(\frac{ds}{dt}\right)_{3,4}$.

Let the associated responses of the following vehicle be a_1, a_2, a_3, and a_4 to correspond with these points. If deceleration responses are considered, then the following relations between the responses can be obtained:

$$a_4 > a_1 > a_3 > a_2 \tag{11}$$

where $a_2 \to 0$.

By using the steady-state flow assumption, $s_{2,3}$ and $s_{1,4}$ can be applied to the free-flow and congested-flow regimes respectively.

Note that the only relation in equation 11 that is not trivial is between a_1 and a_3. Although the driver is able to detect $(ds/dt)_{3,4}$ in large spacing, $s_{2,3}$, he still has time to either switch lanes or remove his foot from the accelerator. On the other hand, in small spacing, $s_{1,4}$, it is not likely that he will have these two choices, and, therefore, he will decelerate with higher magnitude.

In addition, the upper part of Figure 1 includes a chart of the proposed sensitivity function (equation 3) or $\alpha f(s)$ versus the weighting factor A, where, for the α computation, u_f and k_j were taken as 60 mph (95 km/h) and 220 vpm (138 vehicles/km) respectively.

By applying the results in equation 11 to the car-following equation, the relations between the sensitivity values corresponding to the four situations are similar to equation 11, i.e.,

$$[\alpha f(s)]_4 > [\alpha f(s)]_1 > [\alpha f(s)]_3 > [\alpha f(s)]_2$$

where $[\alpha f(s)]_2 \to 0$.

The two sensitivity values corresponding to the congested-flow regime (points 1, 4) will yield values of A in such a way that $A_4 > A_1$; that is, because $a_4 > a_1$, by applying the steady-state speed-concentration relationship in equations 7 and 8 and by using the mathematical properties indicated in equation 10, we see that as A increases the speed decreases (for the same value of concentration) and, obviously, that the speed is proportional to the response magnitude.

Figure 1 shows that the relation $A_4 > A_1$ can be obtained only for $A > 1.0$, since one is concerned with the congested-flow regime where it can be assumed that $k/k_j > 0.5$. For example, following the curve for $k/k_j = 0.6$ shows that the two requirements that $[\alpha f(s)]_4 > [\alpha f(s)]_1$ and $A_4 > A_1$ (for any two states on the curve) are fulfilled only for $A > 1.0$. Similarly, Figure 1 shows that $[\alpha f(s)]_2 \to 0$ only for values of A less than 1.0 but that there are no limitations on the A values for $[\alpha f(s)]_3$. Hence, A values for the free-flow regime should be $[0 < A < 1.0 \cap 0 < A < \infty]$, i.e., for $0 < A < 1.0$. The validity of these results will be shown with real-world data.

In the lower part of Figure 1, the sensitivity component multiplied by spacing can be compared with the constant α_o. Herman and Potts (4) used this constant in their reciprocal car-following model. Their results show that α_o ranges approximately from 18 to 30 in the Lincoln, Holland, and Queens Midtown Tunnels and on the General Motors test track. Thus for the congested-flow regime ($k/k_j > 0.5$), the A values are then approximately greater than 4.0. That is, following the curve for $k/k_j = 0.6$ shows that $18 \leq \alpha f(s) \times s \leq 30$ can be obtained only for $A > 4$, approximately. If one changes u_f and k_j for the α computation, the 4.0 value will be varied but will always be greater than 1.0, another confirmation that, for the congested-flow regime, the A values should be greater than 1.0. Another result from the General Motors test track is that $\alpha_o = 82.6$; this run involved high speed and violent maneuvering. Figure 1 shows that the 82.6 value results in $A < 1.0$ and $k/k_j > 0.75$. Therefore, for $A < 1.0$, high speed can be associated with free-flow regime, and for $k/k_j > 0.75$ violent maneuvering can be associated with small spacing at high speed.

Finally, both graphs in Figure 1 show greater fluctuation of the sensitivity component when $0 < A < 1.0$ than when $A > 1.0$. Inconsistency is greater in the free-flow regime than in the congested-flow regime; therefore, again, $0 < A < 1.0$ best represents the free-flow regime, and $A > 1.0$ best represents the congested-flow regime.

The reasonable range for the weighting factor is $0 < A < e^2$ as was shown in equation 6. If we assume that a better fit to the congested-flow regime is obtained at A values

greater than e^2, this range can be increased within a reasonable limit. If we assume that in very high concentration conditions the spacing is, for example, less than 40 ft (12 m) and the speed is less than 10 mph (16 km/h), it is likely that drivers in a bumper-to-bumper situation will behave differently from those in congested traffic that does not stop. Therefore, from a very high concentration value k', up to k_j, one may not consider the constraint of equation 5, i.e., for $k' \leq k \leq k_j$. Thus, the range for A that is based on the derivation used in obtaining the previous range given in equation 6 can be increased as follows:

$$0 < A \leq e^{2k_j/k'} \tag{12}$$

and the determination of k' from equation 12, at the boundary condition, is

$$k' = \frac{2k_j}{\ell nA} \tag{13}$$

where k_j and A are associated with the congested-flow model.

In addition to the above analysis of deceleration situations, acceleration responses should be considered.

When the lead vehicle accelerates, the spacing increases and the response (if any) of the following vehicle should be positive with an increase in the acceleration magnitude. However, this interpretation results in a progressive ratio between the spacing and the acceleration response, which means that those situations could occur for $A > \exp(2k_j/k')$ and for $A = \exp(2k_j/k')$ where $k > k'$ in a congested-flow regime. Therefore, when the above ranges of A are adopted, the car-following rule cannot be applied in acceleration situations, particularly in the free-flow regime.

The above analysis examines the car-following problem from the standpoint of driver performance when a steady-state stream of vehicles is assumed. However, more accurate consideration can be made for the car-following model in equation 4. It is possible to evaluate the stability of the nonlinear model in equation 4. Furthermore, the dynamic responses of the suggested nonlinear system in equation 4 result in reasonable values for spacing and relative speed, particularly for the two-regime traffic behavior (9).

ANALYTICAL EVALUATION OF MACROSCOPIC DATA

The two-regime traffic flow models based on equation 4 and corresponding macroscopic equations 7 and 8 were calculated by using the 45 speed-concentration data sets. In addition, the two flow regimes were incorporated by means of concentration breakpoint procedure.

Based on the availability of a digital computer an optimization program was used. This program relies heavily on mean deviation, which has proved to be a good indicator of the appropriateness of the data. This mean deviation is definitely preferred to correlation coefficients, particularly in the nonlinear case. The statistical procedure is based on the linearization of the input data (speed and concentration); consequently, a linear regression model of the form $y = ax$ can be applied to determine the free-flow speed, u_f, in the equation

$$u = u_f x \tag{14}$$

Table 1. Two-regime traffic-flow models.

Location	Free-Flow Regime Model				Congested-Flow Regime Model				Two-Regime Model Characteristics				
	A	u_f	k_j	MD	A	u_f	k_j	MD	q_{max}	u_o	k_o	k Break-point	Overlap [k1, k2]
1. Eisenhower at Harlem	0.009	49.9	70	3.69	10.00	58.1	195	3.24	1,868	38.6	48.4	54	
2. Holland Tunnel	1.100	49.8	120	2.84	5.50	34.8	215	1.44	1,305	21.8	59.8	80[a]	$k \rightarrow k_j$
3. Hollywood at Sunset	1.400	50.6	225	5.71	12.00	58.2	205	5.88	1,966	37.6	52.0	52	
4. Hollywood at Sunset	0.090	50.5	140	3.12	12.00	58.3	205	2.13	2,116	44.0	48.0		48, 60
5. Hollywood at Hollywood	0.090	46.4	190	4.16	12.00	61.0	230	3.47	2,117	42.3	50.0		50, 70
6. Hollywood at Hollywood	0.001	45.6	75	3.30	10.00	68.8	200	2.30	2,102	38.1	55.2	66	
7. Hollywood at Bronson	0.001	43.8	55	2.64	11.00	56.1	230	3.63	1,555	37.5	41.4	50[a]	$k \rightarrow 0$
8. Hollywood at Bronson	0.090	54.1	95	3.22	19.00	107.1	175	5.62	2,025	40.5	50.0	50[a]	$k \rightarrow 0$
9. Hollywood at Fifield	1.100	53.9	100	3.16	5.00	43.3	300	3.39	1,448	26.6	54.3	56	
10. Hollywood at Fifield	0.090	43.0	110	4.64	7.00	37.9	300	2.75	1,932	28.3	68.2	80[a]	$k \rightarrow k_j$
11. Hollywood at Franklin	0.500	48.6	145	3.82	7.50	71.2	190	3.23	2,079	26.5	78.4	80[a]	$k \rightarrow k_j$
12. Hollywood at Franklin	0.900	48.3	300	4.46	9.00	70.6	190	4.61	1,965	40.9	48.0	48	
13. Pasadena at College East	0.018	48.3	85	1.41	0.55	29.7	300	4.09	2,057	35.9	57.3		58, 62
14. Pasadena at College East	0.110	53.4	105	1.60	8.00	48.1	260	2.65	2,217	34.5	64.3		68, 72
15. Pasadena at Castelar West	0.110	49.8	110	2.76	7.00	40.3	300	1.90	1,860	28.5	67.0		68, 76
16. Pasadena at Castelar West	1.700	49.8	220	1.44	7.00	48.7	260	1.12	2,285	28.6	80.0		68, 80
17. Pasadena at Castelar East	0.130	48.8	85	2.21	8.00	59.3	220	1.22	1,650	32.1	51.4		40, 60
18. Pasadena at Castelar East	2.000	49.3	215	3.00	7.00	46.7	300	2.84	2,009	30.4	66.0	66	
19. Pasadena at Bishop West	0.400	39.4	300	1.47	8.50	45.5	300	1.59	1,816	34.9	52.0	52	
20. Pasadena at Bishop West	0.800	55.8	185	1.59	8.00	55.9	235	2.58	1,912	30.8	62.0	42	
21. Penn-Lincoln at Laurel	0.380	44.1	300	4.92	9.00	62.5	205	4.47	2,487	37.7	66.0	66	
22. Penn-Lincoln at Laurel	0.080	48.3	105	6.07	7.50	55.3	225	2.61	2,101	32.1	65.5		62, 70
23. Penn-Lincoln at Braddock	0.120	52.5	80	5.66	5.00	31.8	300	4.71	1,640	33.7	48.6		66, 74
24. Penn-Lincoln at Braddock	0.080	54.8	80	4.10	8.00	54.0	245	3.50	1,822	36.4	49.9		58, 66
25. Penn-Lincoln at tunnel	0.070	39.0	105	2.69	15.00	46.4	300	3.89	1,540	32.1	48.0	48	
26. Penn-Lincoln at tunnel	0.400	39.6	200	1.75	7.50	51.4	220	2.59	1,740	32.2	54.0	38	
27. Virginia in lane 1	1.500	62.6	170	2.84	15.50	64.9	205	2.98	1,798	46.1	39.0	39	
28. Virginia in lane 2	0.800	72.5	175	3.01	19.50	98.1	185	4.88	2,416	56.1	43.0	43	
29. Munich-Salzburg in lane 1[b]	0.090	61.5	55	5.41	10.00	85.1	130	2.76	1,383	40.5	34.1	46	
30. Munich-Salzburg in lane 2[b]	0.110	70.6	55	0.92	5.50	74.7	115	2.01	1,060	49.6	33.6	52	
31. Munich-Salzburg in lane 1[c]	1.100	64.0	85	4.95	9.50	70.6	160	3.43	1,396	29.9	46.5	38	
32. Munich-Salzburg in lane 2[c]	0.800	71.7	80	5.22	5.50	71.7	155	7.02	1,680	48.1	34.9	50	

[a]Concentration breakpoint tends to approach either 0 or k_j values as specified by the overlap interval. [b]Northbound. [c]Southbound.

Figure 1. Sensitivity of the weighting factor A.

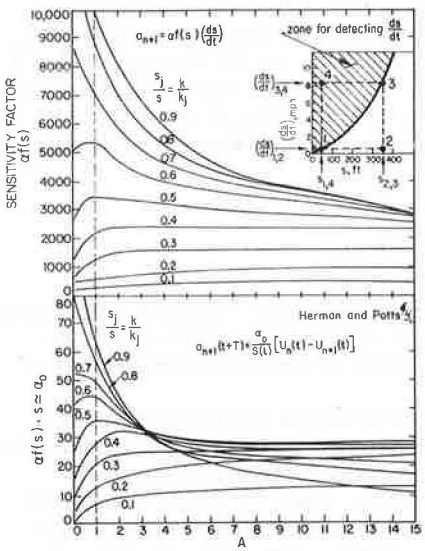

Figure 2. Typical minimization of the mean deviation in two regimes.

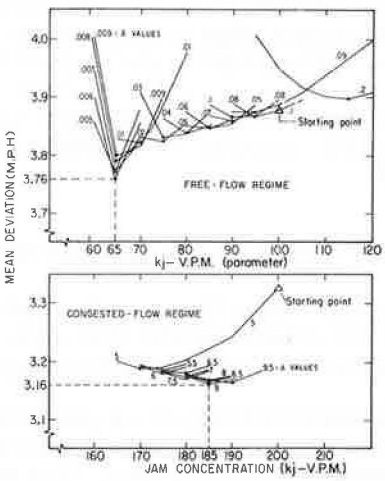

where $x = [1/(A - 1)] (A^{1-k/k_j} - 1)$ for $A \neq 1.0$ and $1 - (k/k_j)$ for $A = 1.0$.

The mean deviation is then determined from the sum of squares of the deviations of the data points from the considered model. Minimization of the mean deviation within certain concentration intervals is satisfactory, and no other criteria, such as those used in the single- and two-regime models based on the generalized car-following model (equation 1), are necessary. However, an upper limit is imposed on k_j such that $k_j \leq 300$ vpm (188 vehicles/km) in order to restrict the time required for running the program.

From inspection of the plot of the data sets, an interval along the concentration axis is determined where it is likely that discontinuity or unstable flow will result. By using a concentration-incremented technique (i.e., within the concentration interval, the concentration range is increased by increments), the program covers this concentration interval separately for each regime. The search for the free-flow regime model considers data points from k = 0 to k = k1 (lower bound) to k = k2 (upper bound) by means of the concentration-incremented technique.

For the congested-flow regime, a similar search is performed by going backward from $k = k_j$ to k = k2 (in the first step) down to k = k1. The optimization policy for finding a breakpoint within the concentration interval is

$$\min_i [(\min MD_i)_{FFR} + (\min MD_i)_{CFR}] \tag{15}$$

for $i = 1, 2, \ldots, (k2 - k1)/\Delta k$ where

FFR, CFR = free-flow regime and the congested-flow regime respectively,
MD = mean deviation,
i = each upper or lower bound, and
Δk = concentration-increment within the concentration interval (k1, k2).

After starting with initial values of A and k_j, in each step the program holds A constant until the k_j associated with minimum MD is found. Then A is changed, by a given increment, until the overall minimum MD is found for a particular A, k_j (after several iterations).

Figure 2 shows part of the minimization procedure, for the two regimes, by using the Eisenhower Expressway data set. In that case, k1 = 45 vpm (28 vehicles/km), k2 = 60 vpm (25 vehicles/km), Δk = 3 vpm (1 vehicle/km), $i_{FFR} = 1$ (data points considered up to k = 45 vpm), and $i_{CFR} = 5$ (data points considered from k = 60 vpm to k_j). It can be seen that the minimum mean deviation is obtained in fewer steps and more smoothly in the congested-flow regime than in the free-flow regime. This figure illustrates a higher consistency in the congested-flow regime than in the free-flow regime.

Results

As mentioned earlier, two groups of data sets were considered. By using a procedure similar to the one used previously (2), the results of the first group of data sets form a basis to estimate the results for the second group. Of the first group of data sets, 28 of 32 are from the center or left freeway lanes. Therefore, the conclusions drawn herein are particularly applicable to freeway facilities.

By running the data sets through the optimization procedure, three cases were identified:

1. Where an absolute breakpoint exists;
2. Where overlap exists, i.e., an unstable zone is created; and
3. Where the data points tend toward single-regime rather than two-regime phenomenon.

The criteria for determining each of the possible cases are as follows.

1. From inspection, a concentration interval is determined. If there is either a breakpoint or an overlap interval, it results within this concentration interval.
2. If an absolute minimum ΣMD, based on equation 15, within the considered interval is found, the program assumes that a breakpoint exists.
3. If either one of the neighboring concentration values to a breakpoint does not have the second minimum ΣMD, an overlap is determined between those concentration values associated with the first and second minimum ΣMD.
4. If the absolute minimum ΣMD belongs to either one of the concentration interval boundaries, then a trend toward a single regime exists.

The results of this investigation of two-regime models using the first 32 data sets are given in Table 1. It should be noted that k_j of the free-flow model and u_f of the congested-flow model are only parameters, but u_f of FFR and k_j of CFR are important traffic characteristics of the two-regime model.

Figure 3 shows different speed-concentration curves. These curves illustrate the above three cases. Also, on the upper right side of each curve the fluctuations of the mean deviations for the two regimes and for both regimes within the considered concentration interval (k1, k2) are shown.

In Figure 3 there are eight numbered curves. To associate each curve with the freeway location, the numbers on the curves are those given in Table 1. In curves 1, 27, and 28 there is a breakpoint, case 1; in curves 4, 24, and 17 there is an overlap that can be interpreted as an unstable zone, case 2; and in curves 8 and 11 a trend toward single regime exists, case 3. Among the eight curves in Figure 3, curve 8 shows a trend toward a single regime, with the use of only the congested-flow model, whereas curve 11 shows the same trend, but with the use of only the free-flow model. The most typical results among the 32 data sets are like curves 1 or 28 (breakpoint exists) and curve 4 (unstable zone exists). In addition, it is interesting to note that curves 27 and 28 are concerned with lane 1 and lane 2 of the same road facility.

Figure 4 shows the 32 data sets in an A, k_j matrix format. These results confirm the following hypotheses:

1. As 25 out of 32 data sets suggest, the free-flow regime models had A values of less than 1.0; and
2. As 31 out of 32 data sets suggest, in the congested-flow regime models the A values were greater than 1.0.

However, it appears that A may have values greater than 1.0 in the free-flow regime when road facilities other than nonshoulder freeway lanes are considered, i.e., tunnel lanes and shoulder lanes. The results for such lanes are indicated in the A, k_j matrix in Figure 4.

Additional 13 Data Sets

The results of the first group of 32 data sets formed the basis to estimate the parameter values for the second group of 13 data sets. That is, in the A, k_j matrix the estimations were that the free-flow regime models associated with freeway lanes will be centered within the region of $0 < A \leq 0.2$, $50 \leq k_j \leq 120$, where the on-ramp and CD road will be scattered above the line where A = 1.0. In the congested-flow regime models the region of $5 \leq A \leq 10$, $150 < k_j < 300$ was estimated for all road facilities. The results of the Santa Monica data sets are given in Table 2 and shown in Figure 5. Generally, these results follow the estimations. However, the congested-flow regime models have somewhat lower A values for the second group of data sets (Figure 5).

From the overall 45 congested-flow regime models, the range of k' that belongs to the constraint in equation 12 was determined. This range was 160 to 250 vpm (100 to 156 vehicles/km), which agrees with the analysis of driver performance mentioned above.

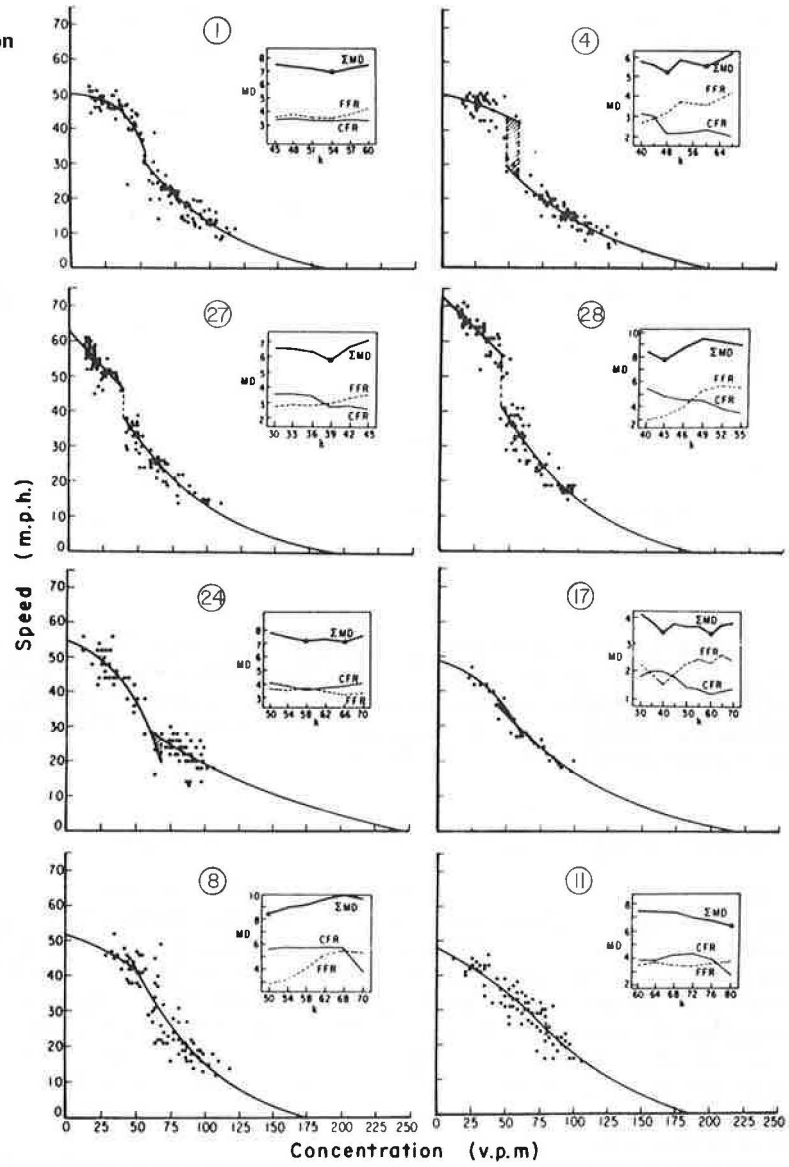

Figure 3. Typical and extreme speed-concentration output curves.

Table 2. Two-regime traffic-flow models (13 data sets).

Station Number	Free-Flow Regime Model				Congested-Flow Regime Model				Two-Regime Model Characteristics				
	A	u_f	k_j	MD	A	u_f	k_j	MD	q_{max}	u_o	k_o	k Break-point	Overlap [k1, k2]
SM-12	0.060	58.2	75	3.93	5.50	52.0	215	0.62	1,892	39.7	47.7	50	
SM-13	0.050	60.3	80	3.70	4.00	62.6	175	1.09	2,150	41.8	51.4	55	
SM-14	0.009	54.6	70	3.32	18.00	76.9	215	2.25	2,042	42.2	48.4		50, 60
SM-15	0.060	58.4	80	2.61	5.00	64.0	175	0.60	2,027	39.9	50.8	60	
SM-16	0.030	60.4	65	3.30	21.00	77.4	200	0.99	1,861	43.6	42.7	50	
SM-17	0.090	62.1	85	2.65	22.50	69.4	230	1.00	2,155	40.9	52.7		55, 65
SM-18	0.090	57.4	75	2.77	6.00	64.0	175	0.88	1,758	37.8	46.5		40, 60
SM-19	0.080	61.7	80	2.90	5.00	59.8	185	1.35	2,052	41.0	50.0	60	
SM-20	0.009	52.9	70	3.33	7.00	74.9	170	1.80	1,978	40.9	48.4		40, 55
SM-21	0.200	61.2	90	2.57	4.50	55.1	195	0.73	1,963	37.2	52.8		40, 60
SM-22	0.400	62.1	90	3.38	4.00	72.5	150	1.06	1,892	34.8	49.7		45, 60
LaBrea (on-ramp)	4.200	47.4	250	2.33	0.50	34.1	200	1.06	2,023	20.1	100.4	80[a]	$k \rightarrow k_j$
Venice (CD-on)	7.000	49.3	165	4.40	9.50	33.5	290	0.88	1,208	20.1	60.2	80[a]	$k \rightarrow k_j$

[a]Concentration breakpoint tends to approach either 0 or k_j values as specified by the overlap interval.

Figure 4. The two-regime models in A, k_j matrix (32 data sets).

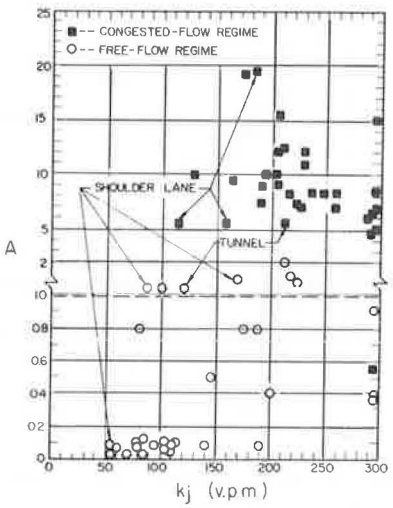

Figure 5. The two-regime models in A, k_j matrix (13 data sets).

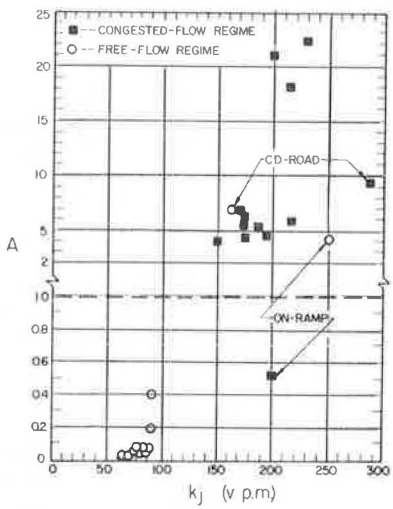

As mentioned earlier, the two flow regimes were incorporated by means of breakpoint evaluation procedures. The results of either the overlap intervals or breakpoints within a specified concentration range are given in Tables 1 and 2. Of the 45 data sets, 22 have a breakpoint and 16 have an overlap interval. The remaining seven data sets have a tendency toward single regime.

Comparison With the Generalized Car-Following Model

The generalized car-following model (equation 1) and the corresponding macroscopic equations were evaluated earlier (2) by using the same 45 data sets analyzed here. However, instead of a breakpoint procedure, in the free-flow regime and in the congested-flow regime only data points with concentration values less than 60 vpm (38 vehicles/km) and more than 50 vpm (31 vehicles/km) respectively were included in analysis of equation 1. Therefore, to form a comparison basis, the proposed model was run along the same concentration ranges. In addition, because no criteria were imposed on the proposed model (excluding the upper limit on k_j), the comparison between the two approaches is based on consideration of only the minimum mean deviation models (2).

A comprehensive comparison of the proposed model and equation 1 is reported elsewhere (9). A summary of this comparison for the free-flow regime models follows:

1. Of the 45 data sets, 36 have lower MD when the proposed model is used than when equation 1 is used, and five data sets have the same MD; and
2. With regard to the preselected criteria (2), 43 and 45 of the data sets meet the q_m and u_f criteria when the proposed model is used, but only 25 and 39 of the data sets meet the q_m and u_f criteria when equation 1 is used.

The summary of the comparison for the congested-flow regime models is as follows:

1. Twenty-five data sets have lower MD when the proposed model is used than when equation 1 is used, and five data sets have the same MD; and
2. Twenty-six of the data sets meet the preselected k_j criterion (2) when the proposed model is used, but only nine of the data sets meet the k_j criterion when equation 1 is used.

CONCLUDING REMARKS

This paper has developed a car-following model based on an analysis of driver performance from which relatively simplified macroscopic models can be derived. The comparison made in this paper is between the suggested model (equation 4) and the generalized car-following model (equation 1), which is found to be representative of previous microscopic and macroscopic theories.

Based on a criterion from previous approaches, a new sensitivity component of the stimulus-response relationship (equation 2) was suggested. Through analysis of driver performance, it becomes apparent that the suggested model is capable of describing both microscopic and macroscopic traffic behavior. The model is particularly useful when the two-regime phenomenon is considered for a single-lane traffic stream in a multilane environment. By using the 45 data sets, a comparison between the new and the generalized car-following models was performed, based on results obtained in the previous work (2). With respect to the two-regime phenomenon one can conclude that the proposed model is superior to the generalized car-following model, particularly in simplicity and clarity. The advantages of the proposed model can be summarized as follows:

1. Better actual data fit;
2. No need for criteria for u_f, k_j, and q_m (excluding an upper limit on k_j);
3. u_f and k_j (boundary characteristics) always defined;
4. Fewer arbitrary parameters in the car-following equation; and
5. Fewer basic macroscopic forms.

Besides the advantage of having a simpler nonlinear model, a stability analysis can be performed on the microscopic proposed model (9). Because drivers do not completely follow any deterministic behavior, the results of the stability analysis are valid at best only in some average sense. However, this analysis provides a method for understanding traffic behavior and the potential for modifying such behavior.

This paper has examined discontinuity, one of the most important characteristics of traffic behavior, under maximum flow conditions. Observations of the data sets suggest that discontinuity can result in an unstable traffic flow zone. It is realized, however, that the considered concentration breakpoint procedure is only one method for evaluating two-regime models. With regard to two-regime traffic behavior, perhaps a more reliable method is to consider the data points with respect to time (9). Such a method sheds light on traffic behavior, particularly under peak conditions. Because additional quantitative information about speed-flow-concentration relationships is required, particularly near the capacity level, future research should examine the traffic-flow behavior under these flow conditions. It is felt, however, that for the interpretation of the discontinuity phenomenon human factors as well as traffic-flow characteristics should be considered (10).

ACKNOWLEDGMENTS

The author gratefully acknowledges Adolf D. May for the support and guidance given during the study reported in this paper. An expression of appreciation is also due to the Division of Highways at Los Angeles, District 7, for supplying the Santa Monica Freeway data sets.

REFERENCES

1. L. C. Edie. Car-Following and Steady-State Theory for Noncongested Traffic. Operations Research, Vol. 9, No. 1, 1961, pp. 66-76.
2. A. Ceder and A. D. May. Further Evaluation of Single- and Two-Regime Traffic-Flow Models. Published in this Record.
3. D. C. Gazis, R. Herman, and R. W. Rothery. Nonlinear Follow-the-Leader Models of Traffic Flow. Operations Research, Vol. 9, No. 4, 1960, pp. 545-567.

4. R. Herman, and R. B. Potts. Single-Lane Traffic Theory and Experiment. Proc., Symposium on the Theory of Traffic Flow, Elsevier, Amsterdam, 1961, pp. 120-146.
5. R. Rothery, R. Silver, R. Herman, and C. Torner. Analysis of Experiments on Single-Lane Bus Flow. Operations Research, Vol. 12, No. 6, 1964, pp. 913-933.
6. L. A. Pipe and C. K. Wojcik. A Contribution to Theory of Traffic Flow. Proc., Symposium on Analysis and Control of Traffic Flow, SAE, 1968, pp. 53-60.
7. B. D. Greenshields. A Study in Highway Capacity. HRB Proc., Vol. 14, 1934, pp. 448-477.
8. R. M. Michaels. Perceptual Factors in Car-Following. Proc., Second International Symposium on the Theory of Road Traffic Flow, London, 1963, pp. 44-59.
9. A. Ceder. Investigation of Two-Regime Traffic-Flow Models at the Micro- and Macroscopic Levels. Univ. of California, Berkeley, PhD dissertation, Jan. 1975.
10. A. Ceder. Drivers' Attention in Simulated Traffic-Flow Conditions. Institute of Transportation and Traffic Engineering, Univ. of California, Berkeley, 1974.

A STUDY OF TRAFFIC PERFORMANCE MODELS UNDER AN INCIDENT CONDITION

We-Min Chow, IBM Thomas J. Watson Research Center, Yorktown Heights, New York

When an incident occurs on a roadway, traffic performance is usually evaluated by means of either the shock wave analysis or the queuing analysis. In this paper, a comparison of these two approaches is given under the assumption that there exists a unique flow-density relationship. It is shown that the two methods of evaluating the performance give the same result if the traffic density is not time dependent.

•TRAFFIC PERFORMANCE under various conditions has been studied for many years. This is an important area not only because of theoretical interests, but also for a better understanding of traffic behavior whereby a good system design and control strategies can be achieved.

In the case of a roadway incident (or accident), two well-known approaches are available to evaluate traffic performance, namely, the shock wave analysis (1, 4) and the queuing analysis. Then a question may arise: How would the results derived from one method be different from those derived from the other? The purpose of this paper is to answer this question by comparing the two approaches from two aspects:

1. Discharge time—the time required to discharge the stored vehicles after the incident is removed, and
2. Total delay—the increment of the total travel time (TTT) due to the incident, i.e., the difference between TTT under the incident case and TTT under the normal case (no incident).

In this paper, it is assumed that a unique flow-density relationship (a q-k diagram) exists. For a given blockage time (the duration that the traffic is blocked by the incident), the discharge time and the total delay will be estimated.

RELATIONSHIP BETWEEN BLOCKAGE TIME AND DISCHARGE TIME

Whenever a freeway incident occurs, traffic conditions are changed because of a reduction in capacity. If the reduced capacity is less than the flow, then the region upstream of the incident location becomes congested, while the traffic situation downstream is improved because of the lower traffic flow. The traffic situations at different stages are given in Table 1. [Note that the normal flow $q(t)$ may be a function of time t. Therefore, the traffic flows before and after an incident may be different.] Figure 1a shows a q-k diagram, and Figure 1b shows a shock wave diagram, which is valid only for constant flow condition. A more realistic case can be shown by letting the flow be a function of time t. Therefore, a generalized shock wave diagram is shown in Figure 1c, where

$L(t)$ = front edge of the shock wave at time t,
$s_1(t)$ = shock wave speed at time t,

Publication of this paper sponsored by Committee on Traffic Flow Theory and Characteristics.

Figure 1. Traffic conditions under incident case: (a) q-k, (b) shock wave with incident occurring at 1 = 0 and constant flow, and (c) shock wave with incident occurring at t = 0 and time-dependent flow.

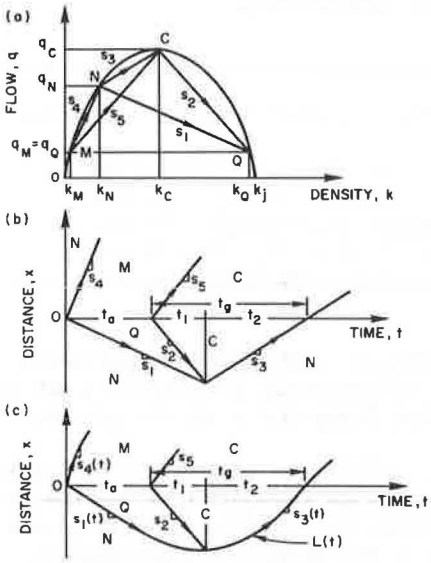

Figure 2. (a) Queuing diagram and (b) shock wave diagram with an incident occurring at t = 0.

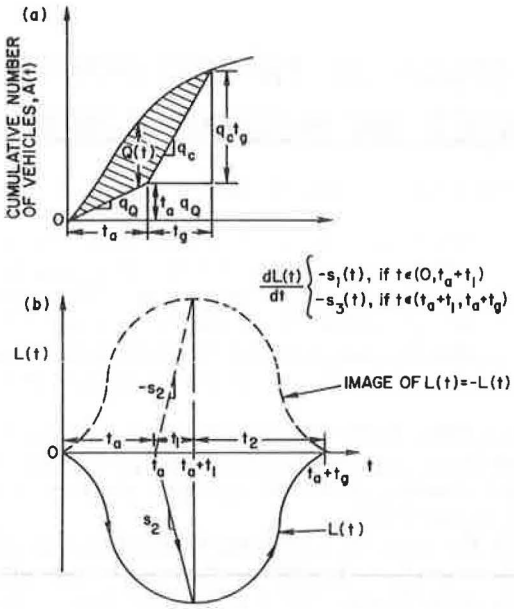

Table 1. Traffic conditions when incident occurs (3).

Events	Upstream	Downstream
Before incident, N	Normal flow, q(t)	Normal flow, q(t)
Incident occurs, Q	Queueing flow, q_Q	Metered flow, q_M
Incident removed, C	Capacity flow, q_c	Capacity flow, q_c
Traffic recovered, N	Normal flow, q(t)	Normal flow, q(t)

q_c = capacity flow,
k_c = capacity density,
q_Q = queuing flow,
k_Q = queuing density,
q(t) = normal flow at time t, and
k(t) = normal density at time t.

Clearly, according to the above definitions, for $L(t) < 0$,

$$\frac{dL(t)}{dt} = \begin{cases} s_1(t) = [q(t) - q_Q]/[k(t) - k_Q], & \text{if } t \in [0, t_a + t_1] \\ s_3(t) = [q_c - q(t)]/[k_c - k(t)], & \text{if } t \in [t_a + t_1, t_a + t_g] \end{cases}$$

where

t_a = blockage time and
t_g = discharge time = $t_1 + t_2$.

Note that the shock wave speeds $s_1(t)$ and $s_3(t)$ are time dependent if the traffic flow q(t) is; s_2 is independent of time if normal capacity and reduced capacity are constant.

This statement is certainly true if the unique relationship between flow q and density k is assumed.

Now, according to Figure 2b, and based on the image of the shock wave diagram with $-L(t) > 0$ (represented by the dashed line), it follows that

$$-L(t_a + t_1) = -\int_0^{t_a + t_1} s_1(t)\, dt \tag{1}$$

$$= -s_2 t_1 \tag{2}$$

$$= \int_{t_a + t_1}^{t_a + t_g} s_3(t)\, dt \tag{3}$$

By using equations 1 and 2,

$$\int_0^{t_a + t_1} \frac{q_Q - q(t)}{k_Q - k(t)}\, dt = \frac{q_c t_1}{k_c - k_Q} - \frac{q_Q t_1}{k_c - k_Q} \tag{4}$$

And equations 1 and 3 imply that

$$\int_0^{t_a + t_g} -s_1(t)\, dt = \int_{t_a + t_1}^{t_a + t_g} [s_3(t) - s_1(t)]\, dt \tag{5}$$

Equations 4 and 5 will give the solution for t_g, if t_a is known. Now, if there is little change in k(t) with respect to time, i.e., $k(t) \approx k$ (some constant), then equation 4 implies

$$\frac{q_Q \times (t_a + t_1)}{k_Q - k} - \frac{A(t_a + t_1)}{k_Q - k} \approx \frac{q_c \times t_1}{k_c - k_Q} - \frac{q_Q t_1}{k_c - k_Q}$$

and equation 5 implies

$$A(t_a + t_g) \approx \frac{q_Q(t_a + t_1)(k_c - k)}{k_Q - k} - \frac{A(t_a + t_1)(k_c - k_Q)}{k_Q - k} + q_c t_2$$

where

$$A(t) = \int_0^t q(r)\, dr \text{ and}$$

$$A(0) = 0.$$

By using these two equations and eliminating the term $A(t_a + t_1)$, it follows that

$$A(t_a + t_s) \approx q_c\, t_s + q_Q\, t_a$$

or

$$\int_0^{t_a} [q(t) - q_Q]\, dt \approx \int_{t_a}^{t_a + t_s} [q_c - q(t)]\, dt \tag{6}$$

Figure 2a shows that the queue length at time t is

$$Q(t) = \begin{cases} \int_0^t [q(r) - q_Q]\, dr, & t \in [0, t_a] \\ Q(t_a) - \int_{t_a}^t [q_c - q(r)]\, dr, & t \in [t_a, t_a + t_s] \end{cases} \tag{7}$$

Because $Q(t_a + t_s) = 0$, equation 7 implies that

$$\int_0^{t_a} [q(r) - q_Q]\, dr = \int_{t_a}^{t_a + t_s} [q_c - q(r)]\, dr$$

The same relationship between t_a and t_s is obtained as in equation 6.

RELATIONSHIP BETWEEN BLOCKAGE TIME AND DELAY

The formula used to calculate the total travel time is

TTT = density × length × time

Therefore, when the shock wave diagram is drawn in a time-distance space (Figure 2b), the formula can be rewritten as

TTT = density × area under the image of L(t)

[The image of L(t) is shown by a dashed line in Figure 2b, which is equal to -L(t).]

Because the delay is the difference between TTT under the incident case and TTT under the normal case, it is legitimate to write the delay in the form

$$D = \int_0^{t_a + t_s} [-L(t) \times \Delta K(t)]\, dt \tag{8}$$

where $\Delta k(t) = k_Q - k(t)$ in the congested region Q and $k_c - k(t)$ in the discharge region C (Figure 2b). From Figure 2b,

$$-L(t) = \begin{cases} \int_0^t [-s_1(r)]\, dr, & t \in [0, t_a + t_1] \\ -s_2 t_1 - \int_{t_a + t_1}^t s_3(r)\, dr, & t \in [t_a + t_1, t_a + t_s] \end{cases}$$

$$D = \int_0^{t_a + t_1} [k_Q - k(t)] \int_0^t [-s_1(r)]\, dr\, dt + \tfrac{1}{2}(-s_2 t_1)(k_c - k_Q) t_1$$

$$- \int_{t_a + t_1}^{t_a + t_s} [k_c - k(t)] \times \left[s_2 t_1 + \int_{t_a + t_1}^t s_3(r)\, dr \right] dt \qquad (9)$$

Again, if $k(t) \approx k$, then it becomes

$$D = \int_0^{t_a + t_s} \int_0^t [q(r) - q_Q]\, dr\, dt - \tfrac{1}{2}(q_c - q_Q) t_1^2$$

$$- t_1 t_2 \frac{q_c - q_Q}{k_c - k_Q}(k_c - k) - \int_{t_a + t_1}^{t_a + t_s} \int_{t_a + t_1}^t [q_c - q(r)]\, dr\, dt$$

$$= \int_0^{t_a + t_s} A(t)\, dt - \tfrac{1}{2} q_Q t_a^2 - \tfrac{1}{2} q_c t_s^2 - q_Q t_a t_s \qquad (10)$$

According to Figure 2a, if the delay is computed by using the simple queuing diagram, then

$$D = \int_0^{t_a + t_s} Q(t)\, dt$$

$$= \int_0^{t_a + t_s} [A(t) - U(t)]\, dt$$

where

$$U(t) = \begin{cases} q_Q \times t, & t \in [0, t_a] \\ q_Q t_a + (t - t_a) q_c, & t \in [t_a, t_a + t_g] \end{cases}$$

$$D = \int_0^{t_a + t_g} A(t)\, dt - \tfrac{1}{2} q_Q t_a^2 - \tfrac{1}{2} q_c t_g^2 - q_Q t_a t_g$$

which is the same relation obtained by using shock wave analysis.

DISCUSSION AND SUMMARY

Two methods have been proposed to compute both the duration of time to discharge stored vehicles and the delay to passing motorists. These two methods (shock wave analysis and queuing analysis) lead to the same results if the density is not dependent on time. In particular, this is the case if the flow rate q(t) varies slowly during the time period $(t_a + t_g)$, and the unique relationship between q(t) and k(t) can be assumed. This result can easily be generalized by letting both flow and density be functions of distance. Furthermore, this result is valid even if q(t) is a random process. In this case, the equivalence of these two methods holds for every realization of q(t), if k(t) is independent of time.

When k(t) is time dependent, these two methods may yield different results. It seems that shock wave analysis has more physical meaning. On the other hand, if queuing analysis is used, computational effort is saved and, in some cases, the delay can be evaluated even when the traffic is stochastic; e.g., if traffic counts form a Poisson process and the duration of the blockage time is exponentially distributed, then the delay can be estimated by using the model developed by Loulou (2). The time-dependent case has not been done in the paper. However, if the explicit form of k(t) is known, numerical comparison can easily be made by using the equations derived in this paper.

ACKNOWLEDGMENT

The author would like to thank A. D. May for his interest and advice. This research was partially supported by the National Science Foundation and the U.S. Department of Transportation.

REFERENCES

1. M. J. Lighthill and G. B. Whitham. On Kinematic Waves, II: A Theory of Traffic Flow on Long Crowded Roads. Proc., Royal Society London, A 229, 1955, pp. 317-345.
2. R. J. Loulou. A Stochastic Model for Highway Accident. Operations Research Center, Univ. of California, Berkeley, ORC 69-32, Sept. 1969.
3. C. J. Messer, C. L. Dudek, and J. D. Friebele. Method for Predicting Travel Time and Other Operational Measures in Real-Time During Freeway Incident Conditions. Highway Research Record 461, 1973, pp. 1-16.
4. M. Wohl and B. V. Martin. Traffic System Analysis for Engineers and Planners. McGraw-Hill, 1967.

MEASURING LEVELS OF SERVICE OF A CITY STREET BY USING ENERGY-MOMENTUM TECHNIQUES

Tom K. Ryden, Department of Civil Engineering, Washington University

A traditional speed and delay study can yield extremely useful information for the evaluation of traffic operations and flow. Unfortunately the results are deterministic, and traffic flow is highly stochastic. Energy-momentum theory recognizes this; however, its applications have primarily been for freeways and expressways. This study applies energy-momentum theory to a city street without access control. Little correlation was found between derived acceleration noise and average speed relationships. Traffic flow inhibited by delay is stochastic, yet, because the number of delays increases, the aperiodic nature of delay frequency does not lend itself to the energy-momentum model. Each delay type must be handled separately.

•DELAY encountered on downtown collector and arterial streets during peak travel times can be frustrating. A countless number of papers have addressed this subject. The primary purpose of this report was to test energy-momentum concepts for monitoring levels of service (1) on a collector street that has a number of traffic flow delay components.

The study site was the Euclid Avenue corridor between Maryland Plaza Drive and Clayton Road in St. Louis. The corridor has traffic problems directly related to the intensity of commercial and hospital activity in the area, a common situation. On a more microscopic level, the study segment is 3,600 ft (1100 m) long, has a curb-to-curb width of 36 ft (11 m) including two lanes with parking, and has an estimated capacity of 600 vehicles per hour per direction at level of service C. Components that contribute to vehicle delay along Euclid Avenue include curbside automobile parking turnover, commercial vehicle loading and unloading, pedestrian interference, bus transit operations, right-of-way restrictions, traffic volume, and type of intersection control. All major intersecting streets except three are controlled by a stop sign. Only Forest Park Parkway, West Pine, and Lindell Boulevard (Figure 1) are signalized, and only the latter two are programmed for synchronization.

Currently two conflicting problems exist. First, the support of the commercial strip by the surrounding community practically demands that Euclid Avenue from Lindell to Forest Park Parkway have further restraints on through traffic to enhance pedestrian and business activity. Second, an excess of through traffic uses Euclid Avenue as a means to travel to and from the Washington University medical complex en route to or from Kingshighway Boulevard (two-way ADT of 46,750) or Forest Park Parkway (two-way ADT of 22,100) (2). The hospital complex is a regional center with more than 8,000 full-time employees (3). If the area grows and develops as it is expected to, the demand for feeder routes like Euclid to and from expressways and principal arterials will increase. As a first step toward the solution of such problems, specific delay components in the traffic flow need to be measured and analyzed.

STUDY PROCEDURE

It seemed appropriate to obtain a continuous record of speeds and speed changes and relate specific changes to particular delays. A standard traffic analyzer was used to

Publication of this paper sponsored by Committee on Traffic Flow Theory and Characteristics.

record speed profiles, vehicle running time, and total operating time of a floating car traveling in the left lane. Enough runs were made to ensure a 95 percent confidence interval of achieving representative results (4). Data were taken during three predetermined peak travel times: 7 to 8 a.m., noon to 1 p.m., and 4:30 to 5:30 p.m. The number of delay complications was greatest during the last period. Speed data were also taken at 2 a.m. when no one else was traveling and the traffic signals were operating on flash. These data were used to determine the mean free speed. Detailed commentary on the causes for delay during each run was tape-recorded. Data were analyzed for the 2 a.m. and p.m. peak travel.

SPEED AND DELAY RECORDS AND SUMMARY

Table 1 gives a typical record of speed and delay for a p.m. peak run on Euclid Avenue. [ΔV stands for the number of 2-mph (3.2-km/h) speed changes used for illustration and comparison.] Data were recorded for both northbound and southbound directions. Statistics (in sec) of the runs were as follows:

Statistic	Northbound	Southbound
Total trip time	303	295
Total stop time	60	56
Total time faster than 10 mph (16 km/h)	150	135
Total time faster than 30 mph (48 km/h)	0	0
Running time	243	239

Table 2 gives delay by type for each direction (5). In both cases, intersection delay due to traffic signals predominated. However, delay due to stop signs was large compared to their frequency of occurrence (twice).

ACCELERATION NOISE CALCULATIONS

The acceleration noise parameter σ, defined as the standard deviation of changes in vehicular speed, was calculated by using Jones and Potts approximation (1) with the conversion factor of 1.465 for converting miles per hour to feet per second:

$$\sigma = \left[\frac{(1.465)^2 (\Delta V)^2}{T} \sum_{i=0}^{T} 1/\Delta T_i \right]^{1/2}$$

where

ΔV = 2-mph (3.2-km/h) speed change,
ΔT_i = running time of vehicle for each speed change, and
T = total running time of vehicle.

This equation was calculated for both northbound and southbound vehicles over defined road segments as shown in Figure 1.

Three components of acceleration noise were defined. Case one took into account the natural roadway noise, neglecting signal control, and vehicle interaction. This component was studied in two sections governed by the stop-controlled intersection at Laclede Avenue. Mean free speeds were determined at this stage. Case two in Figure

Figure 1. Acceleration noise versus distance.

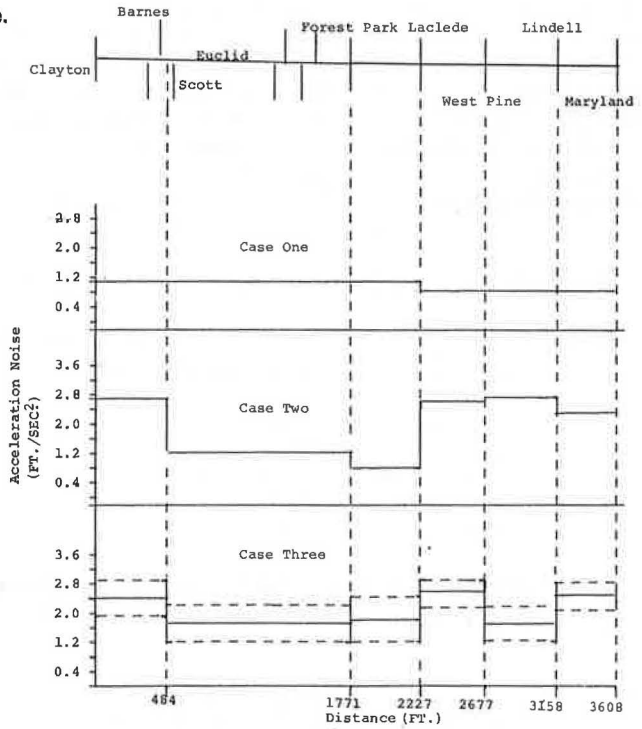

Table 1. Typical speed and delay record.

Start Intersection	Stop Intersection	Delay	Duration (sec)	Total ΔV	Estimated Running Time (sec)
Mayland Plaza	Lindell	Pedestrians	7	25	39
		Signal	36		
Lindell	West Pine	None, made light		10	18
West Pine	Laclede	Midblock	4		
		Crossing	10	29	54
Laclede	Forest Park	None, made light		9	24
Forest Park	Scott	Midblock	4		
		Unloading	15	50	78
		Crossing	15		
Scott	Clayton Road	None		22	30
Clayton Road	Barnes Plaza	Pedestrians	6	24	33
Barnes	Forest Park	Crossing	12	27	63
Forest Park	Laclede	Crossing	12	23	27
Laclede	West Pine	Midblock	4	26	36
		Signal	12		
		Crossing	15		
West Pine	Lindell	None, made light		11	18
Lindell	Maryland Plaza	Crossing	39	26	62
		Pedestrian	20		
		Unloading	15		

Table 2. Percentage of intersection and midblock delay.

Delay	Northound	Southbound
Intersection		
Signal	54	65
Stop sign	21	5
Pedestrian	11	6
Turning movement	3	5
Total	89	85
Midblock		
Loading-unloading	5	8
Block	3	4
Parking	3	3
Total	11	15

1 was also summarized from the mean free speed runs, and it took into consideration the combined effects of vehicle operations due to stop sign and signal control. Case three showed the effects of all delay components. Because the case two data were within the range of case three data (a majority of delay caused by signal control), case two and case three data were grouped so as to make 95 percent confidence intervals about the average (horizontal dashed lines in Figure 1) meaningful. Table 3 gives a summary of acceleration noise data. Table 4 gives additional information on case three data and the symbols used in Figures 3, 4, 5, and 6.

SUMMARY OF ENERGY-MOMENTUM CONCEPTS USED

In the energy-momentum approach for measuring roadway levels of service (1), the total energy of the stream T equals the kinetic energy E plus the internal energy I where

I = σ, the acceleration noise,
E = $\alpha k u^2$,
k = vehicle concentration in vehicles/mile (km),
u = speed of vehicles, and
α = an empirical constant.

The energy can be evaluated for any length of road. Boundary conditions help define the relationship between acceleration noise and E. In general the equation for E is

$$E = \alpha k u_f^2 \left[1 - 2\left(\frac{k}{k_j}\right)^{(N+1)/2} + \left(\frac{k}{k_j}\right)^{N+1} \right]$$

for $N > -1$.

As I approaches 0, E approaches a maximum, which equals T. Theoretically T then equals $\alpha k_m'(u_m')^2$. For the case of N = 1 in the above equation, E can be reduced to

$$E = {}^{4}/_{27}\, \alpha k_j u^2$$

In the other extreme, as E approaches 0, I approaches a maximum σ_{max}. Because energy is neither lost nor gained but merely transferred from one form to another,

$$\sigma_{max} = T = {}^{4}/_{27}\, \alpha k_j u_f^2$$

for N = 1, or

$$\alpha = {}^{27}/_{4}\, \frac{\sigma_{max}}{k_j u_f^2} = 1/\text{capacity of the roadway}$$

T = E + I now becomes

$$\sigma_{max} = \alpha k u^2 + \sigma$$

or

Table 3. Acceleration noise summary data.

Case	Section	Running Time (sec)	ΔV	Average Speed (fps)	σ
One	Maryland Plaza to Laclede	58.0	19	24.0	1.01
	Laclede to Scott (Barnes)	69.4	24	25.1	1.15
Two	Maryland Plaza to Lindell	29.1	17	15.4	2.29
	Lindell to West Pine	24.4	19	19.7	2.66
	West Pine to Laclede	24.5	20	18.4	2.55
	Laclede to Forest Park	24.7	12	18.5	0.99
	Forest Park to Barnes (Scott)	40.5	11	31.8	1.33
	Barnes (Scott) to Clayton	30.0	24	16.2	2.51
Three	Maryland Plaza to Lindell			15.1	
	Lindell to West Pine			22.8	
	West Pine to Laclede			16.3	
	Laclede to Forest Park			16.7	
	Forest Park to Barnes (Scott)			23.4	
	Barnes (Scott) to Clayton			16.2	

Note: 1 fps = 0.3 m/s.

Table 4. Additional acceleration noise summary data.

Section	σ Average	95 Percent Confidence Limits	Segment Symbol
Maryland Plaza to Lindell	2.39	2.39 ± 0.42	○
Lindell to West Pine	1.66	1.66 ± 0.62	□
West Pine to Laclede	2.54	2.54 ± 0.32	△
Laclede to Forest Park	2.03	2.03 ± 0.58	●
Forest Park to Barnes (Scott)	1.90	1.90 ± 0.50	■
Barnes (Scott) to Clayton	2.39	2.39 ± 0.40	▲

Figure 2. General shape of acceleration noise versus freeway speed curve.

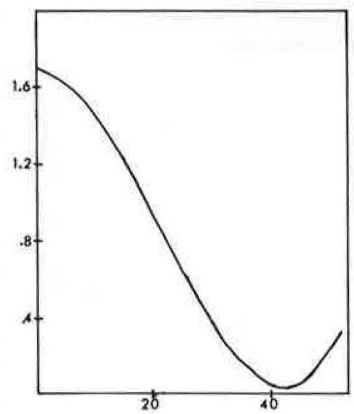

Figure 3. Acceleration noise versus speed for all cases.

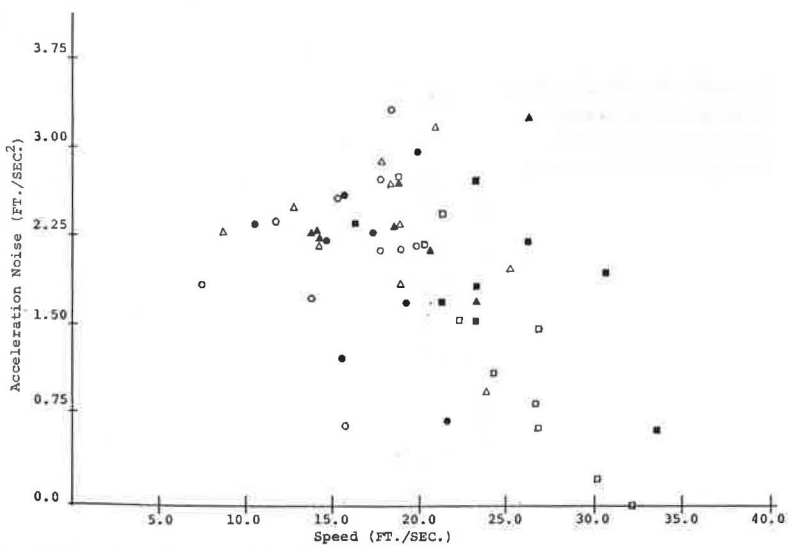

Figure 4. Acceleration noise versus speed for average case three and case one southbound.

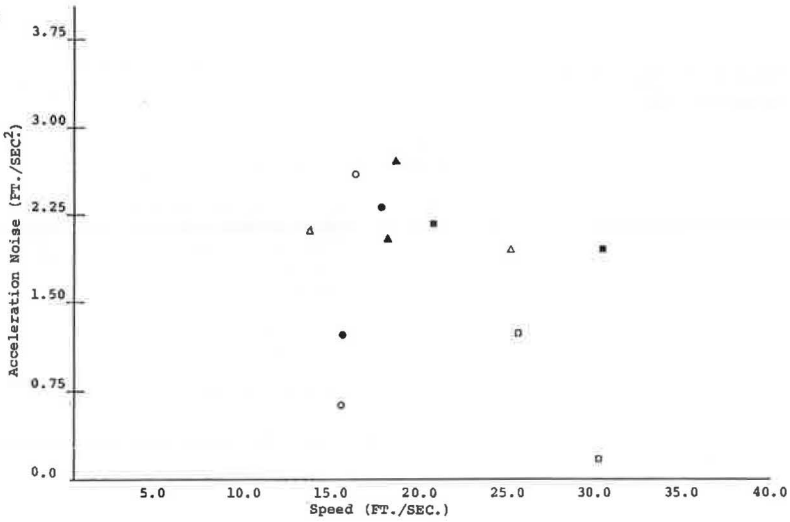

Figure 5. Acceleration noise versus speed for average case three and case one northbound.

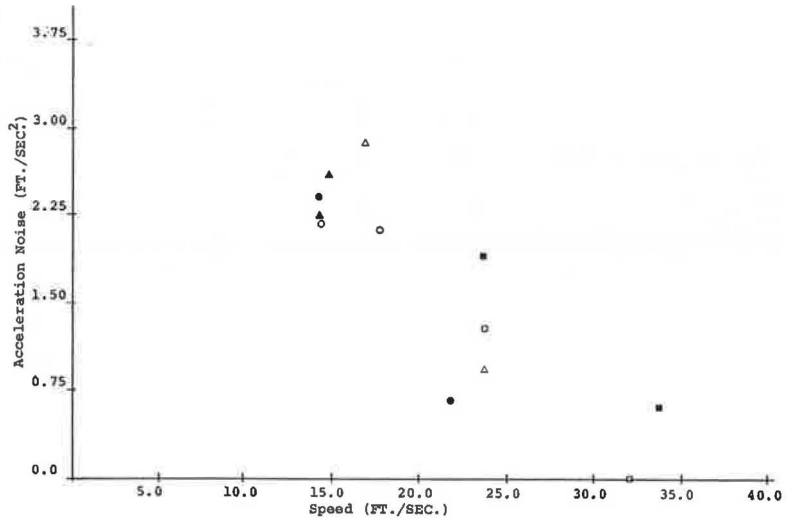

Figure 6. Acceleration noise versus speed for average case three and case one, average of both directions.

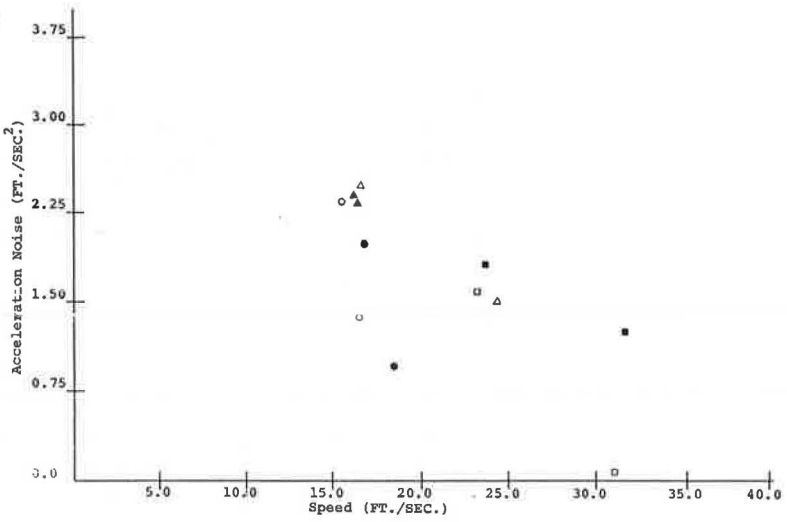

$$\sigma = \sigma_{max} - \alpha k u^2$$

For the case of N = 1,

$$k = k_j(1 - u/u_f)$$

where

k_j = jam concentration, and
u_f = mean free speed.

Substitution gives

$$\sigma = \sigma_{max} - \alpha k_j u^2 + \alpha k_j u^3/u_f$$

Figure 2 shows the general shape of this theoretical relationship fitted with data for a freeway section (1). The results of data from cases one, two, and three of Figure 1 are shown in Figures 3, 4, 5, and 6.

EVALUATION OF RESULTS

Examination of Table 2 shows that intersection delay predominated along Euclid Avenue. Delay due to signal control was the most frequent cause. However, the induced shock wave effects brought about by stop sign and midblock delay can halt traffic for a considerable length of time. Such deterministic results hid an inherently stochastic process. Thus, the acceleration noise results were tabulated to bring to light the variations in traffic flow.

Case one illustrated not only the effect on vehicle operations of the roadway, that is, the pavement type and sight distance conditions along intersecting streets, but also the effect of a stop sign. Without it, ΔV would be reduced 50 percent, cutting σ by a third approximately. In case two, σ between Barnes (Scott) and Laclede was very low in comparison with other segments because for that particular run the Forest Park intersection was cleared without delay. This can be interpreted as a simulation of a well-operating, progressively timed signal system. If the corridor had one, σ would be decreased substantially if other stream delays did not inhibit vehicular platooning. It should be pointed out that, even though it appears that a new minimum σ was obtained, the combined effects of σ between Clayton and Laclede for case two were still higher than those of case one. That is not to say that σ_{min} in case one was an absolute minimum, for it was only the minimum according to the definition of the road segment used.

Case three in Figure 1 contained some very useful results. Maximum dispersion on σ occurs between West Pine and Lindell. Link distance had little to do with it, but intersection control did. As previously mentioned, the Lindell and West Pine intersections are synchronized. The dispersion was the result of the state of the intersections in terms of the number of vehicles waiting to clear before the next platoon desires service. Oftentimes, these two intersections formed bottlenecks because of left-turning traffic. The signals do not have separate left turn indicators. The higher values of σ shown are a direct result of having to stop each time due to stop sign control.

Little correlation exists between Figure 2 and Figures 3, 4, 5, and 6. The energy-momentum theory did not appear to be applicable to a city street with all its stochastic delay components. This may be because the speed ranges in the study were not large enough or the floating car method was not applicable. Although either of these was possible, the biggest factor by far was the aperiodic nature and number of delays en-

countered. For the freeway case, the vehicle stream is most often inhibited by a bottleneck section that induces a shock wave. But this is one type of delay that affects the whole stream in a fairly consistent manner and not the same as the multiple delays encountered on a collector street like Euclid Avenue.

SUMMARY AND CONCLUSIONS

This study set out to examine the use of energy-momentum concepts for measuring levels of service along a city street. The acceleration noise parameter can be extremely useful in pinpointing bottleneck segments when accompanied by accurate speed-delay results. The lack of fit between observed and theoretical results for measuring actual levels of service was due to the number and stochastic nature of the delays found. Through isolation of delays by type, a better fit might be obtained. Realistically speaking, a freeway is the only roadway facility that can exhibit an isolated delay. For the most part as traffic mobility is compromised for traffic accessibility, delays and delay types increase in number and become less independent of one another, producing the scatter shown in Figures 3, 4, 5, and 6.

REFERENCES

1. D. R. Drew. Traffic Flow Theory and Control. McGraw-Hill, 1968.
2. St. Louis Metropolitan Area Traffic Volume Summary. Missouri State Highway Department, May 1974.
3. Washington University Medical Center Transportation Study. Alan M. Voorhees and Associates, Inc., April 1972.
4. L. J. Pignataro. Traffic Engineering: Theory and Practice. Prentice-Hall, 1973.
5. J. E. Baerwald, ed. Traffic Engineering Handbook. Institute of Traffic Engineers, 1965.

EXPERIMENTAL APPLICATIONS OF THE UTCS-1 NETWORK SIMULATION MODEL

Robert A. Ferlis and Richard D. Worrall, Peat, Marwick, Mitchell and Company

The UTCS-1 network simulation model was designed to facilitate the development and evaluation of advanced computer-based traffic control systems. The model can also be used for smaller scale traffic engineering studies. Three series of experimental applications of the model are presented to illustrate the wide range of problems for which the model may be effectively used. In addition, the model is briefly described, and the resource requirements associated with the application of the model are identified. General conclusions are drawn with regard to the utility of the model as a traffic engineering tool.

•IN URBAN AREAS throughout the nation, traffic congestion due to the steadily increasing volume of automotive traffic has demonstrated the need for better use of existing street systems. Evaluation of comprehensive system improvements is complicated by the large number of alternatives available, the interrelationships among the design variables, and the infeasibility of conducting large-scale experiments to test design options. The introduction of computer-based mathematical simulation models has enabled traffic engineers to determine the effectiveness of proposed changes in the transportation system without actually implementing and testing them. Because the cost of using these models is moderate, the designer can evaluate a larger and more innovative selection of alternatives than was previously possible.

The UTCS-1 network simulation model was designed primarily to assist in the development and evaluation of relatively complex network control strategies under conditions of heavy traffic flow. It is particularly appropriate to the analysis of dynamically controlled traffic signal systems based on real-time surveillance of traffic movements. The model may also be used, however, to address a variety of other simpler problems, including the effectiveness of conventional traffic engineering measures (e.g., parking and turn controls, channelization, one-way street systems), bus priority systems, and a full range of standard fixed-time and vehicle-actuated signal control strategies. The research results presented here are documented more fully elsewhere (1).

DESCRIPTION OF THE UTCS-1 MODEL

The UTCS-1 model is based on a microscopic simulation of individual vehicle trajectories through a street network. It can treat all major forms of traffic control encountered in the central areas of American cities. Because the model has a flexible, modular format and a comprehensive set of default input parameters, it can be applied effectively to a wide variety of design problems without the need for detailed calibration.

The logical design of UTCS-1 was described in an earlier report (2). The present configuration of the model consists of three interrelated components. The preprocessor module checks the input data set for accuracy and provides a range of data manipulation options. The simulator module actually executes the simulation. The postprocessor module can be used to compare the standard outputs from two separate model runs and subject the differences to a battery of statistical significance tests. The model is pro-

Publication of this paper sponsored by Committee on Traffic Flow Theory and Characteristics.

grammed in FORTRAN and is operational on IBM 360/370 and CDC 6600 series computer systems.

Operation of the Model

For purposes of simulation, a street network is expressed as a set of unidirectional links and nodes. In the simplest case, a single link represents one direction of travel along one street between two adjacent intersections. Each link may contain as many as five moving lanes. Midblock changes in geometry are accommodated by breaking a single block into two or more successive links. Provision is also made for midblock source-sink nodes representing entrances to parking lots, shopping centers, or minor streets not represented on the full network.

Intersection controls may take the form of stop or yield signs, simple fixed-time traffic signals operating either independently or as part of a coordinated system, vehicle-actuated signals, or more complex signal systems operating under dynamic real-time control. As many as nine signal phases may be incorporated within any given signal cycle. Additional controls in the form of parking restrictions, turn controls, and special channelization are coded directly for each link.

Simulated traffic detectors to provide inputs to real-time signal control algorithms may be located throughout the network. Twelve such detectors may be located at varying points within any one link with a maximum of three in any one lane. In the past, the model was modified to reflect the operation of real-time signal control strategies; however, the present version does not include any detailed coding for such algorithms.

Each vehicle traversing the network is treated as a separate entity. Distinction is made among automobiles, trucks, and buses, and detailed simulation of buses is provided for. The motion of each vehicle is governed by a series of performance characteristics that are assigned probabilistically as the vehicle enters the network. These characteristics in turn are used as input to a set of microscopic car-following, queue-discharge, and lane-switching algorithms.

Vehicles enter the network via a series of entry links or from source nodes located within the network. They are discharged via a set of peripheral exit links or via sink nodes located on each internal link.

The model is operated over a succession of 1-sec time steps. Although each vehicle is processed once every second, individual vehicle trajectories are recorded to a resolution of 0.1 sec. Input conditions such as input flow rates and intersection turning movements are assumed to remain constant over a succession of subintervals. The duration of such subintervals is specified by the user and may vary from as low as 1 min to 30 min or more.

Although many model parameters used for a particular simulation exercise are included in the standard set of user inputs, an additional set of parameters is part of the structure of the model. Most of these parameters were determined during the initial calibration of the model in Washington, D.C., and were felt to be either generally applicable in other situations (e.g., standard vehicle lengths) or difficult to calibrate for every application (e.g., bus dwell time distributions). The values of these parameters are considered default values and can be modified with the use of standard control cards prepared by the user. The default options allow the model to be used at different levels of accuracy depending on the quality of the data available and the experimental objectives. These considerations are treated in greater detail elsewhere (3, 4).

Output Characteristics

The UTCS-1 model provides a comprehensive range of output to describe the input data set, the status of the simulation exercise, and results of the simulation. The input data set for each subinterval is printed out in tabular form. The card listing of the input data is also optionally printed out at the beginning of the simulation.

All input data are checked for completion and consistency by the preprocessor component of the model. When errors are found, execution is aborted and the appropriate error messages are printed. The tabular listing of the input data set is useful in the identification of data or coding errors not detected by the preprocessor (e.g., incorrect input flow rates for an entry link).

A comprehensive set of traffic performance measures is generated either as standard output at the end of each subinterval or as intermediate output at the option of the user. The standard set of output measures is as follows:

1. Vehicle miles of travel,
2. Vehicles discharged from each link,
3. Vehicle minutes of travel time,
4. Total delay time,
5. Ratio of moving time to total travel time,
6. Total travel time,
7. Average travel time per vehicle,
8. Average delay time per vehicle,
9. Average speed,
10. Average occupancy,
11. Average number of stops per vehicle,
12. Average saturation percentage for each link, and
13. Number of cycle failures for each link.

Most of these are produced for each individual link and for the network as a whole. The intermediate output option provides additional detailed information for individual links. These data are useful in the analysis of microscopic traffic behavior over time.

The postprocessor component of the model provides detailed comparisons of the traffic performance measures generated during two separate model runs. These comparisons are made for each individual link and the network as a whole, for each time period (subinterval), and for the entire duration of the simulation. The individual link and network-wide measures are statistically analyzed with the paired-comparison t-test, the Wilcoxin signed-rank test, the Mann-Whitney u-test, and the two-way analysis of variance to determine the level of significance of the difference.

EXPERIMENTAL APPLICATIONS

Although the UTCS-1 model was developed to evaluate sophisticated computer-based traffic control strategies, the model can also be effectively used for other purposes. The following experimental applications are presented to suggest potential uses of the model as an aid to the traffic engineer. The validation exercise illustrates the high degree of accuracy with which the model can simulate actual traffic conditions on a network. The arterial demonstration describes an iterative approach to the design of roadway improvements. The San Jose simulation demonstrates the effectiveness of the model in the analysis and evaluation of network control strategies.

Validation of the UTCS-1 Model

The UTCS-1 model was originally calibrated for a grid network located in downtown Washington, D.C. (Figure 1). The accuracy of the model was determined by assembling a comprehensive set of field data by means of aerial and ground-based time-lapse photography and using the data set as a basis for comparison with two series of model runs, one for a.m. peak and one for a.m. off-peak conditions. The procedures used in performing these analyses paralleled those incorporated in the postprocessor module.

Three model runs (replications) with common sets of inputs for both the a.m. peak and off-peak traffic situations were executed so that the influence of stochastic variations on the test results could be determined. The duration of each test was 32 min of

Figure 1. Validation network.

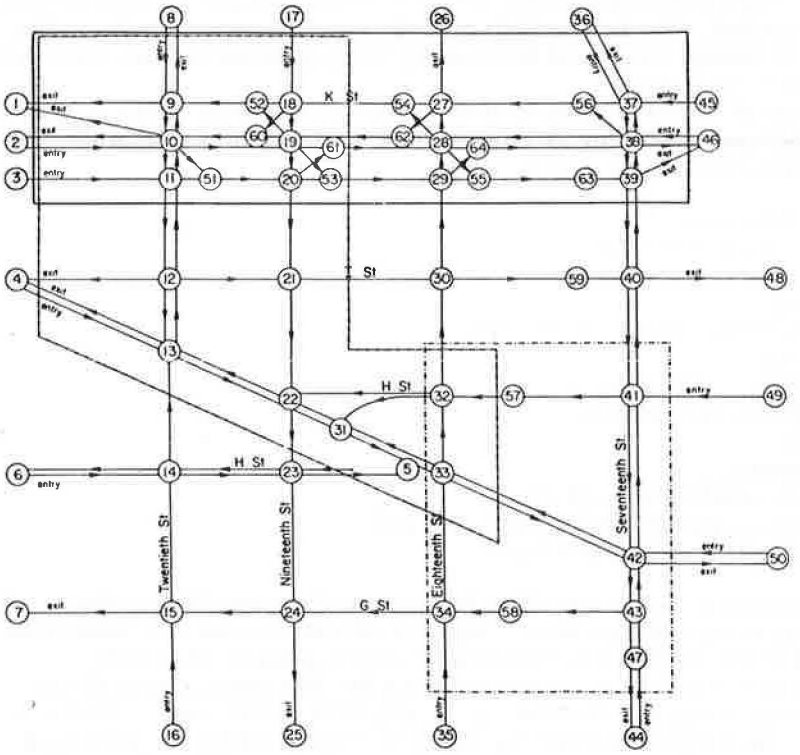

Table 1. Model validation: network-wide comparisons.

Characteristic	Field	Run 1 Amount	Run 1 Difference	Run 1 Percent	Run 2 Amount	Run 2 Difference	Run 2 Percent	Run 3 Amount	Run 3 Difference	Run 3 Percent
Total link output, vph										
Peak	36,108	36,345	237	0.7	36,399	291	0.8	36,368	260	0.7
Off peak	27,433	27,731	298	1.1	27,930	497	1.8	28,007	574	2.1
Vehicles in network										
Peak	328.4	327.9	-0.5	-0.2	332.0	3.6	1.1	329.5	1.1	0.3
Off peak	276.4	246.3	-30.1	-10.9	243.3	-33.1	-12.0	238.7	-37.7	-13.6
Vehicle minutes										
Peak	10,506	10,502	-4	0.0	10,616	110	1.0	10,539	33	0.3
Off peak	8,841	7,891	-950	-10.7	7,781	-1,060	-12.0	7,634	-1,207	-13.7
Vehicle miles										
Peak	1,701	1,705	4	0.2	1,710	9	0.5	1,710	9	0.5
Off peak	1,285	1,293	8	0.6	1,302	17	1.3	1,306	21	1.6
Total delay, vehicle min										
Peak	6,475	6,455	-20	-0.3	6,561	86	1.3	6,483	8	0.1
Off peak	5,806	4,831	-975	-16.8	4,700	-1,106	-19.0	4,541	-1,265	-21.8
Average travel time, min vehicle										
Peak	5.4	5.5	0.1	1.9	5.4	0.0	0.0	5.4	0.0	0.0
Off peak	6.4	6.0	-0.4	-6.3	5.2	-1.2	-18.8	5.1	-1.3	-20.3
Average speed, mph										
Peak	16.43	16.08	-0.35	-2.1	15.99	-0.44	-2.7	16.03	-0.40	-2.4
Off peak	15.35	16.48	1.13	7.4	16.88	1.53	10.0	16.71	1.36	8.9

Note: 1 mile = 1.6 km.

real time, and subinterval durations were 4 min.

The results of the validation exercise are given in Table 1, in which measured and computed values for seven measures of effectiveness are compared. The statistical significance of the difference in the off-peak data was determined by using the Wilcoxin signed-rank test (Table 2).

In the a.m. peak traffic conditions, the model accurately reproduced the actual traffic performance on the network. For all of the measures of effectiveness except average speed, the discrepancies between field and model performance averaged less than 1 percent. The average speed produced by the model appeared to be approximately 2.4 percent below the comparable field measurement. There was little variation among the three replications as illustrated by the network-wide statistics. None of the differences in field and model performance measures was statistically significant at the 5 percent level.

For the off-peak traffic conditions, the pattern was slightly different. The model did not reproduce the field traffic behavior so accurately in the off peak as in the peak period. The discrepancies in average speed ranged from 7.4 to 10.0 percent, and the differences in total delay ranged from 16.8 to 21.8 percent. These differences were significant at the 1 percent level. The model appeared to impede traffic flow less than necessary to reproduce the field data in the off-peak traffic period.

Simple Arterial Network

To illustrate the way in which the model might be used by the traffic engineer as a design tool to aid in the evaluation of alternative improvement schemes, we conducted a series of demonstration runs based on a simple linear arterial network.

The network chosen for the analysis was based on a 1.1-mile (1.8-km) segment of Wisconsin Avenue in Washington, D.C. (Figure 2). Traffic conditions during the a.m. peak were assumed. Because of the extremely low volume of cross traffic on most of the streets intersecting the arterial, the intersecting streets were modeled as artificial links of arbitrary length. All other traffic volume, network geometry, and signal timing data were based on actual conditions. A total of seven model runs were made, each representing approximately 45 min of real time.

The first run was used as a base case for comparison with the remaining six. It simulated the existing pattern of traffic operations for the a.m. peak traffic condition with the assumption of two moving lanes in each direction. The second run assumed reversible lane operation with three lanes in the direction of the major flow and only a single lane in the direction of the minor flow. The third run was designed to assess the impact of selected elimination of left turns. The fourth run was based on the construction of an additional lane in the direction of the major traffic movement and maintained two lanes for the minor movement. The fifth run was designed to measure the impact of instituting simultaneous signal offsets as opposed to the progressive system currently used on the arterial. Runs 6 and 7 evolved out of the first five. They combined a number of elements from each of the first five alternatives and included some modifications of the original inputs. The results of the seven runs are given in Table 3.

Run 2 produced generally poorer overall network performance measures than the base case. An examination of the link-by-link delay statistics generated by the model revealed a consistent pattern of improvement for the major direction of flow, which was more than offset by significant declines in performance for the minor flow.

Run 3 resulted in a significant improvement over the base case. Significant increases in average speed resulted coupled with parallel decreases in delay.

Not surprising, a more significant improvement again was achieved by constructing an additional lane in the direction of the major flow (run 4). This resulted in an increase in overall network speed of more than 30 percent or approximately 3 mph (5 km/h). This was coupled with an even more marked decrease in total delay.

The substitution of simultaneous signal offsets for the existing progressive system had little or no effect on the overall pattern of traffic performance. There was no significant change in either average speed or total delay; there was, however, a signifi-

Table 2. Level of significance of differences in off-peak data in Table 1.

Characteristic	Run 1	Run 2	Run 3
Total link output	0.02	0.01	0.01
Vehicles in network	0.01	0.01	0.01
Vehicle minutes	0.01	0.01	0.01
Vehicle miles		0.02	0.01
Total delay	0.01	0.01	0.01
Average travel time	0.01	0.01	0.01
Average speed	0.01	0.01	0.01

Figure 2. Wisconsin Avenue test network.

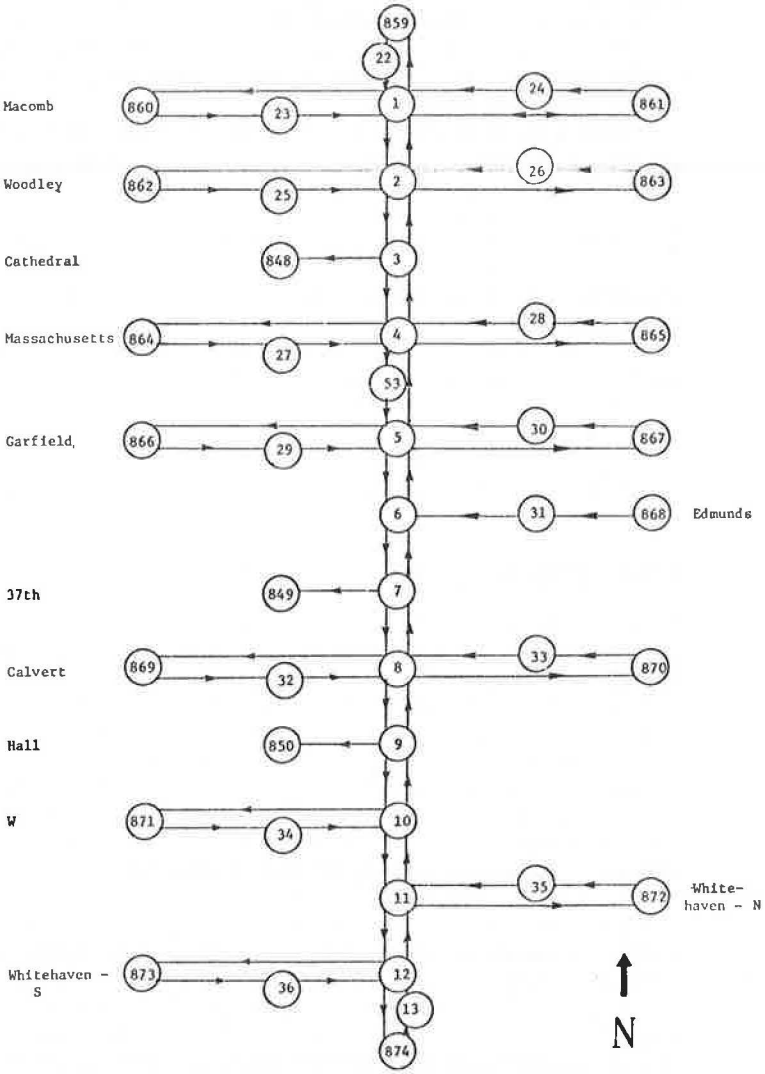

Table 3. Network statistics for Wisconsin Avenue.

Measure of Effectiveness	Base Case	Case 2		Case 3		Case 4		Case 5		Case 6		Case 7	
		Value	Level of Significance	Value	Level of Significance	Value	Level of Significance	Value	Level of Significance	Value	Level of Significance	Value	Level of Significance
Vehicle miles	2,504	2,452		2,525		2,556	0.02	2,516		2,555	0.02	2,565	0.05
Vehicle min	15,242	15,565		13,865	0.01	11,951	0.01	15,279		12,590	0.01	11,267	0.01
Vehicle trips	5,349	5,311		5,345		5,387		5,350		5,389		5,396	
Stops per vehicle	1.98	1.83	0.01	1.97		1.66	0.01	2.18	0.01	1.93		1.64	0.01
Ratio of moving time to total travel time	0.438	0.417		0.483	0.01	0.568	0.01	0.437		0.537	0.01	0.601	0.01
Average speed, mph	9.86	9.46		10.93	0.01	12.83	0.01	9.88		12.18	0.01	13.66	0.01
Mean occupancy	317	323		288	0.01	248	0.01	318		262	0.01	234	0.01
Average delay per vehicle	96.1	102.4		80.4	0.01	57.5	0.01	96.4		65.0	0.01	50.0	0.01
Total delay	8,569	9,067		7,166	0.01	5,158	0.01	8,596		5,834	0.01	4,498	0.01
Delay per vehicle mile	3.42	3.70		2.84		2.02		3.42		2.28		1.75	
Travel time per vehicle mile	6.09	6.35		5.49		4.68		6.07		4.93		4.39	
Percentage of stop delay	82.3	84.4	0.02	78.6	0.01	74.0	0.01	82.2		73.9	0.01	69.7	0.01

Note: 1 mile = 1.6 km.

cant increase in the average number of stops per vehicle when compared with the base case.

This initial set of runs served to identify a number of major traffic problems on the network. It also provided an indication of the improvements in performance likely to be associated with four alternative design-control schemes. Examination of the detailed results generated by the model for each run suggested that the best solution was likely to be obtained by combining features of several of the original schemes. Two additional runs of the model, therefore, were made based on such combinations.

Run 6 was designed to eliminate a number of specific traffic problems at selected locations along the arterial identified as a result of the initial tests. These were relatively limited in scope and resulted in a moderate cost improvement program. Run 7 combined these improvements with the construction of an extra lane in the direction of major flow as reflected in run 4.

The results of these last two runs are also given in Table 3. Both result in significant improvements over the base case. Run 6 yielded a level of improvement significantly above that for runs 2, 3, and 5. Average speed increased approximately 23 percent compared to the base case, and total delay decreased approximately 32 percent. The improvement is not, however, as marked as that associated with the construction of an extra lane (run 4).

Run 7 resulted in the most pronounced improvement of all of the alternatives examined. Average speed increased 38 percent over the base case; total delay decreased approximately 47 percent. Run 7 showed significant additional improvements over run 4. Alternative 7 is, however, by far the most expensive of those tested; it is questionable whether the additional benefits that it provides over alternative 6 justify the additional cost involved.

This simple set of demonstration tests illustrates the potential use of the model as an aid in iterative design. The model was used both to isolate specific traffic problems within the test network and also to assess the benefits associated with an initial set of alternative improvement schemes. These initial analyses were used to generate two refinements to the initial set of improvement proposals. These refinements varied in both cost and potential effectiveness.

Comparison of SIGOP and TRANSYT in San Jose

The third simulation exercise was based on a more complex application for a large network in San Jose, California. The purpose of this test was to illustrate the adaptability of the model to network and traffic conditions that differ significantly from those in Washington, D.C., for which it was originally validated. A secondary objective was to demonstrate the use of the model to evaluate the use of two signal optimization procedures, SIGOP and TRANSYT, under varying traffic conditions and to compare these results with those obtained from a set of parallel field analyses (5).

The simulation study was designed to use the data collected as part of the previous FHWA field comparison. The basic test network included a total of 49 signalized intersections, some of which incorporated relatively complex geometry. This network is shown in Figure 3.

Six series of runs were made in which the model reflected the signal timing plans of SIGOP and TRANSYT for each of three major traffic conditions: morning peak, midday, and evening peak. Signal cycle lengths were set uniformly at 45 sec. Within each time period simulated, all model inputs were maintained constant except for the signal settings generated by the two signal optimization programs. The duration of each simulation run was equivalent to 30 min of real time. Single runs were made for each midday and evening peak condition; multiple replications were made for the a.m. peak condition.

The results of the simulation runs are given in Table 4 in terms of the 12 performance measures generated as part of the model's standard statistical output. The table gives the network-wide value of each performance measure for each run and any significant differences between performance under SIGOP and TRANSYT signal settings

Figure 3. San Jose test network.

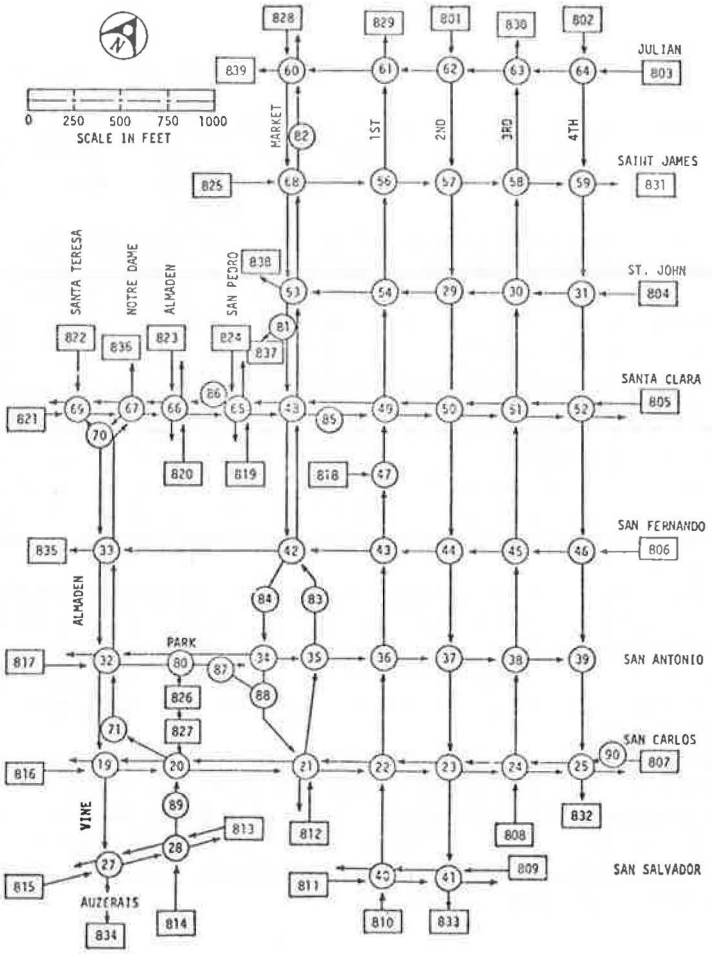

Table 4. Network statistics for San Jose.

Measure of Effectiveness	a.m. Peak					Midday			p.m. Peak		
	SIGOP		TRANSYT		Level of Significance			Level of Significance			Level of Significance
	Run 1	Run 2	Run 1	Run 2		SIGOP	TRANSYT		SIGOP	TRANSYT	
Vehicle miles	3,314	3,295	3,296	3,314		3,273	3,288		4,242	4,227	
Vehicle min	12,279	12,270	11,885	12,142		12,369	12,173		17,397	16,903	0.01
Vehicle trips	5,864	5,854	5,877	5,879		5,447	5,447		7,549	7,524	
Stops per vehicle	2.00	1.99	1.95	2.01		2.36	2.42		2.26	2.19	0.05
Ratio of moving time to total travel time	0.637	0.634	0.654	0.646	0.01	0.625	0.641	0.01	0.574	0.590	0.01
Average speed, mph	16.19	16.11	16.64	16.38	0.02	15.88	16.21	0.02	14.63	15.01	0.01
Mean occupancy	408	408	395	404		411	405		579	562	0.01
Average delay per vehicle	45.7	46.1	42.0	43.9	0.02	51.1	48.2	0.01	58.8	55.3	0.01
Total delay	4,462	4,497	4,110	4,297	0.01	4,635	4,374	0.01	7,403	6,930	0.01
Delay per vehicle mile	1.35	1.36	1.25	1.30		1.42	1.33		1.75	1.64	
Travel time per vehicle mile	3.70	3.72	3.61	3.66		3.78	3.70		4.10	4.00	
Percentage of stop delay	55.7	56.1	51.9	53.0	0.01	56.8	52.0	0.01	63.0	59.3	0.01

Note: 1 mile = 1.6 km.

Table 5. Computer requirements for experimental applications.

Run	Simulation Time (min)	Central Processing Unit Time (min:sec)	Core	Number of Links	Average Number of Vehicles	Bus Traffic Simulation
Washington, D.C.						
Peak validation run 1	32.0	17:31.25	242,000	101	335.0	Yes
Off-peak validation run 1	32.0	16:05.02	242,000	108	251.1	Yes
Arterial demonstration run 1	108.0	17:10.15	242,000	55	297.5	No
Arterial demonstration run 4	108.0	16:21.77	244,000	55	234.5	No
San Jose						
a.m. peak run 1	30.0	21:43.34	262,000	147	408.1	Yes
Noon run 1	30.0	22:31.79	262,000	147	411.2	Yes
p.m. peak run 1	30.0	27:00.92	262,000	147	579.0	Yes

for comparable traffic conditions.

The signal settings generated by TRANSYT produced consistently lower delay and higher average speeds than the equivalent settings generated by SIGOP. This applied uniformly to all traffic conditions. Differences in average speed ranged from 1.7 to 2.6 percent; differences in total delay ranged from 4.4 to 6.4 percent. Most of these differences were statistically significant at the 2 percent level and in one instance at the 1 percent level. The differences were most marked in the p.m. peak case. No significant differences were detected between the comparable results of the a.m. peak replications.

A detailed examination of the link-by-link outputs generated by the model (not tabulated here) yielded a similar pattern. It was found that approximately 65 percent of the individual links for which significant differences in performance existed between the two programs performed better under the TRANSYT signal settings than under the SIGOP settings. Several intersections were identified, however, for which the signal splits appeared to be unreasonable under both signal timing methods. These, in turn, suggested a number of potential improvements that might be made in each timing plan.

MANPOWER AND RESOURCE REQUIREMENTS

The precise requirements associated with a particular application may vary considerably depending on the size and complexity of the network, the level of traffic flow, and the characteristics of the control strategies to be evaluated. The estimates presented here, based on the three series of experimental applications, should be interpreted only as approximate guidelines.

Manpower Requirements

Any simulation model that offers the flexibility and realism that UTCS-1 does is bound to require a certain degree of sophistication and effort in study design and input preparation to produce optimal results. The time and manpower resources associated with the application of the model depend on a number of factors. Of these, the most important is the availability of basic data on input flow rates, current signal timing, and network geometry. These data are typically available, at least in approximate form, in existing traffic engineering records. The remaining areas of resource commitment are as follows:

1. Verify and complete raw data assembly,
2. Reduce and code field data,
3. Keypunch and verify input cards,
4. Prepare input decks and test execution,
5. Perform production runs, and
6. Analyze outputs.

The actual extent of the work involved is dependent on the size and complexity of the network, the nature of the alternatives to be tested, and the selection of user options.

In the case of the simple arterial demonstration test described earlier, a total of approximately 6 person-weeks was devoted to input preparation. Another 6 person-weeks was expended in the performance of the production runs and the analysis of the outputs. In the case of the San Jose demonstration tests, a total of approximately 8 person-weeks was devoted to input preparation, building upon data generated in the earlier Federal Highway Administration field study. The performance of the production runs and the analysis of the resultant outputs consumed roughly 6 additional person-weeks.

Computer Requirements

Computer requirements for running the model are a function of several factors: the size of the test network, the level of traffic flow, the type and frequency of output reports, the desired number and length of simulation runs, and the like. Factors that significantly affect computer core requirements include the maximum number of nodes, links, and vehicles permitted in the network and the selection of user options, e.g., bus traffic, transient flow blockages (rare events), and actuated signal control. Computer running time is affected by the duration of the simulation, the number of links, the number of vehicles, and the specification of user options.

The computer resources expended for the experimental application described earlier are given in Table 5. All of these tests were executed on an IBM 360/65 computer. For most practical applications a real time-simulation time ratio of approximately 2:1 may be anticipated when the IBM version of the model is used. On CDC 6600 series computers, this ratio should improve to a value of approximately 5:1.

The UTCS-1 model, in both IBM and CDC forms, is available to potential users through the Federal Highway Administration. The model has been extensively tested and has been used by FHWA in support of programs in Los Angeles, Dallas, and Washington, D.C. In addition, UTCS-1 has been applied by the Ontario Ministry of Transportation and Communications, the state highway departments of California and Utah, and consultants.

SUMMARY AND CONCLUSIONS

A series of experimental applications of the UTCS-1 model were performed to illustrate some potential uses of the model. The validation experiment demonstrated the ability of the model to reproduce actual traffic patterns on a grid network. The arterial demonstration described the utility of the model in the development of traffic system improvement plans. The SIGOP-TRANSYT comparison in San Jose illustrated the model's ability to analyze the effectiveness of large-scale traffic control strategies. Several conclusions may be drawn from these experiments.

1. The flexibility of the model systems permits the investigation of a broad spectrum of traffic problems on varying levels of detail. An individual application can be closely tailored to the objectives of the experiment and the limitations of the data.
2. The UTCS-1 model can accurately represent the behavior on individual segments and the network as a whole. The model is sensitive to variations in traffic conditions and to the specification of system characteristics.
3. The performance measures produced by the model can facilitate the development of effective programs of traffic system improvements. The facility with which the impacts can be modified, once the basic network has been developed, stimulates the investigation of additional (and perhaps more innovative) alternatives.
4. Alternative improvement programs can be effectively evaluated, in both relative and absolute terms. The quantitative performance information produced by UTCS-1 facilitates the identification of trade-offs and serves as input to the determination of the cost effectiveness of traffic system design strategies.

ACKNOWLEDGMENTS

The UTCS-1 network simulation model was developed by Peat, Marwick, Mitchell and Company, together with its subcontractors, KLD and Associates, Inc., under contract to the Office of Research, Federal Highway Administration, U.S. Department of Transportation. The experimental applications described in this paper formed the final phase of this contract activity.

Numerous people were involved in the development of the model. The authors would like to acknowledge, in particular, the contributions of Guido Radelat, FHWA contract

manager; Edward Lieberman and David Wicks, KLD and Associates, Inc., who were responsible for its basic programming; and Jeffrey Bruggeman, Peat, Marwick, Mitchell and Company, who directed its final implementation and testing. Any errors or shortcomings in the text are, of course, the sole responsibility of the authors.

REFERENCES

1. Peat, Marwick, Mitchell and Co. and KLD Associates, Inc. Network Flow Simulation for Urban Traffic Control System—Phase II: Technical Report for UTCS-1 Network Simulation Model. Federal Highway Administration, U.S. Department of Transportation, Rept. FHWA-RD-73-83, March 1974.
2. E. B. Lieberman, R. D. Worrall, and J. M. Bruggeman. Logical Design and Demonstration of UTCS-1 Network Simulation Model. Highway Research Record 409, 1972, pp. 46-56.
3. Peat, Marwick, Mitchell and Co. and KLD Associates, Inc. Network Flow Simulation for Urban Traffic Control System—Phase II: Volume 4, User's Manual for UTCS-1 Network Simulation Model. Federal Highway Administration, U.S. Department of Transportation, Rept. FHWA-RD-73-86, March 1974.
4. Peat, Marwick, Mitchell and Co. and KLD Associates, Inc. Network Flow Simulation for Urban Traffic Control System—Phase II: Volume 5, Applications Manual for UTCS-1 Network Simulation Model. Federal Highway Administration, U.S. Department of Transportation, Rept. FHWA-RD-73-87, March 1974.
5. Alan M. Voorhees and Associates, Inc. SIGOP/TRANSYT Evaluation: San Jose, California. Federal Highway Administration, U.S. Department of Transportation, Rept. FH-11-7822, July 1972.

VEHICULAR HEADWAY DISTRIBUTIONS: TESTING AND RESULTS

J. E. Tolle, Transportation Research Institute, Carnegie-Mellon University

Numerous investigations and studies have been performed concerning the spacings and headways of vehicles in the traffic stream. This paper briefly reviews, examines, and tests some of the mathematical models with real world data collected for both two-lane roadways and urban freeways. These testing methods include both graphical fits and statistical fits, and the results are presented, along with conclusions on the appropriateness of the model representations. The results indicate the composite exponential, Pearson Type III, and log-normal distributions best represent conditions; generally the log-normal distributions are the best for a wide range of traffic volumes.

•THE SPACINGS and headways of vehicles in the traffic stream have been the concern of many investigations and studies. Normally spacing refers to the physical distance between vehicles in feet (meters), and headway is the time between successive vehicles in seconds. There have been numerous attempts to mathematically describe vehicle spacing and headways in the traffic stream. This paper examines these models and presents the results obtained by using the log-normal distribution.

Before attempting to develop a model, one should ask why a mathematical description of headways is desired. One reason is for input to a simulation model of traffic flow on a digital computer such as an intersection, car-following, or other simulation. If such a simulation model exists, then the problem of generating traffic data as input arises. At least two methods of solving this problem exist. The first is the reading in of actual data, which has two disadvantages:

1. The reading in of data consumes a lot of computer and data collection time, and
2. Because only actual observed volumes are used, one benefit of simulation, that of investigating situations that are extremely difficult to observe in the real world, is lost.

The second method eliminates these disadvantages because it allows the computer to generate its own data. The problem of time is then solved, since computer generation of data requires only a fraction of the required read-in time. Also, situations that are difficult to observe in the real world can be investigated. The one problem with internal generation of data is that a mathematical model is needed with which to accurately generate data that agree with the real world situation.

PREVIOUSLY PROPOSED DISTRIBUTIONS

The Poisson distribution has been successfully used to obtain the arriving rate of vehicles. Under conditions of free flow, i.e., most vehicles are able to choose their desired speed, this gives satisfactory results.

Assume that free-flow conditions exist, and consider the probability of x vehicles

Publication of this paper sponsored by Committee on Traffic Flow Theory and Characteristics.

arriving per t time interval. This is known as the arriving rate of vehicles. If the hourly volume Q is known, then the Poisson probability function is

$$P(x) = \begin{cases} \exp(-m_a x)/x! & \text{for } x = 0, 1, \ldots \\ 0 & \text{otherwise} \end{cases} \quad (1)$$

This is a discrete distribution, i.e., it takes on different values only at the integer points. It is appropriate at this time to recall the differences between counting distributions and time headway distributions. The counting distribution is always discrete, and the time headway distribution is continuous. This is clear from the fact that only a whole number of vehicles may arrive in a given time interval, but a time gap may be a fractional value.

If we write the Poisson function in the form

$$P(x) = \frac{1}{x!}\left(\frac{Qt}{3,600}\right)^x \exp(QT/3,600) \quad (2)$$

where t is the time interval to be considered in seconds and Qt/3,600 is the average number of vehicles per t seconds, this corresponds to the m-value that represented the mean value in equation 1. Then P(x) is the probability of x vehicles arriving during the given time interval t.

One of the first distributions tested for headways was the negative exponential, which may be derived from the Poisson by considering the probability of zero arrivals in the time interval. If $\lambda > 0$,

$$P(t) = \begin{cases} \lambda \exp(-\lambda t) & \text{for } t > 0 \\ 0 & \text{otherwise} \end{cases} \quad (3)$$

Then the probability of a gap greater than or equal to T seconds is the integral from T to infinity of the negative exponential; i.e., for $T > 0$,

$$P(t > T) = \exp(-\lambda t) = \exp(-QT/3,600) = e \quad (4)$$

The negative exponential cannot be satisfactory because it assigns a higher probability to very low headways, and as the time approaches zero the probability increases. From observed results this is not true; however, there is normally a peak number of headways around 0.5 to 2 sec, and the probability of a zero headway is by necessity zero.

Gerlough (5) suggested a method of possible correction for the negative exponential that consists of shifting the negative exponential away from the origin. The difficulty with that method is that small gaps are impossible, which does not satisfy the known conditions. Equation 5 represents the shifted exponential (shift of a to the right).

$$f(t) = \begin{cases} \exp[-\lambda(t - a)] & \text{for } t > a \\ 0 & \text{otherwise} \end{cases} \quad (5)$$

Other distributions that may be evaluated are the composite exponential and the Pearson Type III.

COMPOSITE EXPONENTIAL

Schuhl (13) proposed a composite exponential in which vehicles are classified as constrained or free flowing. A constrained vehicle is one that is prevented from passing, and a free-flowing vehicle is able to pass. We then have the following definitions:

$$n = \frac{\text{volume of constrained vehicles}}{\text{total volume}},$$

$$1 - m = \frac{\text{volume of free-flowing vehicles}}{\text{total volume}},$$

b_1 = average headway of constrained vehicles = 3,600/number of constrained vehicles,

b_2 = average headway of free-flowing vehicles = 3,600/number of free-flowing vehicles,

Δ = minimum headway required by constrained vehicle, and

t = headway in seconds.

The composite exponential probability distribution function is as follows:

$$P(t) = P_r(g < t) = \begin{cases} (1 - n)(1 - e^{-t/b_2}) + n[-e^{-(t-\Delta)/(b_1 - \Delta)}] & \text{for } t > 0.5 \\ 0 & \text{for } t < 0.5 \end{cases} \tag{6}$$

That is, the probability of a headway less than t seconds is $P(t)$.

Intervals of a half second were used except for the last one to test the composite exponential and to apply a chi-square test for goodness of fit. Figures 1 through 6 show the plots of the theoretical and observed distribution functions. Only one statistically good fit was obtained with a volume of 339 vehicles per hour, but graphically the fits for some volumes were fairly close, indicating that there is some merit for considering the composite exponential.

PEARSON TYPE III

The Pearson Type III distribution may be stated as follows for $x > 0$:

$$f(x) = \frac{\lambda^k e^{-\lambda} x^{k-1}}{\Gamma(k)} \tag{7}$$

If k is an integer, $\Gamma(k) = (k - 1)!$

Equation 7 is the probability density function. If $k = 1$, equation 7 simply reduces to the previously discussed negative exponential distribution. Figure 7 shows the effect of varying k and holding λ constant. From equation 7 it is seen that the distribution function is

$$F(x) = P(X < x) = \int_0^x \frac{\lambda^k e^{-\lambda x} x^{k-1}}{\Gamma(k)} dx \tag{8}$$

Figure 1. Observed and theoretical cumulative headway distributions for volumes of 339 and 442 vph.

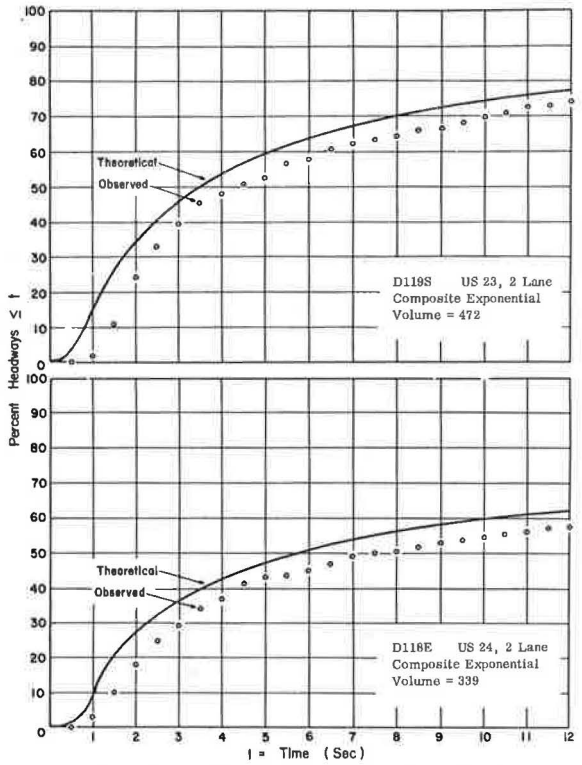

Figure 2. Observed and theoretical cumulative headway distributions for volumes of 445 and 515 vph.

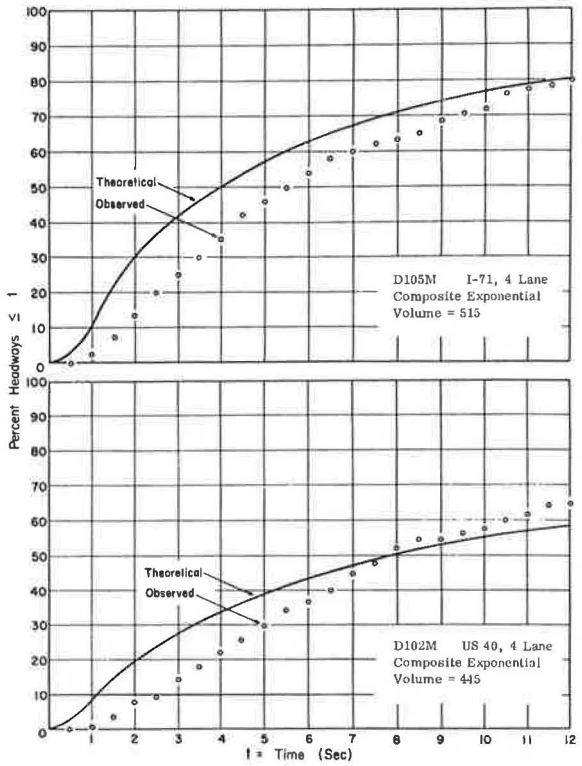

Figure 3. Observed and theoretical cumulative headway distributions for volumes of 551 and 659 vph.

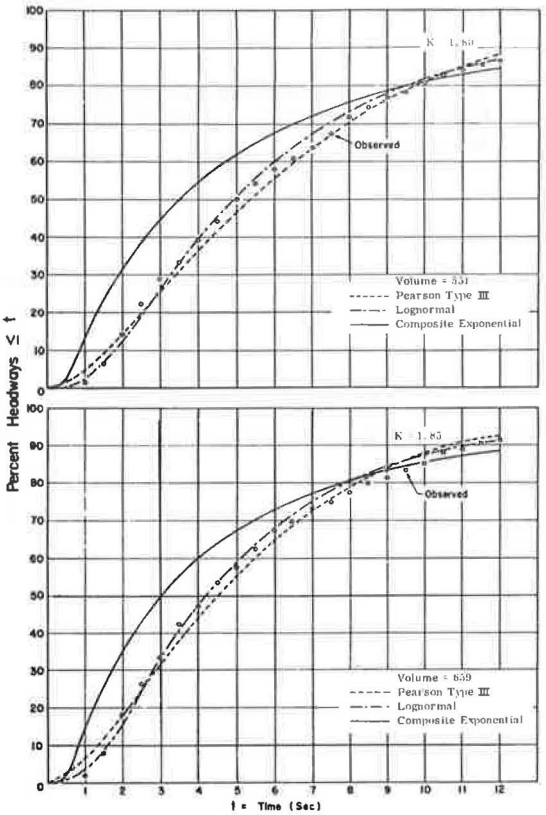

Figure 4. Observed and theoretical cumulative headway distributions for volumes of 781 and 902 vph.

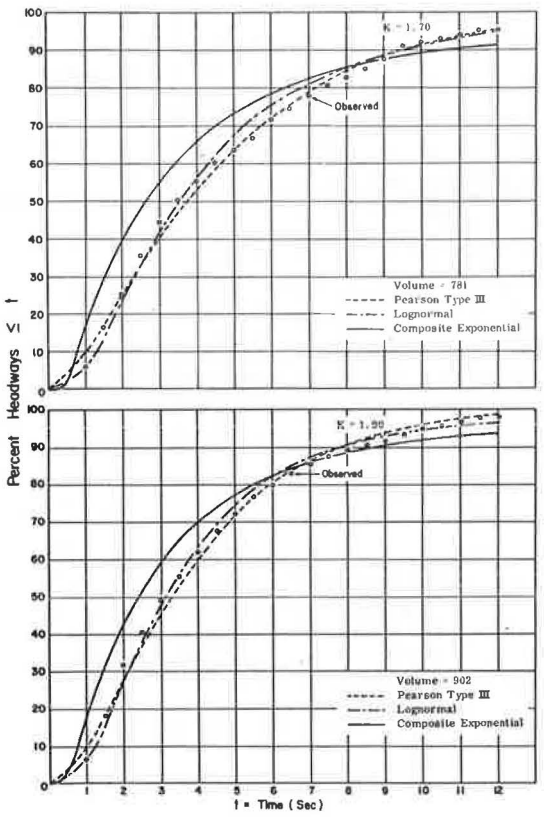

Figure 5. Observed and theoretical cumulative headway distributions for volumes of 1,026 and 1,128 vph.

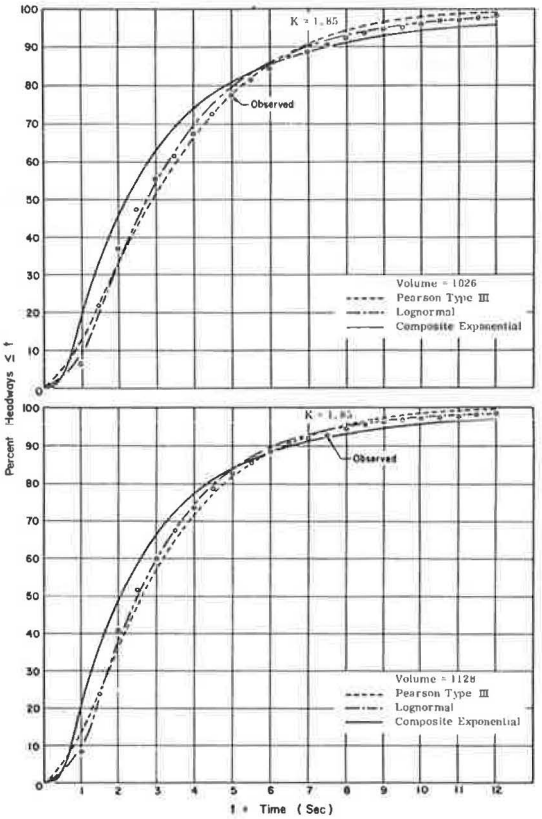

The reduction of F to a simple formula is easily done for integer values of k. For noninteger k-values, it is necessary to evaluate the gamma function with a table or algorithm and use an approximation for the integral.

In the evaluation of the data collected, the parameter λ was set at k divided by the average gap length in seconds. Again a chi-square test was used, but no good statistical fits were found. Graphs of the theoretical and observed distribution functions are very close and an improvement over the composite exponential (Figures 3 through 6). The use of noninteger k did not improve the statistical fits, and these graphs were not plotted.

LOG-NORMAL DISTRIBUTION

Consider now the log-normal distribution. The log-normal distribution is the distribution of a variate whose logarithm obeys the normal law of probability. A number of names have been given the log-normal distribution such as the Galton-McAlister, Kapteyn, and Gibrat distribution. Although this is a relatively new application of the log normal, its origin dates back to 1879, and it has been used extensively in economic theory.

Consider a random variable X that ranges from zero to infinity, i.e., $0 < X < \infty$. By making the transformation $Y = \lg X$, where lg is the natural logarithm, then Y is again a random variable having an infinite range; that is, Y takes on values between minus and plus infinity, $-\infty < Y < \infty$.

If Y is normally distributed, then by introducing the following notation:

$$L(x|\mu,\sigma^2) = P(X < x) \text{ and } N(y|\mu,\sigma^2) = P(Y < y)$$

the relation becomes

$$N(y|\mu,\sigma^2) = N(\lg x|\mu,\sigma^2)$$

That is, L and N are the distribution functions of X and Y respectively. Because X and Y are related by $L(x) = N(\lg x)$ for $x > 0$,

$$L(x) = \int \frac{1}{\sqrt{2\pi}\sigma} \exp\left[-(\lg t - \mu)^2/2\sigma^2\right] dt \qquad \text{for } x > 0$$

By differentiating L with respect to x

$$\frac{dL}{dx} = \frac{1}{x\sigma\sqrt{2\pi}} \exp\left[-(\lg x - \mu)^2/2\sigma^2\right] dt \qquad \text{for } x > 0$$

it follows immediately that the probability density function of X is

$$f(x) = \frac{1}{x\sigma\sqrt{2\pi}} \exp\left[-(\lg x - \mu)^2/2\sigma^2\right] \qquad \text{for } x > 0$$

Evaluation of the distribution was again carried out on the computer by using a system subroutine to evaluate the normal distribution. Because Y is normally distributed

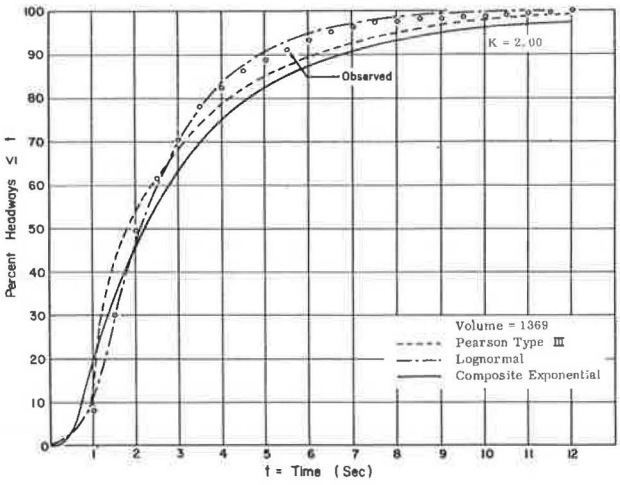

Figure 6. Observed and theoretical cumulative headway distributions for volume of 1,369 vph.

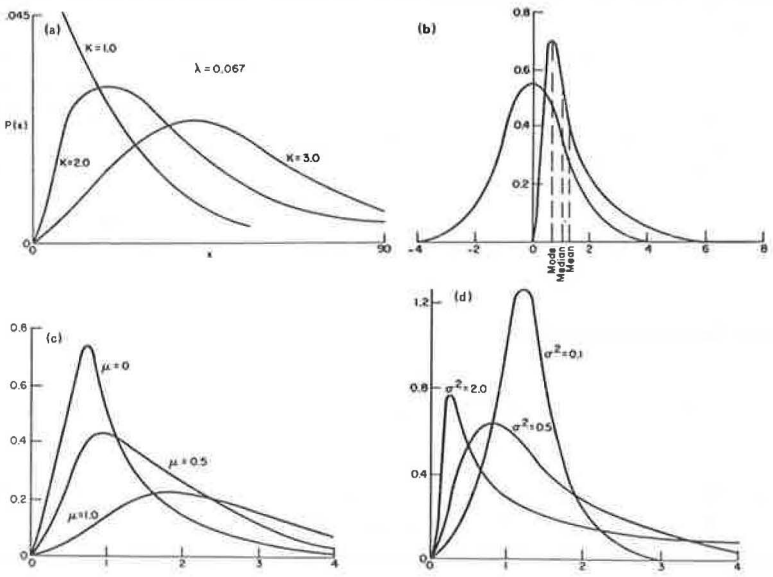

Figure 7. Frequency curves for (a) Type III distribution for various values of K, (b) normal and log-normal distributions, (c) log-normal distribution for different μ, and (d) log-normal distribution for different σ^2.

Table 1. Summary of distributions.

Distribution	Type	Comments	Equation
Poisson	Counting		$f(x) = \begin{cases} \frac{e^{-m}m^x}{x!} & \text{for } x = 0, 1, \ldots \\ 0 & \text{otherwise} \end{cases}$
Generalized Poisson	Counting		$P_n = \sum_{i=1}^{k} \frac{e^{-\lambda t}(\lambda t)^{nk+i-1}}{(nk+i-1)!}$ for $t = 0, 1, \ldots$
Negative exponential	Gap	Unsatisfactory	$f(x) = \begin{cases} \lambda e^{-\lambda x} & \text{for } x \geq 0 \\ 0 & \text{otherwise} \end{cases}$
Shifted exponential	Gap	Unsatisfactory	$f(x) = \begin{cases} \lambda e^{-\lambda(x-a)} & \text{for } x \geq a \\ 0 & \text{otherwise} \end{cases}$
Composite exponential	Gap	One out of 11 good fits. Good fit at 515 vph on 4-lane highway using 38 deg of freedom.	$P(g < t) = \begin{cases} (1-n)(1-e^{-t/b_2}) + n\left[1 - e^{\frac{(t-\Delta)}{b_1-\Delta}}\right] & \text{for } t \geq \Delta \\ 0 & \text{for } t < \Delta \end{cases}$
Pearson Type III	Gap	No good fits. Actual graphic prediction better than implied by no good fits.	$f(x) = \begin{cases} \frac{\lambda^k e^{-\lambda x} x^{k-1}}{(k-1)!} & \text{for } x \geq 0 \\ 0 & \text{for } x < 0 \end{cases}$
Log normal	Gap	Four out of 7 good fits with selected 5-min data. Two out of 4 good fits with 1 hour of data. Zero out of 2 good fits with 515 vph on 4 lanes and 339 vph on 2 lanes. Graphically predictions all seem close.	$f(x) = \begin{cases} \frac{1}{x\sigma\sqrt{2\pi}} e^{\frac{(\ln x - \mu)^2}{2\sigma^2}} & \text{for } x > 0 \\ 0 & \text{for } x \leq 0 \end{cases}$

with mean μ and variance σ^2, $z = (Y - \mu)/\sigma$ has a normal distribution with mean 0 and variance 1. As estimates for the parameters

$$\hat{\mu} = \frac{\sum_{n} \lg x_i}{n}$$

$$\hat{\sigma}^2 = \frac{\sum_{n} (\lg x_i - \hat{\mu})^2}{n - 1}$$

Figure 7 shows a comparison of the normal probability function and the corresponding log-normal probability function and also the effect of varying μ and σ^2 on the log normal. Figures 3 through 6 show the theoretical and observed frequencies in graphical form. Four out of seven good statistical fits were obtained. Graphically all of the plots were close to the actual data.

DATA COLLECTION

Data were collected on I-71, a four-lane Interstate highway in Ohio, in order to evaluate these distributions. The distributions have been tested in two ways. First, 22 hours of data were collected and in turn were divided into hourly data, resulting in representative volumes of 882, 930, 1,040, and 1,278 vehicles per hour per lane.

Next the 22 hours of data were separated into 5-min intervals. Based on these intervals, hourly volumes were constructed from representative 5-min volumes. For example, 12 intervals with volumes ranging from 55 to 60 vehicles were chosen to obtain an hourly volume of between 660 and 720 vehicles. Using this method gave representative volumes of 551, 659, 781, 902, 1,026, 1,128, and 1,369 vehicles per hour per lane.

Finally, 1 hour of data was collected from each of the following sites in Ohio:

Highway	Number of Lanes	Vehicles per Hour
US-40	4	445
I-71	4	515
US-24	2	339
US-33	2	472

CONCLUSION

Table 1 gives a summary of the distributions. Table 2 gives a comparison of the three distributions tested.

Of the distributions previously used for headway distributions, two of these, the composite exponential and the Pearson Type III, were chosen to be tested. One good statistical fit was obtained for the composite exponential at a low volume of 339 vph on a two-lane highway. The Pearson Type III was more representative at higher volumes. Although no other good statistical fits were obtained with these distributions, this may be considered more the rule than the exception, since there is such a variation in traffic flow due to factors that cannot be taken into consideration when vehicles are counted. To partially correct for this, we chose representative intervals to obtain an hour's data of specific volume. The closest fits for the Pearson Type III occurred, as expected,

Table 2. Comparison of results of the three distributions.

Volume (vehicles per hour per lane)	Composite Exponential		Pearson Type III		Log Normal	
	Chi Square	Good Fit	Chi Square	Good Fit	Chi Square	Good Fit
549	91.38	No	60.31	No	36.40	Yes
659	86.96	No	64.32	No	32.76	Yes
781	237.75	No	76.37	No	71.27	No
902	289.92	No	61.07	No	42.12	Yes
1,026	446.58	No	108.83	No	52.18	No
1,128	1,078.95	No	128.02	No	42.11	Yes
1,369	2,247.21	No	231.62	No	75.39	No

when noninteger values for the parameter k were used, although this does not improve the fit enough to be statistically good.

The resulting statistically good fits with the log-normal distribution were actually better than expected. They indicate as the plots tended to suggest that the log normal is a better prediction of headways than the other two distributions.

ACKNOWLEDGMENTS

The research reported in this paper was sponsored by the Ohio Department of Highways in cooperation with the Federal Highway Administration while the author was associated with Transportation Research Center, Ohio State University.

REFERENCES

1. W. F. Adams. Road Traffic Considered as a Random Series. Journal of Institute of Civil Engineers, 1936.
2. J. Aitchison and J. A. C. Brown. The Lognormal Distribution. Cambridge Univ. Press, New York, 1957.
3. J. M. Aitken. Simulation of Traffic Conditions at an Uncontrolled T-Junction. Traffic Engineering and Control, Oct. 1963.
4. J. Evidente. Vehicular Headway Distribution on Upgrades of 2-Lane Rural Highways. Dept. of Civil Engineering, Ohio State Univ., MS thesis, 1964.
5. D. L. Gerlough. Traffic Inputs for Simulation on a Digital Computer. HRB Proc., Vol. 38, 1959, pp. 480-492.
6. B. D. Greenshields and F. M. Weida. Statistics With Applications to Highway Traffic Analyses. Eno Foundation, 1952.
7. F. A. Haight. The Generalized Poisson Distribution. Annals of Institute of Statistical Mathematics, Tokyo, Vol. 11, No. 2, 1959, pp. 101-105.
8. F. A. Haight, B. F. Whisler, and W. W. Mosher, Jr. New Statistical Methods for Describing Headway Distribution of Cars. HRB Proc., Vol. 40, 1961, pp. 557-564.
9. Investigation and Measurement of Traffic Dynamics. Ohio State Univ., Rept. EES202C-1, 1965.
10. J. P. Kinger. Application of the Theory of Probability to Problems of Highway Traffic. Proc., Institute of Traffic Engineers, 1934.
11. A. D. May and F. A. Wagner, Jr. Headway Characteristics and Interrelationships of Fundamental Characteristics of Traffic Flow. HRB Proc., Vol. 39, 1960, pp. 524-547.
12. K. Pearson. Tables of the Incomplete Gamma Function. Cambridge Univ. Press, 1922.
13. A. Schuhl. The Probability Theory Applied to Distribution of Vehicles on Two-Lane Highways. In Poisson and Traffic, Eno Foundation, 1955.
14. J. E. Tolle. The Lognormal Headway Distribution. Traffic Engineering and Control, Vol. 13, No. 11, 1971.
15. J. E. Tolle and J. Treiterer. The Distribution of Vehicular Headways—A Stochastic Model. In Investigation of Traffic Dynamics by Aerial Photogrammetry Techniques, Ohio State Univ., Rept. EES278-2, 1969.

APPLICATIONS OF TRAFFIC FLOW THEORY IN MODELING NETWORK OPERATIONS

Sam Yagar, University of Waterloo, Ontario

ABRIDGMENT

Certain characteristics of roadway traffic flow, though conceptually simple in isolation, can create modeling problems in a network context. The following phenomena must be accurately represented in any network model used for evaluating traffic control measures: queue spillback, cost of queuing on each link, flow-dependent capacities of weaving and merge sections, and dynamic sharing of merge capacity by its approaches. Some methods for modeling these traffic network idiosyncracies are outlined. These methods were incorporated in the development of the CORQ traffic model, which has been validated against field data and has been found sufficiently sensitive to be applied in evaluating detailed traffic control schemes.

•AN ASSIGNMENT technique (1) that introduced the concept of queuing analysis for treating time-varying demands was found to be too general for use as a tool for evaluating traffic operations. It left a number of important questions related to road-specific networks unresolved. These were addressed (2) in the development of CORQ, a model for predicting traffic flows and queues in a corridor.

The CORQ model is based on a dynamic traffic assignment procedure (1) that divides a time period (e.g., a peak period) into a set of time slices, each of which is sufficiently short that the demand rates between origin-destination (O-D) pairs can be considered constant. There is a separate O-D matrix for each time slice. These O-D matrices are assigned to the network in order. Queuing is allowed, and its effect on travel time is reflected in the path choice phenomenon. After each time slice the network is cleared of all flows and queues. The queued vehicles are represented in the next time slice by being added to the demands for that time slice. They are then reassigned to their destinations.

This paper identifies some traffic flow characteristics that should be represented in a flow prediction model and outlines some methods for accomplishing this. The procedures used to simulate these phenomena in the CORQ model are described. The following types of phenomena had to be represented in the CORQ model:

1. Queue spillback,
2. Cost of queuing on each link,
3. Flow-dependent capacities of weaving and merge sections, and
4. Dynamic sharing of merge capacity by its approaches.

Because the general assignment technique could not simulate the effects of queue spillbacks, queue costs were attributed to the use of the bottlenecks rather than the use of the links, where the delay time is actually spent. The capacities of weaving and merge sections on freeways can vary with the flows in these sections. Therefore, neither flows nor capacities are known in advance. Further, the sharing of capacity at merge sections (e.g., freeway on-ramps) by competing approaches to the merge is a function of the demands at each of those approaches. There is little difficulty in describing and understanding these idiosyncracies of road traffic. However, preservation of their traffic flow properties in the context of a traffic assignment model is an-

Publication of this paper sponsored by Committee on Traffic Flow Theory and Characteristics.

other matter. They must be represented sufficiently accurately for use in a micro type of model. The model must be precise enough to evaluate various traffic control schemes. The procedures used to represent the above traffic idiosyncracies in the CORQ model are outlined briefly herein. They are described in greater detail elsewhere (2).

QUEUE SPILLBACK

If a queue spills back through a diverge or an intersection it can delay vehicles that do not even use the bottleneck, i. e., vehicles that leave the queue downstream of that bottleneck and create no delay for other users. Users of the link with the bottleneck are generally not delayed further, regardless of the physical length of the queue.

Whenever a link absorbs vehicles at a greater rate than it can discharge them, its queue grows at a rate equal to the difference of these rates. This is caused by a limited ability of a downstream link to absorb vehicles because of flow capacity or a spillback of its own. The physical size of a queue is not important until spillback occurs, which causes delays to vehicles that will not even use the bottleneck.

The spillback process can be modeled by keeping track of the number of queued vehicles on each link and comparing this to the average physical queue capacity of the link. Because the physical queue on a link has no effect on other links until it backs through a node to another link, this additional information is sufficient. When a queue does spill upstream, the delay attributed to each link should be proportional to the size of the queue on that link divided by its discharge rate at the prevailing conditions.

REPRESENTATION OF LINK COSTS

The cost of using a link is a combination of

1. Flow, the unit cost of travel corresponding to the flow on the link, and
2. Queuing, the cost of being delayed in queue if there is a physical queue on the link.

The total cost for the link is treated as if the user drives along the link at a constant speed until he reaches the tail of the queue, where he begins to drive more slowly toward the downstream end and waits his turn to leave the link. The flow cost represents the time spent in reaching the tail of the queue. The queue cost represents the time that he is moving to the downstream end of the queue. The latter is not all delay, for he is simultaneously working his way to the downstream end of the link. It has been treated as above to take accurate account of time spent on a link and to count the time spent moving in the queue only once. This method is compatible with the modeling procedure of CORQ and takes full account of the time spent on a link without requiring the detailed space-time trajectories of the vehicles.

The unit cost of travel on a link, excluding queuing, can be obtained as a function of flow (less than capacity) in a straightforward manner such as a floating vehicle technique. This function is then approximated by piecewise linear sublink components (2) for use in the model's incremental assignment procedure. When there is queuing on the downstream portion of the link, the flow cost for the link is factored down to represent the actual cost for just the upstream portion of the link that allows flow in the nonqueuing mode.

The unit cost of queuing is also approximated by piecewise linear components. The queue service rate is estimated dynamically within the model as a function of existing conditions within the network. It is always proportional to the rate at which vehicles are discharged at the downstream end of the queue. In the simplest case, it is equal to the saturation flow rate for the downstream link serving the queue. The treatments of more complicated cases, such as a merge or diverge, are described elsewhere (2).

CAPACITY OF WEAVING SECTIONS

A traffic flow prediction model should contain a technique to dynamically estimate weaving capacities as estimates of traffic flow change. However, even the estimation of weaving capacities based on known flows does not seem fully resolved. Weaving studies to date (3, 4) have emphasized design of weaving sections rather than estimation of capacity for existing weaving flows.

MERGE CAPACITIES

The total capacity of a merge can vary, and, furthermore, the capacities of its approaches generally depend on one another's flow. These relationships can best be determined empirically for a given merge. Because the ultimate values of flow-dependent capacities cannot be known before the flows are known, they should be reestimated dynamically as the estimates of the flows change during the network loading process. These problems are outlined below, along with some methods for dealing with them.

Capacity of the Downstream Section

Except for weaving sections, capacity of the downstream link of a merge is generally affected only by a breakdown in flow. The occurrence of breakdowns seems random, but their incidence increases greatly as flow levels approach or even exceed the average capacity of a section.

Total merge capacity is generally treated as independent of the approach flow mix, inasmuch as breakdown and queuing generally begin just downstream of the merge after the flows on the competing approaches have successfully merged. The queuing is therefore caused by excessive merging traffic overloading the downstream link and not by friction caused by the merge. Buckley and Yagar (5) argue that the occurrence of a merge may even boost capacity.

The throughput capacity of a poorly designed merge could vary with the flow mix on the approaches. However, a preliminary study of some actual merges indicated that the approach flow ratio generally does not affect capacity, so that merge capacity can be treated as independent of the flow mix on the approaches. In isolated cases where this approximation is not accepted, the total equivalent through flow could be restricted at the merge to reflect any effect of flow mix variation on the merging capacity. The CORQ computer program (2) already has provision for this.

Sharing of Merge Capacity by the Approaches

Even where the total merge capacity is independent of its flow mix the approaches to the merge have component capacities that depend on one another's flow. When the total merge capacity is independent of the flow mix, the approach capacities are complementary. When each approach has greater demand than the merge will absorb from it, queues build upstream on both approaches. In this particular case the capacity of each approach depends on its ability to discharge vehicles into the merge during this state of competition for the merge. This particular capacity is defined as the capacity entitlement of the approach, for it is always available to the approach. These entitlements can be determined by counting the respective merging rates when there is queuing on both approaches. When one approach does not require all of its entitlement, the other approach can make use of the unused entitlement.

Estimating Capacities From Entitlements and Extrapolated Partial Flows

The phenomenon of capacity sharing at a merge section can be modeled quite easily if the demands on the two competing approaches are known. However, the flows cannot be assigned until the capacities are known, while the merge capacities in turn depend on the competing demands. To simulate the sharing of merge capacity when the flows are not known in advance, the CORQ model has a dynamic capacity borrowing routine and a dynamic entitlement updating routine.

Capacity-Borrowing Routine

This routine is considered after each increment (6) of assignment. If one of the approaches is out of capacity and another is projected to have an excess at the end of the time slice, the latter may lend some capacity to the former.

The capacity-borrowing routine also has some optimization characteristics. A common goal of freeway operations is to operate a bottleneck merge at capacity without having a queue on the freeway. The traffic analyst can model this by simulating traffic-responsive metering to predict its effects in the corridor. The analyst merely gives the main-line approach sufficient entitlement (perhaps even the total merge capacity) that it will not have a queue and uses the capacity-borrowing routine in the simulation. The merge capacity not needed by the main-line approach is passed on to the on-ramp. Use of the incremental assignment technique may result in poor projections of ultimate link flows. This might be countered by further iterations of incremental assignments using new capacity entitlements.

Entitlement-Updating Routine

Varying the capacity entitlements based on the results of the previous iteration tends to give oscillating results if a significant number of drivers have a path choice that is sensitive to merge capacities, resulting in their swinging from one approach to the other of the same merge. However, the amplitude of the oscillation tends to decrease with each iteration. In the applications (2) that were performed by the author it was found that four to six iterations generally gave reasonably good results.

The user who can estimate his merge demands sufficiently well without the routines for merge sharing or entitlement updating need not use these options and may go immediately to the final step. However, the author's experiences have found these routines to be very helpful in closing in on the final merge entitlements in spite of the problems in using them.

SUMMARY

To be practical, a model for evaluating strategies of traffic operations and control must be precise. Certain properties of traffic flow that previously did not require detailed treatment are critical in models that assign traffic to a network. For the CORQ model, it was necessary to address the phenomena of queue spillback, cost of temporary queuing on a link, dynamic determination of the capacities of weaving and merge sections, and dynamic sharing of merge capacity by the approaches to a merge. Routines were developed for modeling the occurrences and effects of these phenomena in a manner compatible with the needs of CORQ. Although these problems have not necessarily been fully resolved, they have been at least identified. Furthermore, the interim treatment that they received was sufficient to create a model that has been validated against field data (7) and found sufficiently sensitive (8) to be applied in evaluating a variety of detailed traffic control schemes.

Although the outlined routines have served as an interim measure to bridge a gap

for the needs of the CORQ model, there is room for improvement especially in those related to dynamic estimation of weaving capacity and dynamic sharing of merge capacity. Further, some improvement in modeling of the merge-sharing phenomena to further automate applications could reduce the time and effort requirements of the user. The extent to which this could in fact be accomplished is limited by the use of an incremental type of assignment technique that is good for modeling queuing processes but tends to oscillate among various shortest paths.

REFERENCES

1. S. Yagar. Dynamic Traffic Assignment by Individual Path Minimization and Queuing. Transportation Research, Vol. 5, 1971, pp. 179-196.
2. S. Yagar. Dynamic Assignment of Time-Varying Demands to Time-Dependent Networks. Transportation Development Agency, Ministry of Transport of Canada, 1974.
3. L. J. Pignataro et al. Weaving Areas: Design and Analysis. NCHRP Rept. 159, 1975.
4. L. J. Pignataro, W. R. McShane, K. W. Crowley, B. Lee, and R. P. Roess. Weaving Area Operations Study: Analysis and Recommendations. Highway Research Record 398, 1972, pp. 15-30.
5. D. J. Buckley and S. Yagar. Capacity Funnels Near On-Ramps. Proc., International Symposium on Transportation and Traffic Theory, Sydney, Aug. 1974, pp. 87-104.
6. S. Yagar. Emulation of Dynamic Equilibrium in Traffic Networks. Proc., International Symposium on Traffic Equilibrium Methods, Montreal, Nov. 1974.
7. S. Yagar. An Analysis of the Morning Peak Traffic Problems in the Eastbound Corridor Serving Ottawa. Ministry of Transportation and Communications, Ontario, April 1973.
8. S. Yagar. Measures of the Sensitivity and Effectiveness of CORQ. Transportation Research Record 562, 1976.

FIRST-YEAR EFFECTS OF THE ENERGY CRISIS ON RURAL HIGHWAY TRAFFIC IN KENTUCKY

Kenneth R. Agent, Donald R. Herd, and Rolands L. Rizenbergs,
Kentucky Department of Transportation

The Arab oil embargo in mid-October 1973 curtailed availability of gasoline. Fuel conservation measures resulted in reduced travel and lower traffic speeds. On March 1, 1974, posted speed was set at 55 mph (88 km/h) on rural highways in Kentucky. Traffic volumes, speeds, and accidents for the rural highway during the period known as the energy crisis and its aftereffects were compared to those during the corresponding period a year earlier. Traffic volumes began to decline in December 1973 and continued through September 1974. Total travel in the 12 months through November 1974 decreased by 2.3 percent; traffic increased by 5 percent in 1973. Accident rates during this period decreased by 13.5 percent, and the largest decreases were associated with the highways experiencing the greatest reductions in travel speed. Accident rates decreased substantially as traffic speeds decreased. Differences between wet-surface and dry-surface accident rates were especially significant and were more so for Interstate than for two-lane highways. Improved wet-pavement skid resistance due to lower speeds obviously contributed to a reduction in accident rates. Continuation of the 55-mph (88-km/h) speed limit on all rural highways would seem advisable.

•THE energy crisis became a reality to motorists during the last months of 1973. Previously, the public had ignored warnings of fossil fuel shortages. Events, however, demonstrated the seriousness of the problem. Gasoline availability became critical. Voluntary (later mandatory) adherence to lower speed limits reduced traffic speed. Traffic volumes decreased. The public's rush to purchase smaller cars exhausted inventories. Driving habits and life-styles changed. Speculation concerning effects on accident experience abounded in the press and in the professional community. Significant and perhaps lasting changes in highway transportation were being shaped.

The gasoline shortage became critical soon after the Arab oil embargo began. The Arab oil-producing nations began withholding oil from the United States in mid-October 1973. On November 7, 1973, the President addressed the nation on the criticality of the situation and requested voluntary energy conservation measures such as reducing travel and lowering travel speeds. Gasoline allocation to service stations was initiated. In December 1973 came gasless Sundays; most service stations were closed from 9 p.m. Saturday until Monday morning. The truckers' strike in February 1974 intensified the awareness of the gasoline shortage. On March 1, 1974, Kentucky's speed limits were reduced to 55 mph (88 km/h). The oil embargo ended in mid-March. Gasoline again became plentiful but at a much higher price.

This report presents data and analysis of traffic volumes, speeds, and accidents on rural highways in Kentucky as affected by the energy crisis.

Publication of this paper sponsored by Committee on Traffic Flow Theory and Characteristics.

PROCEDURE

Accident and traffic volume data were collected for each month between December 1971 and November 1974. Accident data were obtained from computer tapes containing all accidents for rural areas reported by state police. Therefore, only rural accidents (including cities with less than 2,500 population) were considered. Five of the more populous counties were excluded, inasmuch as local police investigate most accidents within those counties.

The report deals with the total rural system as well as the various highway types comprising the total system. The highway system was divided into the following types:

1. Two-lane,
2. Three-lane,
3. Four-lane, undivided,
4. Four-lane, divided (no access control),
5. Interstate, and
6. Parkway (toll road).

Volume data for each month were obtained from the automatic traffic recording (ATR) stations located throughout the state. Volumes were converted into vehicle miles (kilometers) of travel for each type of highway. The total vehicle miles (kilometers) of travel for 1972 (1) were used as the base or reference. Data from the ATR stations were summarized by month. The percentage of the total traffic counted in 1972 was calculated for each month. The total vehicle miles (kilometers) of travel on a particular highway type from 1972 were then multiplied by an adjustment factor for each month to obtain the monthly volumes. These volumes were also adjusted for new highway openings. There were 29 ATR stations on two-lane highways but none on three-lane highways. The factors obtained for the two-lane highways were used for three-lane highways. There was only one usable ATR station for rural four-lane highways. The factors obtained from this station were used for both four-lane divided and undivided highways. Five ATR stations were located on rural Interstate highways. The monthly factors for parkways were obtained from monthly counts of total traffic on the toll road system made available by the Kentucky Toll Road Authority. Annual growth factors from 1971 to 1972, 1972 to 1973, and 1973 to 1974 were then calculated for each month and used to find the monthly traffic volumes in 1971, 1973, and 1974. Volumes from the ATR stations were used in the analysis of traffic volumes. Inasmuch as sections of new highways were added during the study period, vehicle miles (kilometers) of travel used for rate calculations reflect changing road lengths.

From the accident and volume data, monthly accident rates [accidents per 100 million vehicle miles (accidents per 160 million vehicle kilometers)] were calculated for each highway type. Accident severity was studied, and the number of fatalities and injuries for each month was obtained.

Traffic speed data were obtained at two Interstate locations, one four-lane highway location, and two two-lane highway sites before and after initiation of the 55-mph (88-km/h) speed limit. The average, median, and 85th percentile speeds and speed distributions were determined as well as the 10-mph (16-km/h) pace and the percentage of vehicles in the 10-mph pace. The pace is the increment of speed including the greatest number of vehicles.

RESULTS

The findings presented here pertain to the total rural highway system, approximately 23,000 miles (37 000 km) of roads, and its major components in Kentucky. Monthly data of one year were compared to the data of the corresponding month in the preceding year. This method best illustrated changes occurring during otherwise comparable periods of time. Three-lane and four-lane undivided highways, however, will not be discussed here because of their limited mileage.

Figure 1. Monthly traffic volumes for total rural highway system.

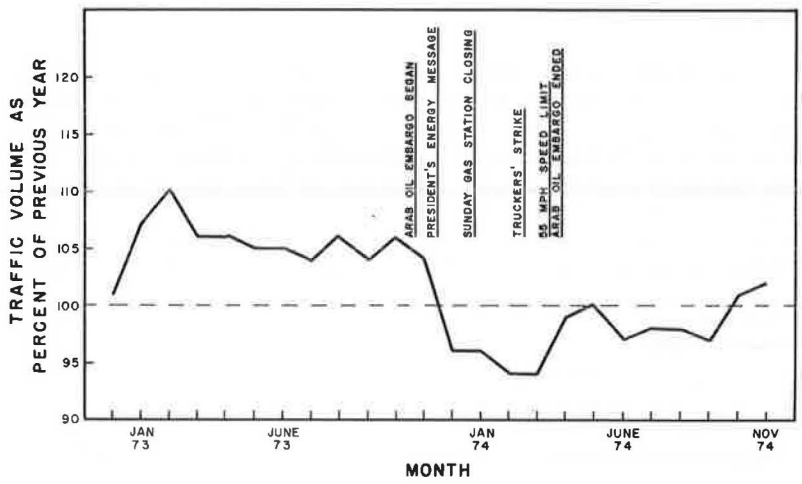

Figure 2. Monthly traffic volumes by highway type.

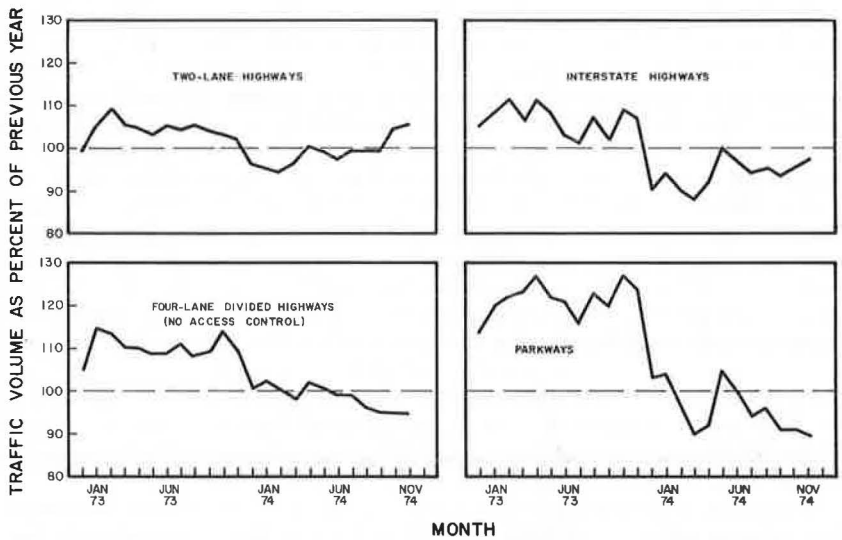

Table 1. Summary of volume data by highway type.

Highway	Period[a]	Volume (MVM)[b]	Volume Decrease (percent)
Two-lane	1973	8,979	
	1974	8,864	1.3
Four-lane divided (no access control)	1973	659.9	
	1974	649.4	1.6
Interstate	1973	2,267	
	1974	2,131	6.0
Parkway	1973	579.0	
	1974	555.0	4.1
Four-lane undivided	1973	113.6	
	1974	109.6	3.5
Three-lane	1973	52.1	
	1974	51.6	0.8
Total system	1973	12,650	
	1974	12,361	2.3

[a]1973 is Dec. 1972 through Nov. 1973; 1974 is Dec. 1973 through Nov. 1974.
[b]Million vehicle miles (1.61 million vehicle kilometers).

Traffic Volume

An evident effect of the energy crisis has been the reduction in traffic volume. Monthly volumes for the total rural system are shown in Figure 1. December 1973 was the first month in which volume dropped below the corresponding month of the previous year. In the past, volumes increased by about 5 percent annually as exhibited by the months preceding December 1973. The decrease in traffic volume after December 1973 continued through September 1974 and reached a maximum in March 1974. In October and November 1974, traffic volumes increased compared to the previous year. The effect of the energy crisis on traffic volumes appeared to have lessened. For a 12-month period (December 1973 through November 1974), the total vehicle miles (kilometers) driven decreased by 2.3 percent compared to the same period a year earlier. The decrease was significant in light of a 5 percent increase experienced previously.

Major events of the energy crisis are also shown in Figure 1. Traffic volumes began to drop shortly after the start of the oil embargo in October 1973 and continued to drop until the end of the oil embargo in March 1974. Reduction in traffic volumes gradually lessened. By October and November 1974, volumes exceeded those of the same months of the previous year.

Trends in volume changes for the various highway types were similar (Figure 2). In all cases, December 1973 was the first month that showed a large decrease compared with the preceding year. The maximum reductions occurred in February and March 1974. Interstate highways and parkways showed the largest reduction in volume. This is as expected because minimizing long-distance travel by the public was considered foremost. The increase in parkway volume in 1973 was partially due to the opening of a new parkway in December 1972. The volume on the parkway, however, was minimal compared to the whole highway system. Two-lane and four-lane divided (no access control) highways had a smaller decrease in volume because of the local traffic on these types of highways. A comparison of traffic volumes for the 12-month period (December 1973 through November 1974) with those for the same period a year earlier is given in Table 1. There was a large reduction in Interstate and parkway volumes in comparison to two-lane and four-lane divided (no access control) highways. Data in this table include some new sections of highways opened during the study period.

Speed

Imposition of the 55-mph (88-km/h) speed limit placed a definite constraint on traffic speed. Even before then, conservation efforts by drivers had resulted in reduced travel speeds. Table 2 gives the average, median, and 85th percentile automobile and truck speeds and 10-mph (16-km/h) pace on Interstate highways. In June 1973, the median speed was 69.1 mph (111.2 km/h) for cars and 62.0 mph (99.8 km/h) for trucks. Some speed reduction occurred by November and again in February for all vehicles. In March 1974, after the speed limit was changed, median speeds dropped by 14.2 mph (22.9 km/h) for cars and 8.5 mph (13.7 km/h) for trucks compared with June 1973. Car and truck speeds have increased slightly since the initiation of the lower speed limit. A comparison of November 1974 speeds with March 1974 speeds shows that the median speed has increased by 1.0 mph (1.6 km/h) for cars and 1.9 mph (3.1 km/h) for trucks. However, the 85th percentile speed has remained around 60 mph (97 km/h) for both cars and trucks.

An important aspect of traffic speed is uniformity. An index to uniformity is the 10-mph (16-km/h) pace, which is the speed range in which the greatest percentage of vehicles operate. Table 3 gives the percentage of vehicles on Interstate routes in the pace and shows that the percentage increased as traffic speed decreased. This means that the average variance in speeds between vehicles has decreased. This may contribute to a reduction in accidents (2).

Average driving speeds and 10-mph (16-km/h) paces for four-lane divided (no access control) and two-lane highways are given in Table 3, which includes data from before and after the speed limit reduction. The changes in speeds on both types of highways

were similar. Median automobile speeds decreased by about 4 mph (6 km/h), and median truck speeds decreased by about 2 mph (3 km/h). No significant change in percentages of vehicles in the pace was evident on the four-lane divided (no access control) highways. On two-lane roads, the percentage of vehicles in the pace increased.

Table 4 gives the percentage of vehicles that exceeded the posted speed both before and after the energy crisis. The percentages of trucks that exceeded the speed limit on Interstate roads after the speed reduction are similar to those for automobiles. On two-lane highways, the truck speed limit was increased from 50 to 55 mph (80 to 88 km/h). The increased speed limit reduced the percentage of trucks exceeding the posted limit from 32 to almost zero.

Accidents

December 1973 was also the first month that experienced fewer accidents compared to the year before. Except for January 1974, the number of accidents in the first months of 1974 was considerably less than that for the corresponding months in 1973. During the months preceding December 1973, accidents had increased on the average by more than 10 percent over the year before. The largest decrease in accidents occurred in March and April 1974, after the speed limit was reduced on March 1, 1974. There were also decreases in volume. The number of accidents in the later months of 1974 remained below 1973 levels, but the reductions in numbers of accidents lessened.

All four highway types experienced a decrease in accidents for almost every month in 1974. March and April 1974 showed the largest decreases. Interstate and four-lane divided (no access control) highways had the most dramatic drop in accidents. The number of accidents on parkways has fluctuated widely, but the largest decrease occurred in March 1974. The decrease in accidents continued through November 1974. On two-lane highways, the monthly percentage of accidents first dropped below that of the previous year in December 1973. This decrease continued through November 1974 to 76 percent in April. The decrease lessened in the late months of 1974. On four-lane divided (no access control) highways, the number of accidents has remained below that of the previous year since August 1973, except for January and June 1974.

Monthly accident rates on the total rural system first showed a significant decrease compared to the year before in March 1974, although there were indications of a decreasing accident rate before then (Figure 3). In November and December 1973, the accident rate dipped slightly below that of the same months in 1972. In January 1974, there was an increase, but the rate again decreased in February. After the speed limit reduction on March 1, 1974, the accident rate reduced sharply compared to that of the year before. The reduced accident rate has continued through November 1974, and reached a minimum during April. The accident rate for the period between December 1973 and November 1974 was 186 accidents per 100 million vehicle miles (160 million vehicle kilometers) but was 215 during the same period a year earlier. Between 1970 and 1972, the rate was 204 (1).

The monthly variation in accident rates for the various highway types is given in Figure 4. Except for two-lane highways, there was a large variation in the monthly accident rates. March 1974 showed the largest decrease in accident rates for all highway types. The reduction in accident rates was greater for Interstate than for two-lane highways. This might be related to the fact that speeds decreased more on Interstate than on two-lane highways.

Pavement surface conditions (dry, wet, snow, or ice) should be considered whenever accident occurrences are compared. Weather conditions for the months of December 1973 through November 1974 were, therefore, compared to those for the corresponding months in the preceding year. Large differences were found for several months. The number of hours of snow and ice in January 1974 approximately doubled in comparison to January 1973; this may partially account for the increased accident rates, especially on Interstate highways. In April and July 1974, the hours of inclement weather decreased by about 50 percent compared to the same months a year earlier; this may have contributed to reduced accident rates for those months. There was also a 35

Table 2. Driving speeds and 10-mph (16-km/h) pace for Interstate highways.

Date	Speed (mph)						10-mph Pace			
	Average		Median		85th Percentile		Percent		Range (mph)	
	Cars	Trucks	Cars	Trucks	Cars	Trucks	Cars	Trucks	Cars	Trucks
June 1973	68.4	62.6	69.1	62.0	75.4	67.6	50	68	64 to 73	59 to 68
Nov. 1973	64.3	60.7	64.4	60.7	69.5	65.2	64	70	61 to 70	51 to 66
Feb. 1974	62.5	59.9	61.3	58.8	67.4	64.3	64	66	57 to 66	55 to 64
March 1974	55.9	53.8	54.9	53.5	59.1	51.1	79	76	51 to 60	49 to 58
May 1974	59.0	57.4	57.8	56.2	62.8	60.3	74	79	55 to 64	53 to 62
July 1974	58.8	59.1	57.2	57.5	61.8	62.6	82	79	53 to 62	53 to 62
Sept. 1974	58.1	54.2	56.9	53.7	61.8	57.7	75	74	53 to 62	49 to 58
Nov. 1974	56.9	56.3	55.9	55.4	60.3	59.1	72	82	51 to 60	51 to 60

Note: 1 mph = 1.6 km/h.

Table 3. Driving speeds and 10-mph (16-km/h) pace for two-lane and four-lane divided (no access control) highways.

Highway Type	Date	Speed (mph)						10-mph Pace			
		Average		Median		85th Percentile		Percent		Range (mph)	
		Cars	Trucks	Cars	Trucks	Cars	Trucks	Cars	Trucks	Cars	Trucks
Two-lane	1972	56.0	47.7	54.9	47.3	60.2	53.4	61	55	53 to 62	41 to 50
	1974	52.0	46.2	50.3	46.0	56.4	51.3	70	63	45 to 54	43 to 52
Four-lane divided (no access control)	1972	57.2	53.2	56.5	53.0	61.6	57.3	66	69	53 to 62	47 to 56
	1974	53.7	50.9	52.9	50.1	58.3	55.9	65	62	49 to 58	47 to 56

Table 4. Percentage of vehicles exceeding posted speed limit before and after energy crisis.

Highway Type	Posted Speed Limit (mph)	Percentage of Vehicles Exceeding Limit	
		Cars	Trucks
Interstate	70	40	6[a]
	70 ± 5[b]	16	
	55	58	55[c]
	55 ± 5[b]	18	
Two-lane	60	19	
	55	19	0[d]
Four-lane, divided	60	28	
	55	35	

Note: 1 mph = 1.6 km/h.

[a]One percent exceeded 75 mph (121 km/h).
[b]Consideration of 5-mph (8-km/h) tolerance.
[c]Twelve percent exceeded 60 mph (97 km/h).
[d]Before speed limit was increased from 50 to 55 mph (80 to 88 km/h), 32 percent of trucks exceeded limit.

Figure 3. Monthly accident rates for the total rural highway system.

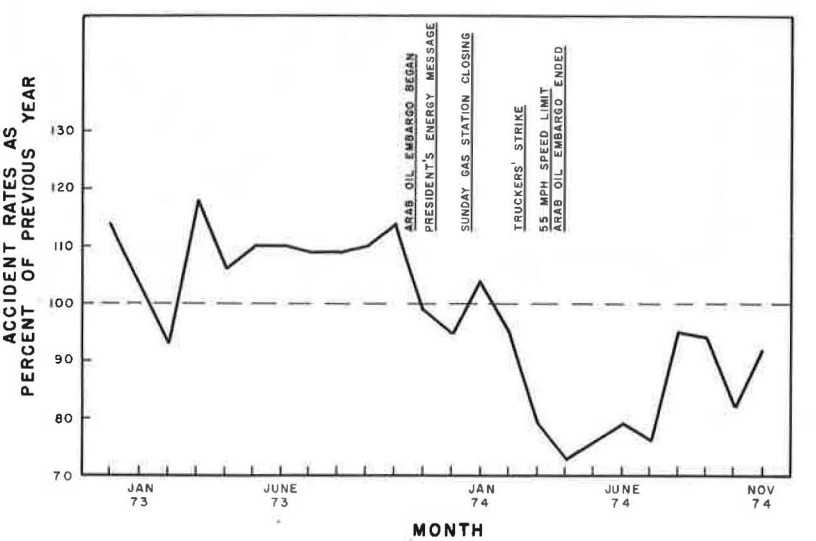

Figure 4. Monthly accident rates by highway type.

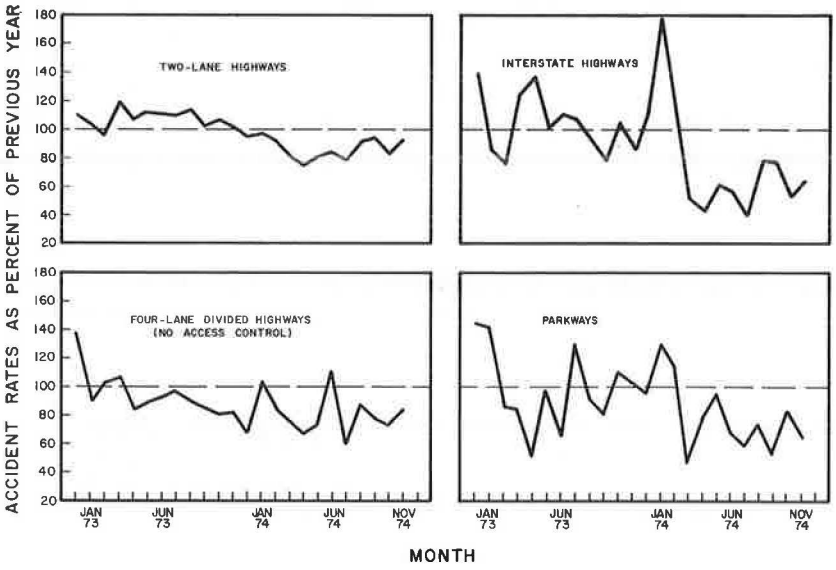

Figure 5. Monthly injury rates for the total rural highway system.

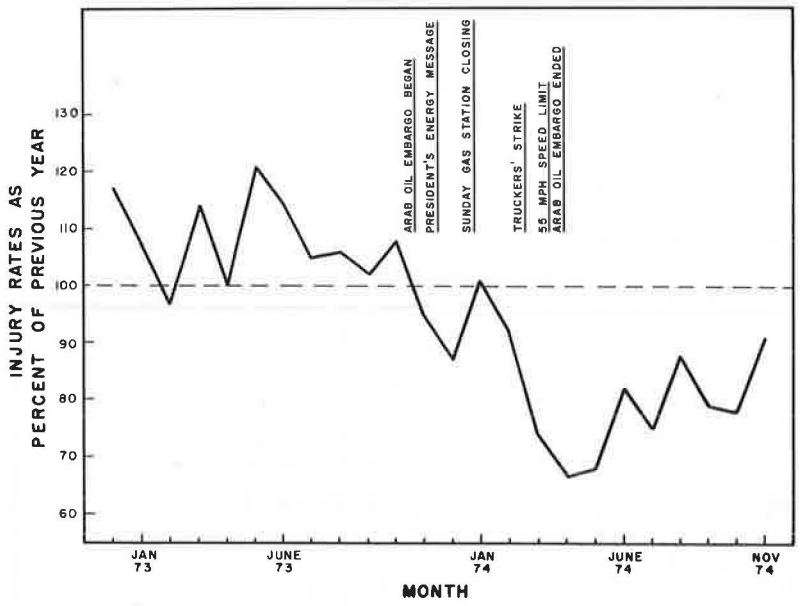

percent reduction in inclement weather in October 1974, which may explain the large accident rate decrease that month. In August and September 1974, hours of inclement weather more than doubled and the number of accidents increased. However, when the 12-month periods were compared, there was a difference of only 4 percent in inclement weather (1974 was slightly higher). Weather, therefore, should not have affected the total accident experience significantly.

Fatalities

The monthly variation in fatalities has fluctuated considerably. The number of fatalities has remained below that of the preceding year from December 1973 through November 1974. The total number of fatalities from December 1973 (when the energy crisis seemed to have an impact) through November 1974 was compared to that of the same time periods 2 years earlier. The number of fatalities dropped from 832 to 555, a reduction of 32 percent. At the same time, vehicle miles (kilometers) driven dropped by only 2.3 percent.

The average change in fatalities, based on the average of the 2 previous years, was a 32 percent decrease for two-lane highways, a 76 percent decrease for parkways, a 14 percent increase for four-lane divided highways, and a 40 percent decrease for Interstate highways.

A very wide fluctuation in fatality rate was also observed for the total rural system during the study period. As with fatalities, the fatality rate has remained below the rate of the preceding year (December 1973 through November 1974) except for 2 months. The lowest fatality rate occurred in December 1973. The fatality rate for the period December 1973 through November 1974 was 4.5 fatalities per 100 million vehicle miles (160 million vehicle kilometers); the rate was 6.6 fatalities per 100 million vehicle miles (160 million vehicle kilometers) for the same period a year earlier. The drop in fatality rate, therefore, was considerable (32 percent).

The fatality rate decreased on all major highway types except on four-lane divided (no access control) highways, where the rate increased by 23 percent. The decreases in fatality rate were 81 percent on parkways, 34 percent on Interstate highways, and 31 percent on two-lane highways. The largest decreases, therefore, were on those highway types where the previous speed limit was 70 mph (113 km/h).

Injuries

There was a pronounced change in the number of injuries since December 1973. In the months preceding December 1973, the number of injuries increased on an average of more than 10 percent over that of the previous year. In April 1974, the injuries reached a minimum of only 66 percent compared to April 1973. The reduction in injuries lessened in the later months of 1974.

All highway types had a reduced number of injuries in 1974; the greatest decreases occurred in March, April, and May. Interstates and parkways had the largest decrease: a 40 percent reduction for the 12-month period. The number of injuries on two-lane highways first dropped below that of the previous year in December 1973 and remained lower through November 1974. For four-lane divided (no access control) highways, the number of injuries has fluctuated widely.

The change in the injury rate for the total rural system (Figure 5) since the beginning of the energy crisis was very similar to the change in the number of injuries. With the exception of January 1974, every month since November 1973 has been below the corresponding month in the preceding year. The large drop in the injury rate occurred in March 1974 and has continued through November 1974, although the reductions have lessened.

The variation in injury rates by highway type is shown in Figure 6. For Interstate, parkway, and four-lane divided (no access control) highways, injury rates have fluctuated above and below the rates for the previous year since the first months of 1973,

Figure 6. Monthly injury rates by highway type.

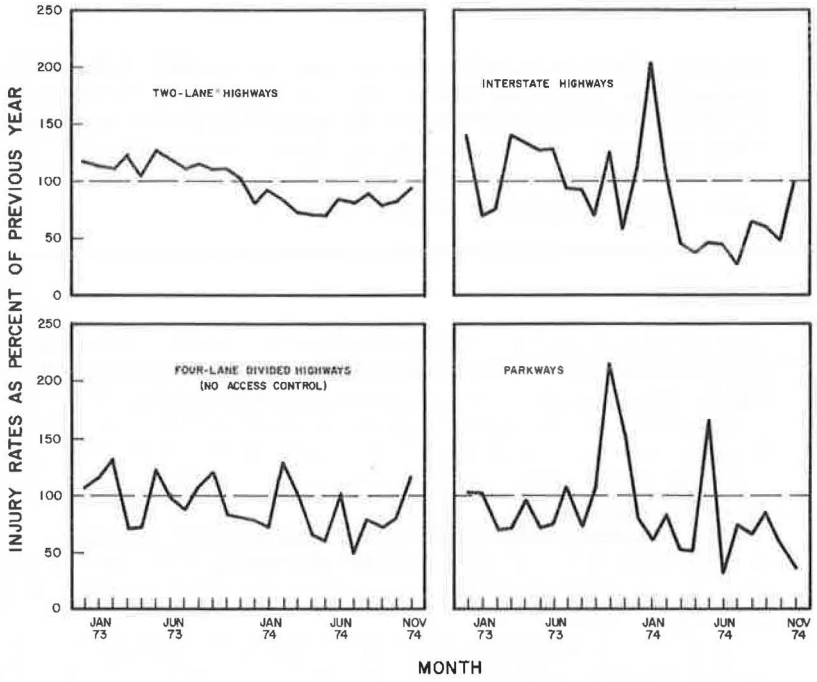

Table 5. Summary of accident data for various pavement surface conditions.

		All Accidents			Dry-Surface Accidents			Wet-Surface Accidents			Snow or Ice Accidents		
Highway Type	Period	Number*	Rate	Rate Decrease (percent)	Number	Rate	Rate Decrease (percent)	Number	Rate	Rate Decrease (percent)	Number	Rate	Rate Decrease (percent)
Two-lane	1973	23,197	258		17,138	229		5,468	414		591	313	
	1974	20,106	227	12.0	14,805	202	11.8	4,370	371	10.4	931	250	20.1
Four-lane divided (no access control)	1973	1,051	159		736	134		271	279		44	317	
	1974	809	125	21.4	585	109	18.7	175	203	27.2	49	179	43.5
Interstate	1973	2,082	92		1,361	72		554	166		167	348	
	1974	1,390	65	29.3	908	52	27.8	211	74	55.4	271	301	13.5
Parkway	1973	373	64		260	54		82	96		31	254	
	1974	288	52	18.8	196	43	20.4	41	56	41.7	51	219	13.8
Total system	1973	26,703	214		19,495	185		6,375	343		833	318	
	1974	22,593	185	13.6	16,494	164	11.4	4,797	296	13.7	1,302	254	20.1

*Includes only accidents where surface condition was stated.

Figure 7. Monthly accident rates and volumes for total rural highway system.

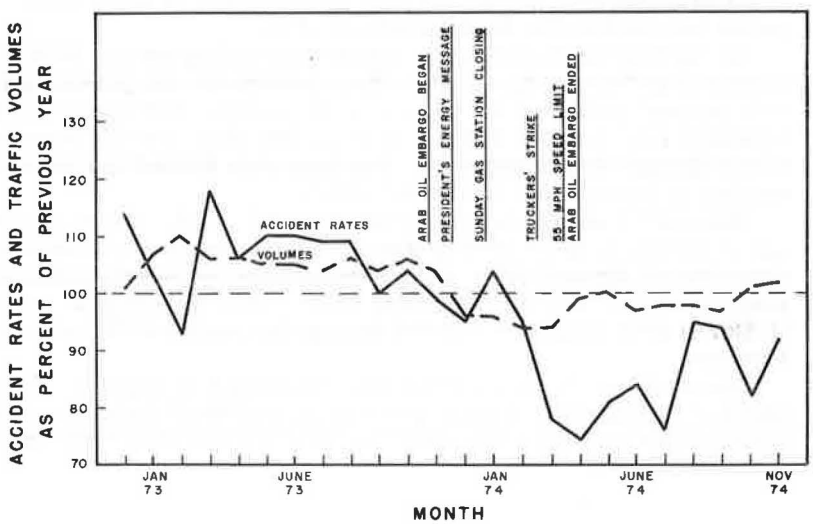

but the injury rate did decrease in 1974. The injury rate on two-lane highways first dropped below that of the previous year in December 1973 and reached 70 percent in April and May 1974.

Surface Conditions

Accident rates are higher on wet pavements than on dry pavements. Furthermore, research has shown that accident rates tend to increase as wet skid resistance diminishes (3). Table 5 gives accident rates in accidents per 100 million vehicle miles (160 million vehicle kilometers) for dry, wet, and snow or ice surface conditions for two periods of time. Accident rates were calculated from adjusted vehicle miles (kilometers) of travel under each surface condition by using precipitation data for the Lexington area. The assumption was made that Lexington weather data applied statewide and that traffic volumes did not differ for different surface conditions. The latter assumption in particular is not entirely true. Some reduction in travel probably occurs in wet weather, and travel certainly diminishes during snow or ice conditions. The accident rates in contrast to those cited in Table 5, therefore, would be lower for dry surfaces, somewhat higher for wet surfaces, and substantially higher for ice or snow surfaces.

Under dry conditions, the greatest accident rate decrease occurred on Interstate roads (27.8 percent) and parkways (20.4 percent). As shown earlier, the speed decreases were much larger on these highway types. It is important to note the substantial decrease in wet-weather accident rates on Interstates (55.4 percent) and parkways (41.7 percent). The reductions were far in excess of the corresponding decreases during dry conditions. Obviously, improved skid resistance at the lower travel speeds provides an added margin of safety and, therefore, contributes to a reduction in accidents. A similar decrease was found for four-lane divided (no access control) highways: 27.2 percent when wet and 18.7 percent when dry.

On two-lane highways, the decrease in wet-weather accidents (10.4 percent) was somewhat similar to that for dry-surface accidents (11.8 percent). It must be pointed out, however, that even a modest error in the precipitation data used in one of the periods could substantially influence the results.

During conditions of snow or ice, decreases in accident rates are evident on all highways as a result of lower posted speeds. The decreases were below those shown for dry and wet conditions for Interstates and parkways and above those for two-lane and four-lane divided (no access control) highways. No data were available to compare travel speeds under these conditions. It may be reasonable to assume, however, that traffic normally responds to severely hazardous driving conditions and reduces speeds accordingly. Changes in posted speeds, therefore, may not affect driving speeds to the same extent during inclement weather as during favorable weather. Again, assumed applicability of weather data may introduce errors.

DISCUSSION OF COMPARISONS

It was shown that fatalities, accidents, and injuries, as well as fatality rates, accident rates, and injury rates, have decreased since the beginning of the energy crisis. The question remains whether these decreases resulted from changes in traffic volumes, speeds, and the like or from any combination of contributing factors. As shown in Figure 7, the decrease in volume, which began in December 1973, corresponds to a reduced accident rate. Although volume reductions lessened in April and May, the accident rate reached its lowest point in April. In March 1974, the accident rate decreased dramatically, but the reduction in volume remained the same. Also, traffic volumes in October and November 1974 increased above those of the previous year, but the accident rate remained lower. The large accident rate decrease, therefore, corresponded with the lowering of the speed limit to 55 mph (88 km/h) on March 1, 1974. Total travel during the 12-month period decreased by 2.3 percent, and the accident rate decreased by 13.5 percent.

Figure 8. Relationship between median traffic speed (adjusted for automobiles and trucks) and accident rate for Interstate highways.

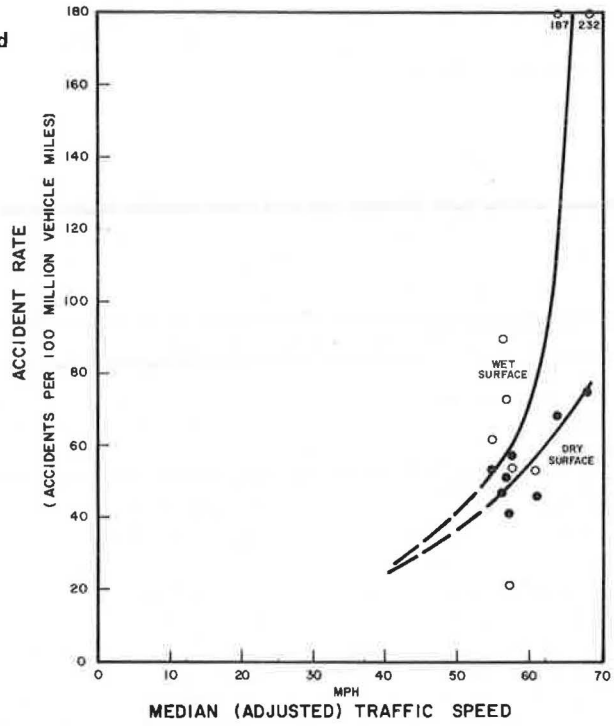

Figure 9. Relationship between median traffic speed (adjusted for automobiles and trucks) and accident rate for two-lane highways.

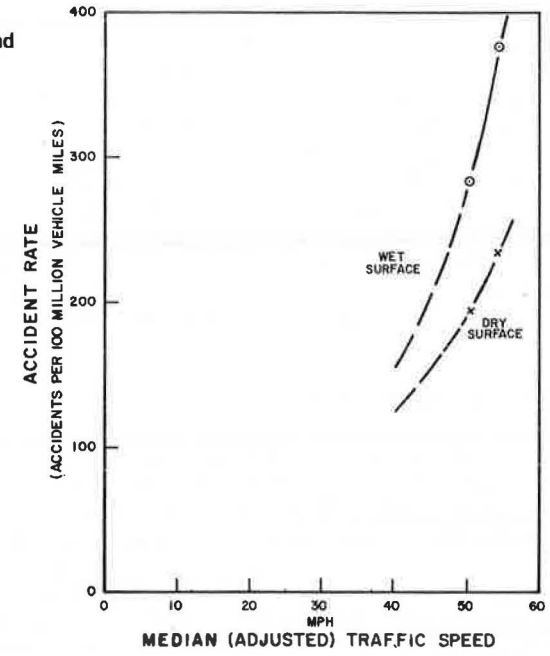

Table 6. Summary of accident data for various highway types.

Highway Type	Period	Accidents			Fatalities			Injuries			Severity Index
		Number	Rate	Rate Decrease (percent)	Number	Rate	Rate Decrease (percent)	Number	Rate[c]	Rate Decrease (percent)	
Two-lane	1973	23,276	259		715	8.0		15,132	169		2.78
	1974	20,209	228	12.0	486	5.5	31.2	12,256	138	18.3	2.66
Four-lane divided (no access control)	1973	1,054	160		17	2.6		650	98		2.50
	1974	815	126	21.2	21	3.2	23.1[a]	506	78	20.4	2.51
Interstate	1973	2,078	92		65	2.9		1,456	64		2.64
	1974	1,395	65	29.3	41	1.9	34.5	865	41	35.9	2.65
Parkway	1973	369	64		21	3.6		268	46		3.21
	1974	288	52	18.8	4	0.7	80.6	167	30	34.8	2.70
Total system[b]	1973	27,183	215		832	6.6		17,768	140		2.77
	1974	23,043	186	13.5	555	4.5	31.8	14,016	113	19.3	2.65

[a]Increase. [b]Includes three-lane and four-lane undivided (no access control) highways.

The relationship between traffic speed and accident rate for Interstate highways is shown in Figure 8 and for two-lane highways in Figure 9. Very limited (but precious) data points were available for plotting. The data points, of course, are subject to errors because of uncertainties on traffic speeds and volumes associated with various weather conditions. The plots do, however, bring to attention a disproportionate increase in accident rates as speed increases. The differences between wet-surface and dry-surface accident rates are especially significant and more so for Interstate highways than for two-lane highways. Improved wet-pavement skid resistance at the lower speeds obviously contributed to a reduction in accident rates. Reduced speed, therefore, has a greater effect on accident rates during wet-surface than during dry-surface conditions.

A summary of accident experience for various highways is given in Table 6. Fatality and injury rates decreased more than accident rates. The most dramatic impact, of course, must be the 277 lives saved between December 1973 and November 1974 when compared to the same period a year earlier. Whereas traffic volume and other contributing factors may account for some of the decrease in accident rates since the beginning of the energy crisis, lower travel speeds certainly stand out as the single most important reason why accident, fatality, and injury rates have decreased.

CONCLUSION

Decreases in accident rates associated with reducing the speed limit to 55 mph (88 km/h) from 70 mph (113 km/h) on Interstates and parkways and 60 mph (97 km/h) on two-lane roads have been dramatic. To safeguard the public from undue hazards associated with higher speed driving, continuation of maximum speed limit at 55 mph on all rural highways seems advisable.

REFERENCES

1. K. R. Agent. Relationships Between Roadway Geometrics and Accidents—An Analysis of Kentucky Records. Division of Research, Kentucky Department of Transportation, April 1974.
2. A Policy on Geometric Design of Rural Highways. American Association of State Highway Officials, 1965.
3. R. L. Rizenbergs, J. L. Burchett, and C. T. Napier. Accidents on Rural Interstate and Parkway Roads and Their Relationship to Pavement Friction. Division of Research, Kentucky Department of Transportation, Oct. 1973.

TRAFFIC CHARACTERISTICS OF SHOPPING CENTERS IN SOUTH AFRICA

P. W. B. Kruger, Olaus A. W. van Zyl, and Taylor N. Withrow,
Bruinette, Kruger, Stoffberg and Hugo, Pretoria

The existence of large regional shopping centers in South Africa is a relatively recent occurrence. As the scale, diversity, and number of all sizes of centers expanded, it became increasingly apparent that the applicability of overseas, particularly U.S., traffic design data often used should be tested. A different life-style and different hours of operation dictated that design standards for South African conditions needed to be reconsidered. This report summarizes such research.

•SHOPPING CENTERS in the Pretoria-Johannesburg metropolitan region were surveyed (Table 1). The classification of centers follows that commonly used (6); however, the scale is not of the same magnitude. Neighborhood centers are dominated by a supermarket and have less than 45,000 ft^2 (4180 m^2) of gross leasable floor area. Community centers are dominated by a department store and have from 45,000 to 200,000 ft^2 (4180 to 18 580 m^2) of gross leasable area (GLA). Regional centers have two or more department stores with over 300,000 ft^2 (27 870 m^2) of GLA. Hours of operation were generally 8:30 to 5:30 on weekdays and 8:30 to 1:00 on Saturdays. Surveys were normally conducted from a half hour before opening to a half hour after closing. Transit users and walk-in trade were negligible at all centers. The distinction between shopping and convenience goods followed the usual designation (2). Convenience goods include items purchased frequently and regularly such as food, drugs, and hardware. Shopping goods are items purchased selectively such as furniture, appliances, clothing, and jewelery. All indexes were related to GLA.

The traffic planner is mainly interested in two sets of shopping center activity values. One set measures the center activity during the street peak period and the other measures activity during the peak period of the center itself. The afternoon street peak period for the most part coincides with the weekday shopping peak period. Trip generation figures for this hour on an average weekday are needed to evaluate the effect of shopping center traffic on street traffic. (Some planners might prefer a peak weekday.)

The general sales patterns for South Africa indicate typical peak shopping activity at the end of each month and shortly before Christmas. The highest and lowest end-of-month peaks occur the week prior to Christmas and the last week in January, respectively. It was therefore assumed that center peak values of interest to the designer would fall within the range of values found for these 2 weeks. Such surveys would determine the high and low extremes of these peak design values.

STUDY FINDINGS

Design Day

Tables 2 and 3 give comparisons of various characteristics for the 2-week-long surveys and show that Thursday is the nearest to an average weekday for survey purposes.

Publication of this paper sponsored by Committee on Parking and Terminals.

Table 1. Shopping center statistics.

Shopping Center	Classification	Gross Leasable Area (ft^2)	Percentage of GLA for Shopping Goods	Present Parking Index (spaces/ 1,000 ft^2 of GLA)
A. Glenfair	Neighborhood	27,450	20	6.6
B. Superand	Neighborhood	37,030	40	—[a]
C. Waterkloof	Neighborhood	43,530	40	2.3
D. Esperanto	Community	47,360	60	11.9[b]
E. Bryanston	Community	52,630	70	5.6
F. Killarney	Community	72,560	50	5.4
G. Rand Park	Community	105,000	40	6.9
H. Southdale	Community	122,920	80	6.5
I. Hyde Park	Community	123,890	80	4.6
J. Kempton City	Regional	316,670	60	3.8
K. Sandton City	Regional	344,440	80	6.7

Note: 1 ft^2 = 0.09 m^2.

[a]No parking layout designated. [b]Allows for future expansion.

Table 2. Weekly variation in daily trip generation and percentage of traffic.

Characteristic	Mon.	Tues.	Wed.	Thur.	Fri.	Sat.
Daily trip generation (trips/1,000 ft^2 of GLA)						
Community center, Dec. 18-23, 1972[a]	65.4	75.5	70.5	73.6	95.2	63.9
Community center, Jan. 29-Feb. 3, 1973[b]	57.4	59.8	64.0	62.6	75.6	67.8
Regional center J, Dec. 18-23, 1972	30.9	33.0	34.0	34.4	45.6	24.4
Regional center J, Jan. 29-Feb. 3, 1973	24.8	23.7	24.6	23.8	26.2	23.8
Percentage of total weekly traffic						
Community center, Dec. 18-23, 1972[a]	14.9	17.0	15.9	16.5	21.3	14.4
Community center, Jan. 29-Feb. 3, 1973[b]	14.8	15.5	16.5	16.2	19.5	17.5
Regional center J, Dec. 18-23, 1972	15.3	16.3	16.8	17.0	22.6	12.0
Regional center J, Jan. 29-Feb. 3, 1973	16.9	16.1	16.7	16.2	17.8	16.2

Note: 1 ft^2 = 0.09 m^2.

[a]Unweighted average of centers G, H, and I. [b]Unweighted average of centers G and H.

Table 3. Weekly variation in peak-hour trip generation and parking accumulation.

Characteristic	Mon.	Tues.	Wed.	Thur.	Fri.	Sat.
Peak-hour trip generation (trips/1,000 ft^2 of GLA)						
Community center, Dec. 18-23, 1972[a]	9.3	9.6	8.8	9.8	13.1	17.0
Community center, Jan. 29-Feb. 3, 1973[b]	8.0	8.4	8.4	8.6	10.4	17.3
Regional center J, Dec. 18-23, 1972	4.2	4.4	4.6	4.8	5.8	5.9
Regional center J, Jan. 29-Feb. 3, 1973	4.0	2.9	3.1	3.1	3.9	5.9
Maximum parking accumulation index (vehicles/1,000 ft^2 of GLA)						
Community center, Dec. 18-23, 1972[a]	4.8	4.0	4.1	4.8	5.1	5.7
Community center, Jan. 29-Feb. 3, 1973[b]	2.2	2.4	2.6	2.5	2.9	5.4
Regional center J, Dec. 18-23, 1972	1.3	2.0	2.1	1.9	3.4	2.5
Regional center J, Jan. 29-Feb. 3, 1973	1.1	1.0	1.1	1.0	1.1	2.9

Note: 1 ft^2 = 0.09 m^2.

[a]Unweighted average of centers G, H, and I. [b]Unweighted average of centers G and H.

Table 4. Traffic characteristics for an average weekday.

Center	Daily Trip Generation[a] (trips/ 1,000 ft^2 of GLA)	Shopping Center Peak Hour	Trip Generation During Center Peak Hour (trips/1,000 ft^2 of GLA)	Street Peak Hour	Shopping Center Trip Generation During Street Peak Hour (trips/1,000 ft^2 of GLA)
Neighborhood					
A	118.6	4:30 to 5:30	21.6	4:45 to 5:45	21.3
Community					
D	60.0	4:45 to 5:45	9.6	4:30 to 5:30	9.3
E	57.7	1:30 to 2:30	6.9	4:30 to 5:30	6.6
G	67.6	2:45 to 3:45	8.9	4:45 to 5:45	7.8
H	63.3	4:15 to 5:15	9.0	4:30 to 5:30	8.8
I	46.4	4:00 to 5:00	6.1	4:45 to 5:45	4.7
Average	59.0		8.1		7.4
Regional					
J	22.4	4:15 to 5:15	3.4	4:30 to 5:30	3.4

Note: 1 ft^2 = 0.09 m^2.

[a]Refers to the 10-hour period from 8:00 a.m. to 6:00 p.m.

The last Saturday in January followed an end-of-month payday. On this day about the same number of cars used the centers as on any weekday in that week but in fewer hours. Also the Saturday at the end of January gave the same hourly trip generation intensity and parking accumulation as any day prior to Christmas. Activity on the Saturday following an end-of-month payday was further tested by conducting vehicle counts at four centers on all Saturday mornings during a 2-month period. These counts showed that the end-of-month Saturday was indeed the busiest and that there was little variation between end-of-month Saturdays.

These findings led to the decision to use any normal Thursday as a representative design day of average weekday conditions at shopping centers and the Saturday at the end of any month as a design day for access and parking requirements.

Average Weekday

Data from surveys conducted on Thursdays are given in Tables 4 and 5. (Shopping center J was the only regional center surveyed on a weekday. Because its market area was not yet fully developed, there are some doubts about the survey values.) Figure 1 shows the average variation in shopping center traffic flow during a weekday at community centers D, E, G, H, and I. Figure 2 shows the daily variation in parking accumulation for a weekday at the same community centers, and Figure 3 shows the shopping center trip generation during the street peak hour versus GLA.

Daily trip generation rates for a weekday at community centers varied from a high of 95.2 trips per 1,000 ft^2 (93 m^2) of GLA in the week before Christmas to an average of 59.0. In comparison with U.S. values, Keefer (1) found an average of 16.08 trips per 1,000 ft^2 of GLA, LARTS (2) found a value of 46 trips per 1,000 ft^2 of GLA for community centers, and Miller (3) found a range of 45 to 101 trips per 1,000 ft^2 for three community centers. Daily trip generation rates for South Africa appear to be generally higher than those for U.S. centers.

For most centers studied, the shopping center and weekday afternoon street peak hours tend to coincide. From Figure 2 a range of values for street peak-hour trip generation for different center sizes can be determined. This trip generation tends to decrease as center size increases. The average value found for community centers was 7.4 peak-hour trips per 1,000 ft^2 (93 m^2) of GLA for a street peak period between 4:30 and 5:45 p.m. with an approximately 50-50 directional split in shopping center traffic.

For an average weekday the trip generation rate at community centers was 8.1 trips per 1,000 ft^2 (93 m^2) of GLA for a center peak occurring between 1:30 and 5:45 with an approximately 50-50 directional split.

Vehicle occupancy was lowest in the morning and increased in the afternoon after schools were out. Vehicle occupancy for a weekday averaged 1.6 for neighborhood and community centers and 1.8 for regional centers.

For an average weekday the daily trip generation rate for service vehicles was 6.0, 4.3, and 2.4 trips per 1,000 ft^2 of GLA for neighborhood, community, and regional centers respectively. The trip generation rate for the peak hour of service vehicle activity on an average weekday was 1.2, 0.7, and 0.3 trips per 1,000 ft^2 of GLA for neighborhood, community, and regional centers respectively. The peak period for service vehicle activity occurred between 11 a.m. and 1 p.m. with a directional split of approximately 50-50. The service vehicle activity during the street peak period is minimal.

On an average weekday the average maximum parking accumulation index was 0.3, 0.2, and 0.1 vehicle per 1,000 ft^2 of GLA for neighborhood, community, and regional centers respectively. The peak accumulation could be expected to occur between noon and 2 p.m. Parking duration increased only slightly from neighborhood to regional centers and averaged about 30 min.

Sixty percent of the peak accumulation of service vehicles required a loading dock with a preferred height of 3 ft 6 in. (1.1 m). Less than 6 percent of service vehicles at all centers were tractor-trailers. Seventy-four percent of the service vehicles were between 13 and 26 ft (3.9 and 7.9 m) long; 18 percent were less than and 8 percent were

Table 5. Parking characteristics for an average weekday.

Center	Maximum Parking Accumulation Index (vehicles/ 1,000 ft² of GLA)	Time of Peak Parking Accumulation	Parking Duration (min)	Parking Turnover (vehicles/ stall/day)
Neighborhood				
A	3.2	10:30	22	9.0
Community				
D	3.4	3:15	41	1.8
E	2.8	12:30	34	3.4
G	5.2	3:00	50	5.1
H	2.7	1:15	44	4.9
I	3.4	Noon	42	5.0
Average	3.5		42	4.0
Regional				
J	1.1	4:45	94	3.0

Note: 1 ft² = 0.09 m².

Figure 1. Variation in shopping center traffic flow for a weekday at a community center.

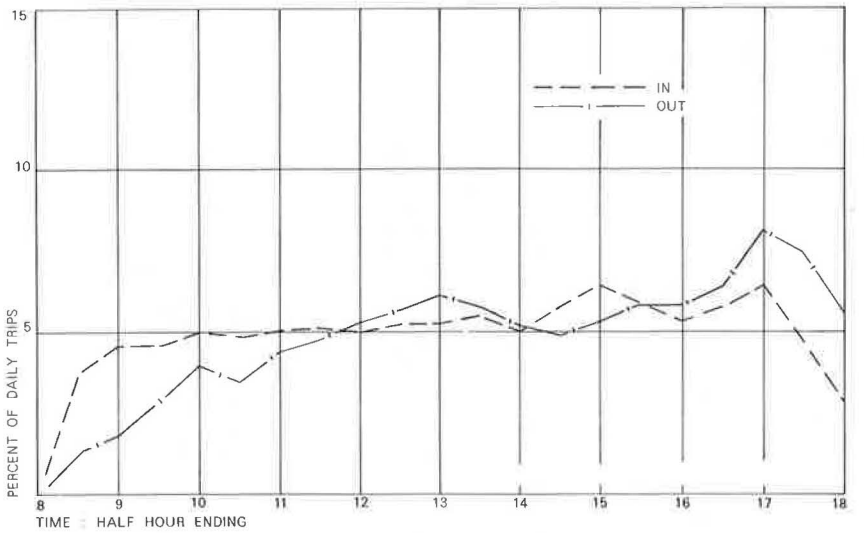

Figure 2. Variation in parking accumulation for a weekday at a community center.

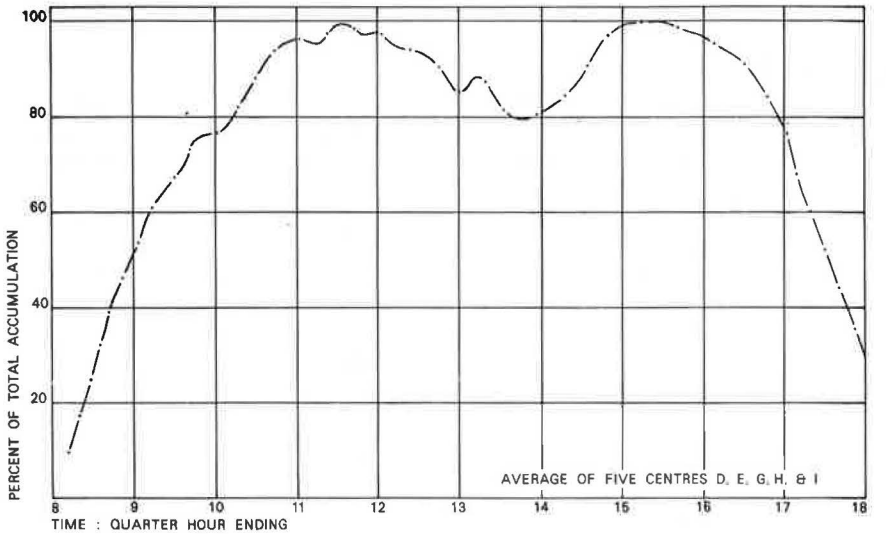

Figure 3. Variation in weekday shopping center trip generation versus size of center.

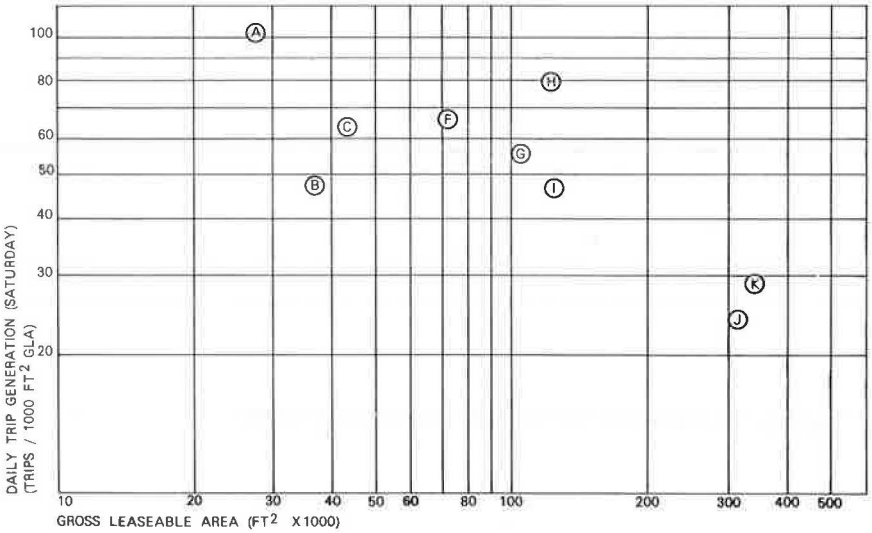

Table 6. Traffic characteristics for a design Saturday.

Center	Daily Trip Generation (trips/ 1,000 ft² of GLA)	Trip Generation During Center Peak Hour (trips/1,000 ft² of GLA)	Peak Hour for Shopping Center Traffic
Neighborhood			
A	102.7	27.4	11:45 to 12:45
B	47.5	13.7	11:30 to 12:30
C	63.9	17.4	10:15 to 11:15
Average	71.4	19.5	
Community			
F	66.5	17.4	10:15 to 11:15
G	55.6	13.7	10:30 to 11:30
H	80.1	20.9	11:30 to 12:30
I	46.8	19.6	10:30 to 11:30
Average	62.2	17.9	
Regional			
J	23.8	5.9	10:30 to 11:30
K	28.7	7.9	10:30 to 11:30
Average	26.2	6.9	

Note: 1 ft² = 0.09 m².

Table 7. Parking characteristics for a design Saturday.

Center	Maximum Parking Accumulation Index (vehicles/ 1,000 ft² of GLA)	Time of Peak Parking Accumulation	Parking Duration (min)	Parking Turnover (vehicles/ stall/day)
Neighborhood				
A	5.6	10:45	–	15.5
B	3.8	Noon	19	–
C	5.5	11:15	38	12.6
Average	5.0		28	14.0
Community				
F	5.8	10:45	62	6.4
G	3.6	12:15	–	4.0
H	7.3	11:30	–	6.2
I	5.7	11:15	47	5.0
Average	5.6		54	5.4
Regional				
J	2.9	11:15	–	3.1
K	5.7	11:15	91	2.3
Average	4.3		91	2.7

Note: 1 ft² = 0.09 m².

Figure 4. Variation in shopping center traffic flow for a design Saturday at a community center.

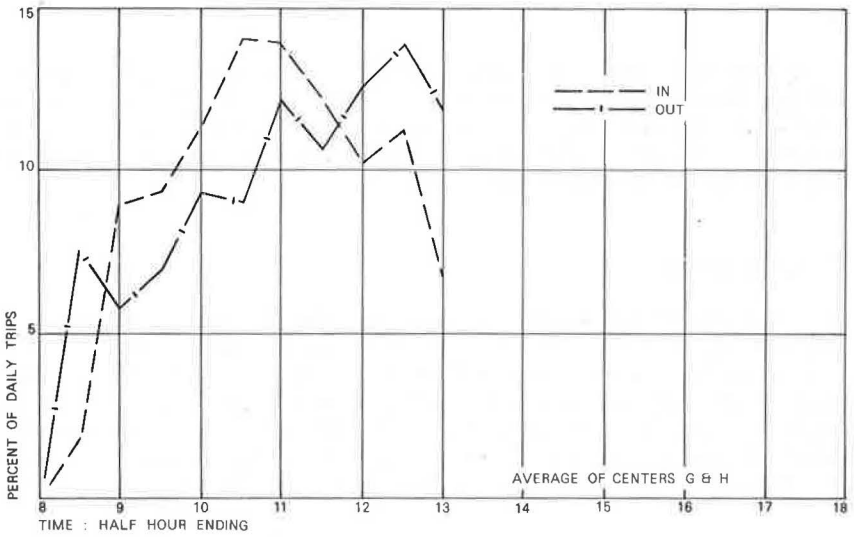

Figure 5. Variation in shopping center trip generation for a Saturday versus size of center.

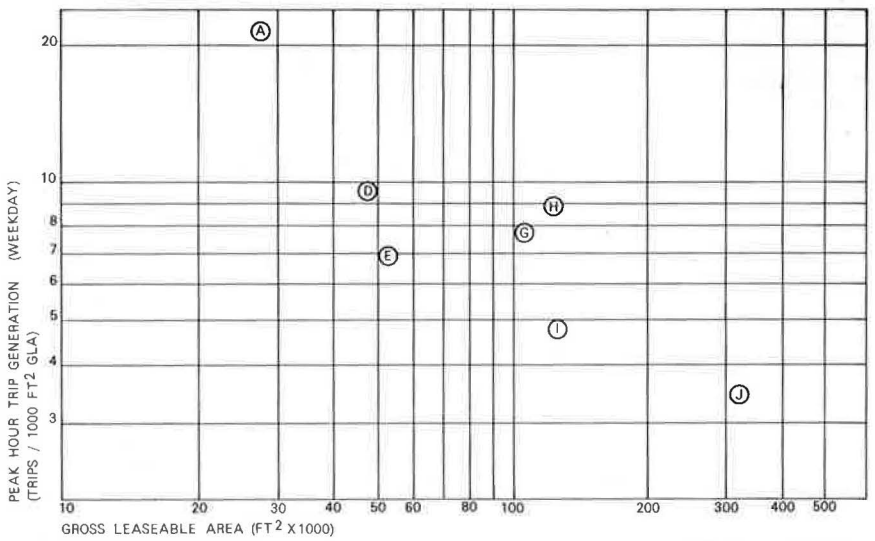

Figure 6. Variation in peak-hour trip generation for a design Saturday versus size of center.

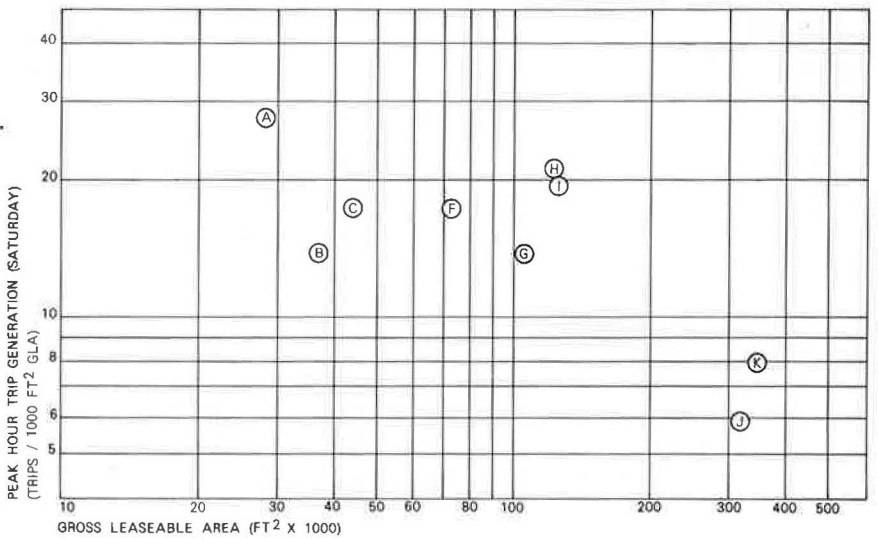

more than this range. In loaded height, 29 percent were less than 6.5 ft (1.9 m), 50 percent were between 6.5 and 10 ft (1.9 and 3 m), and 22 percent were more than 13 ft (3.9 m). In terms of gross vehicle weight, 50 percent of the service vehicles were between 11,000 and 33,000 lb (4990 and 14 970 kg), 43 percent were less than 11,000 lb, and 7 percent were more than 33,000 lb.

Design Saturday

Data from surveys conducted on end-of-month Saturdays are given in Tables 6 and 7. Figure 4 shows the variation in shopping center traffic flow on such a design Saturday at community centers. Figure 5 shows the daily trip generation rate versus GLA and again illustrates the decreasing daily generation rate with increasing center size. Figure 6 shows how the design Saturday peak trip generation rate decreases with increasing center size, and Figure 7 shows the daily variation in parking accumulation at community centers. Figure 8 shows the variation in parking index with center size.

Figure 7. Variation in parking accumulation for a design Saturday at a community center.

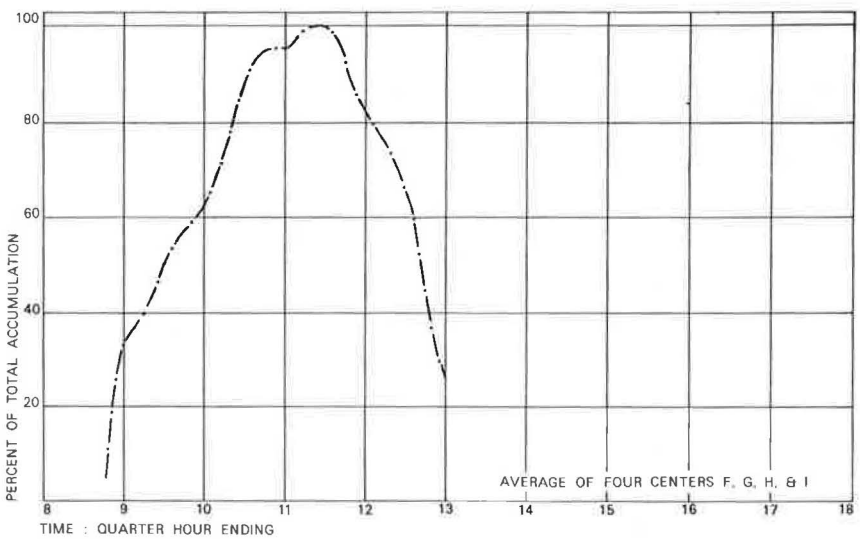

Figure 8. Variation in parking accumulation index for a design Saturday versus size of center.

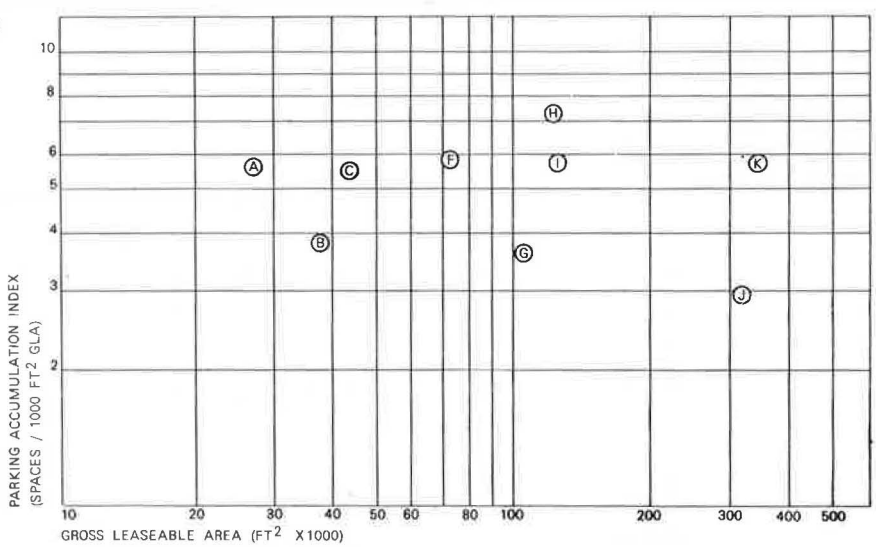

Average values for daily trip generation of 71.4, 62.2, and 26.2 trips per 1,000 ft^2 (93 m^2) of GLA were found for neighborhood, community, and regional centers respectively. For a design Saturday, the peak trip generation rates are 19.5, 17.9, and 6.9 trips per 1,000 ft^2 of GLA for neighborhood, community, and regional centers respectively. The shopping center peak period occurs from 10:00 a.m. to 12:30 p.m. with an approximately 50-50 directional split.

For a design Saturday the average maximum parking accumulation index was 5.0, 5.6, and 4.3 spaces per 1,000 ft^2 (93 m^2) of GLA for neighborhood, community, and regional centers respectively. For the middle range of centers, the data support the Urban Land Institute value of 5.5 spaces per 1,000 ft^2 of GLA found for U.S. centers. Because data are lacking for centers at the ends of the size scale, Figure 8 and Table 5 include the authors' recommendation of higher parking index values for smaller centers and lower values for larger centers (4, 5). The peak demand can be expected to occur between 10:45 a.m. and 12:15 p.m.

Parking duration on a Saturday averaged 28 min for neighborhood centers, 54 min for community centers, and 91 min for regional centers. The short duration and high generation rates for neighborhood centers lead to a daily turnover rate for Saturday of 14.0 vehicles per stall. Community centers show a turnover of 5.4 vehicles per stall and regional centers 2.7 vehicles per stall. Higher daily generation rates for South African centers cause the daily turnover rates to be proportionately higher than U.S. values.

Vehicle occupancy increased through the morning. Vehicle occupancy was 1.8 for neighborhood and community centers and 2.0 for regional centers, slightly higher than for weekdays.

SUMMARY

Certain South African shopping center traffic characteristics correlate very well with U.S. data, but others do reflect local life-style differences.

Any normal Thursday seems to provide acceptable average values of typical weekday shopping center traffic characteristics. The pre-Christmas shopping peak is well represented by any end-of-month Saturday and any such Saturday can be used as a design day for access and parking requirements at shopping centers.

For an average weekday the shopping center peak generally coincides with the afternoon street peak hour. The vehicle trip generation rate during this p.m. street peak hour is important in determining the effect of shopping center traffic on street traffic. For a community center the value of 7.4 trips per 1,000 ft^2 of GLA was found. Vehicle occupancy was 1.6 persons per vehicle, parking duration 42 min, and parking turnover 4.0 vehicles per stall per day.

For an end-of-month Saturday the shopping center peak-hour trip generation is important for the design of access points. The maximum parking accumulation index is necessary for determining the required number of parking spaces. For a community center the peak-hour trip generation rate is 17.9 trips per 1,000 ft^2 of GLA and the maximum parking accumulation index is 5.6 vehicles per 1,000 ft^2 of GLA. Vehicle occupancy was 1.8 persons per vehicle, parking duration was 54 min, and parking turnover was 5.4 vehicles per stall per day.

REFERENCES

1. L. E. Keefer. Urban Travel Patterns for Airports, Shopping Centers and Industrial Plants. NCHRP Rept. 24, 1966.
2. J. W. Shaver. Los Angeles Regional Transportation Study 1961 Shopping Center Study. Presented at Fourteenth California Street and Highway Conference, Institute of Transportation and Traffic Engineering, Univ. of California, Los Angeles, Jan. 1962.
3. F. D. Miller. Trip Generation at Shopping Centers. Traffic Engineering, Sept. 1969, pp. 32-35.

4. G. W. Barton. Design Criteria for the Traffic Planning of Suburban Shopping Centers. Proc., Ninth International Study Week in Traffic and Safety Engineering, Munich, Sept. 9-13, 1968.
5. Parking Principles. HRB Special Rept. 125, 1971.
6. J. R. McKeever. Shopping Centers Restudied. Urban Land Institute, Technical Bulletin 30, Part 1, Feb. 1957.

DRIVER RESPONSE TO THE 55-MPH MAXIMUM SPEED LIMIT AND VARIATIONAL CHARACTERISTICS OF SPOT SPEEDS

Tenny N. Lam, University of California, Davis; and
Paul Wasielewski, General Motors Research Laboratories

ABRIDGMENT

Spot speed observations were made on a four-lane suburban freeway from November 8, 1973, to June 13, 1974, when speeds were influenced by fuel conservation measures. Speeds were recorded in 15-min intervals in mid-afternoons on 39 days. The mean speed of cars dropped from 63.4 mph (102 km/h) in early November to 60.4 mph (97.2 km/h) in late November to early March and was further reduced to 57.4 mph (92.4 km/h) after the posted speed limit was changed from 70 to 55 mph (113 to 88 km/h) on March 3, 1974. A multiple classification analysis of the 15-min mean speeds showed that the variance of these means was not significantly affected by factors such as time of day, day of the week, traffic flow, and truck composition, although an effect due to different observers was found. The residual variance of the 15-min means after systematic effects were removed was significantly greater than would be expected from sampling errors if the speeds of individual cars were identically distributed. The implications of these results with respect to the planning and design of before and after speed studies are discussed.

•THE RECENT introduction of a 55-mph (88-km/h) nationwide speed limit as a fuel conservation measure offered an unprecedented opportunity for studying driver responses to changes in maximum speed limit laws.

The fuel situation was brought to public attention by the President's televised speech on November 7, 1973. Since then, the public has been urged to reduce fuel consumption through various voluntary and regulatory measures, including speed reductions. Since March 3, 1974, speed reductions have been made mandatory nationwide through the imposition of 55-mph (88-km/h) maximum speed limits.

To observe the driving public's response to the speed limit change, we made a series of spot speed observations at a suburban freeway in the Detroit metropolitan area where the speed limit had been 70 mph (113 km/h). A number of studies have been made to determine the effect of the new speed limit (1, 2). One aim of the present study was to obtain information on the detailed characteristics of driver response in a more or less continuous manner over a relatively long time span. Hence, observations were made several times a week during periods immediately before and after the new speed limit took effect and at less frequent intervals in other periods from early November 1973 to November 1974.

This extensive series of speed measurements is also of interest from a more fundamental point of view. As a second aspect of this study, a statistical analysis has been made of the variational characteristics of observed mean speeds in 15-min periods. Attempts were made to relate the variations to characteristics of the traffic stream, such as the total volume and the number of trucks, and observational conditions, such as

Publication of this paper sponsored by Committee on Traffic Flow Theory and Characteristics.

the time of day, day of the week, and observer. The results of the analysis are important for the planning and design of spot speed studies.

DATA COLLECTION

Speed observations were made on Mich-59, a four-lane freeway in a suburban setting about 20 miles (30 km) north of Detroit, where influences of curves, grades, and nearby exits or entrances were judged to be minimal. All observations were made in good weather on weekday afternoons between 1:40 and 3:50 p.m. The traffic flow was generally between 200 and 450 vehicles per lane per hour, including about 10 percent trucks. New speed signs were posted on this road by March 4, 1974, the day after the law became effective.

Speeds of individual vehicles were recorded in 15-min intervals for the westbound traffic by using a radar speed meter located off the freeway right-of-way. The entire data system was calibrated and checked in the field by recording the speed of a test vehicle with a calibrated speedometer. Individual speeds could be measured to a precision of ±1.0 mph (±1.6 km/h). Trucks were separated from light-duty vehicles. It was not always possible to single out the speeds of individual vehicles when bunches of vehicles passed through the radar beam, but this was not an important factor under the prevailing light flow. On a typical day, observations were made during six 15-min intervals and about 800 individual speeds were recorded.

The first measurements were made on November 8 and 9, 1973, the days immediately following the President's first televised speech on the energy situation. Additional measurements were made at irregular intervals in November and December 1973, and January and early February 1974. More frequent measurements were made in late February and in March in order to provide a detailed picture of driver response during the period immediately before and after the Michigan statutory speed limit went into effect on March 3. State police enforcement of the new law began on March 16, 1974. Since April 1974 observations have been continued on a less frequent basis. All together, 259 observations in 15-min intervals were made on 46 days.

In July 1974, the observation point had to be moved about 1 mile (1.6 km) downstream because of roadside developments. Observed speeds at the new site were about 1.1 mph (1.8 km/h) higher than at the previous site. Because this effect may be due to the new site, these data have not been included in the statistical analysis discussed below.

DRIVER RESPONSES

The results of the observations are shown in Figures 1 and 2. Figure 1 shows the mean and standard deviation of the speeds of passenger cars and light-duty trucks for each day on which speeds were observed. The Michigan speed limit for trucks was 55 mph (88 km/h) before March 3 and thus was not affected by the new law. Observed truck speeds have a mean of 55.8 mph (89.8 km/h) with no statistically significant change over the observation period. The discussion below refers only to the speeds of light-duty vehicles.

The observed reduction in car speeds seems to have taken place in two distinct steps. The first reduction of 2.9 mph (4.7 km/h) occurred between the observations on November 8-9, 1973, just after the President's speech, and those in late November. There was no further change from late November until early March when speed reductions were still on a voluntary basis. An additional drop of 2.8 mph (4.5 km/h) occurred between March 1 and March 5, apparently as a result of the imposition of the statutory 55-mph (88-km/h) speed limit in Michigan on March 3. After police enforcement began on March 16, there was a drop in the standard deviation but no significant reduction in mean speeds. Thus the mean speed dropped by a total of 5.7 mph (9.2 km/h) between early November 1973 and early November 1974. At the same time, the standard deviation fell by 2.1 mph (3.4 km/h).

A more detailed picture of the evolution of the speed patterns over this period is

shown in Figure 2, which gives the fraction of speeds less than 55, 60, 65, and 70 mph (88, 97, 105, and 113 km/h) on each day.

The effectiveness of the public appeal for voluntary speed reductions is illustrated by the reduction in mean speeds between the observations on November 8-9 and those on November 29-30, 1973. We have no comparable measurements for the period preceding the President's November 7 speech, so we cannot assess the full extent of the speed reduction on Mich-59. However, the Michigan Department of State Highways and Transportation measured an average speed of 67.9 mph (109.3 km/h) in October 1973 for typical rural freeways in Michigan. In spite of the observed reduction in mean speeds, there were very few drivers who complied fully with the suggested voluntary limit of 50 or 55 mph (80 or 88 km/h), indicating that drivers apparently responded by reducing their speeds only to the extent that they deemed appropriate, rather than by following the letter of the President's appeal.

The further reduction in speeds after the imposition of the statutory 55-mph (88-km/h) limit suggests that measures backed by law are more effective in altering driving patterns than those depending on voluntary cooperation alone. Even for the most recent observation period, only about 30 percent of the observed vehicles were below 55 mph, compared to 11 percent in early November. On the other hand, cars with speeds of more than 60 mph (97 km/h) dropped from 64 to 27 percent between the two periods.

In addition to the governmental measures for reducing highway speeds, the period from November 1973 to March 1974 witnessed a steady increase in the price of gasoline and a reduction in its availability. They may have induced drivers to conserve gasoline for reasons of economy and convenience. Conversely, the period from March 1974 through June 1974 was characterized by stabilized gasoline prices and increased availability. One might have expected that condition to lead to a trend toward increasing speeds. However, the mean speeds from March 1974 through June 1974 seem to have remained stable. The observed speed changes in the period from November 1973 to June 1974 appear to have developed in discrete steps associated with governmental actions rather than as a continuous trend either upward or downward. The observations from July 1974 through November 1974 show a small increase of 1.1 mph (1.8 km/h), as mentioned above, but this may be due to a change in the observation site.

VARIATIONAL PROPERTIES OF OBSERVED MEAN SPEEDS

In traffic engineering practice (3, 4), statistical analyses of spot speed studies have usually been based on the assumption that speeds observed under similar conditions, such as time of day, day of the week, flow, and truck volume, are random samples drawn from identical distributions. Statistically significant differences between samples are then regarded as an indication of the effect of a change in conditions.

The data obtained in this study provide a convenient opportunity to test the assumption of identically and independently distributed observed individual speeds. Under this assumption, the mean of a 15-min sample of observed speeds is expected to have a variance given by

$$\sigma_{\bar{v}}^2 = \sigma_v^2/n \qquad (1)$$

where

n = sample size,
σ_v^2 = variance of the individual observations, and
$\sigma_{\bar{v}}^2$ = variance of the sample mean $\bar{v}$.

An estimate of $\sigma_{\bar{v}}^2$ is usually provided by a sample estimate of σ_v^2 given by

Figure 1. Mean and standard deviation of passenger car speeds observed on individual days.

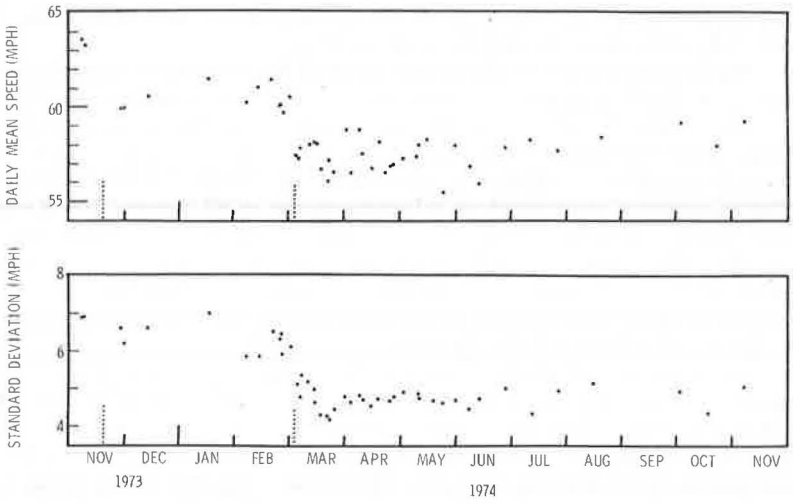

Figure 2. Fraction of car speeds less than 55, 60, 65, and 70 mph (88, 97, 105, and 113 km/h) on different days.

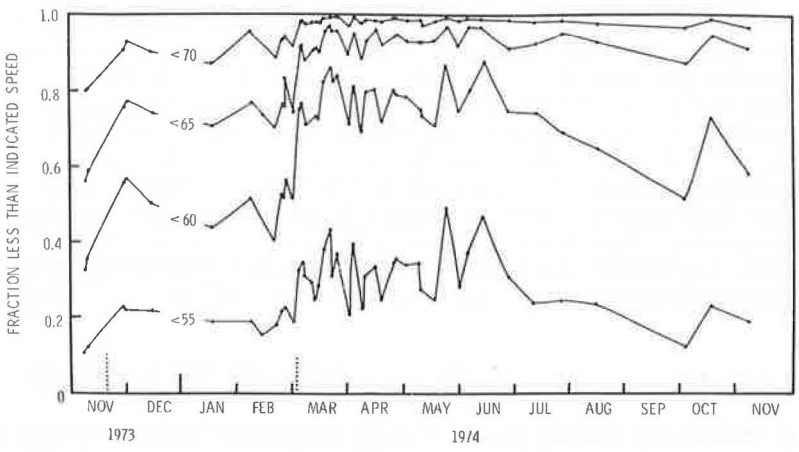

Table 1. Result of multiple classification analysis for all data.

Predictor Variable	Degrees of Freedom	Sum of Squared Deviations	F-Ratio
Period	3	666.8	204.8[a]
Day of week	4	10.3	2.4
Time of day	2	1.4	0.7
Observer	3	21.2	6.5[a]
Volume of cars	8	4.6	0.5
Volume of trucks	5	5.4	1.0
All predictors	25	696.8	24.9[a]
Residual variance	196	212.8	

[a]Significant at the 1 percent level.

Table 2. Result of multiple classification analysis for all data with date as predictor variable.

Predictor Variable	Degrees of Freedom	Sum of Squared Deviations	F-Ratio
Date	38	700.8	27.8[a]
Time of day	2	1.3	1.0
Observer	3	22.1	8.6[a]
Volume of cars	8	2.8	0.7
Volume of trucks	5	6.0	1.9
All predictors	56	802.9	22.0[a]
Residual variance	165	106.6	

[a]Significant at the 1 percent level.

$$s_{\bar{v}}^2 = \sum_{i=1}^{n} (v_i - \bar{v})^2/(n - 1) \quad (2)$$

where v_i = observed speed of an individual vehicle in the sample. The sample estimate, $s_{\bar{v}}^2$, of $\sigma_{\bar{v}}^2$ is then obtained by using equation 1. An independent estimation $S_{\bar{v}}^2$ can be obtained from repeated observations in samples of approximately n vehicles under similar conditions. The estimate of $\sigma_{\bar{v}}^2$ is then calculated from the observed mean speed $\bar{v}_i$ of each individual sample. Comparing the results from the two approaches allows a study of the stability and stationarity of the speed distributions observed under similar or different conditions.

The 222 speed samples obtained in 15-min intervals between November 8, 1973, and June 13, 1974, have been divided into four periods: November 8 to November 9, 1973; November 28, 1973, to March 1, 1974; March 5 to March 15, 1974; and March 18 to June 13, 1974. In each of these periods the daily means and standard deviations appear to be stationary.

In addition to the observed effects due to the change in conditions associated with the four time periods, each 15-min sample is also characterized by a number of other factors that may contribute systematically to the observed mean speed (5, 6). Although this study was planned so that the range of flow and time of day would be narrow, a statistical analysis was made to study possible influences from

1. Volume of cars,
2. Volume of trucks,
3. Observer,
4. Time of day, and
5. Day of week.

The variability of the 15-min samples reflects not only the inherent variability due to sampling but also possible nonstationarity in the samples and contributions from the variables mentioned above. A study of the variational properties and the contributions from the various sources of the observed 15-min mean speeds is described below.

An appropriate approach for analyzing this set of data is to adjust the observed 15-min mean speed for systematic effects due to the various variables and to compare the variance of the adjusted mean speeds with the variance expected from identical and independent observations drawn from a single speed distribution. The method used to carry out this procedure must reflect two characteristics of the data. First, some of the predictors or independent variables, such as day of the week, are nonnumerical. Second, some of the independent variables are correlated; for instance, the volume generally increased later in the day, so that volume and time of day are correlated variables. A convenient and appropriate way of dealing with data of this type is a statistical technique known as multiple classification analysis (7). In essence, this technique estimates the fraction of the variance explained by the independent variables. The significance of the explanatory power of each variable can then be tested by using the F-ratio test. Similarly, the residual or unexplained variance, with the systematic effects removed, can be compared with the variance expected under the assumption of independently and identically distributed individual speeds.

The results of the multiple classification analysis are given in Table 1. (The sum of squared deviations explained by all the predictors together is not equal to the sum of the individual contributions because of correlations among the predictor variables.) The largest fraction of the variance is predicted by the division of the data into the four apparently distinct periods. The only other predictor variable that accounts for a significant fraction of the variance is the observer recording the speed data. This effect, involving a spread of 0.7 mph (1.1 km/h) among four observers, may be due to different reaction times in reading the speed meter. It is interesting to note that there was no consistent significant effect due to varying flow rates within the range observed in the study.

The residual variance given in Table 1 is a measure of the random variability of the 15-min mean speeds after adjustment is made for systematic contributions from the six predictor variables. This quantity, which is a combination of the variations due to sampling and nonstationarity, may be compared with the variation due to sampling alone. The variability in the mean speeds due to sampling may be calculated from the observed speed distributions by using equation 1.

The individual speeds in the 15-min samples, unfortunately, also exhibit variations from sample to sample, as well as a significant difference before and after March 3, 1974. It is, therefore, not possible to make an exact comparison between the residual variance of the mean speeds estimated from the multiple classification analysis and the expected variance in the mean speeds due to sampling. The residual variance in the mean speeds has been estimated to be 1.09 $(mph)^2$ [2.8 $(km/h)^2$]. This may, however, be qualitatively compared with the range of variances due to sampling as derived from equation 1 for individual samples. The range was 0.18 to 0.83 $(mph)^2$ [0.47 to 2.2 $(km/h)^2$] during the period before March 3 and 0.07 to 0.39 $(mph)^2$ [0.18 to 1.01 $(km/h)^2$] during the period after March 3. The residual variance, which is in all cases larger than the variance attributable to sampling alone, indicates certain nonstationarity in the 15-min samples of individual speeds.

It is also of interest to determine whether the speed fluctuations among observations on the same day are as great as those among observations on different days. This question can be answered by repeating the multiple classification analysis calculation by using the observation date as a predictor variable instead of the period and the day of the week. The results are given in Table 2. The residual variance is reduced to 0.65 $(mph)^2$ [1.7 $(km/h)^2$], which is significantly less than the value of 1.09 $(mph)^2$ [2.8 $(km/h)^2$] obtained in the earlier calculation; this indicates that the variance from day to day is greater than that within a day. However, the residual variance is still larger than most of the variances due to sampling as calculated from individual 15-min speed distributions.

CONCLUSIONS AND DISCUSSION

Mean speeds of cars on the Mich-59 freeway were reduced from 63.3 to 57.6 mph (102 to 92.7 km/h) during the period of the study, and the standard deviation of the speed distribution fell from 6.9 to 5.1 mph (11.1 to 8.2 km/h).

An important aspect of freeway speeds is the connection between speed and accidents. It is well known that lower speeds lead to reduced accident severities. Traffic safety research has also shown that greater uniformity of speeds leads to reduced accident rates. The reduction in the standard deviation of speeds on Mich-59 suggests that speeds have become more uniform and hence that the freeway may have become safer.

The variational properties of observed 15-min mean speeds do not agree with the results expected if the individual speeds are identically and independently distributed, even after corrections are made for possible systematic effects. The variances in the mean speeds from day to day of 1.09 $(mph)^2$ [2.8 $(km/h)^2$] and from 15-min interval to 15-min interval of 0.65 $(mph)^2$ [1.7 $(km/h)^2$] exceeded the expected sampling variations if the speed distribution were stationary. Factors such as volume and time of day do not have strong influences on the mean speed within the range of relatively light flow under which the study was conducted.

The results indicate that, although the mean speed of 15-min observations is stochastically stationary under similar conditions, it is nonetheless a statistically distributed quantity and hence must be estimated with repeated measurements of sample means. A large sample of individual vehicle speeds on the same day, even under approximately constant conditions, is not sufficient to predict the mean speed from day to day or from one part of one day to another of similar conditions. In before and after studies, it would be more desirable to sample speeds in individual short intervals over a number of days before and after the change in conditions and then use the individual sample means as the basic data for statistical comparisons.

ACKNOWLEDGMENTS

We thank R. Herman, head of the Traffic Science Department, General Motors Research Laboratories, for many constructive comments and useful discussions. We are also grateful to S. B. Koziel, G. D. Kotila, and G. Gorday for assistance in data collection and instrumentation and to R. Swann of the Michigan Department of State Highways and Transportation for providing us with data from the state speed survey program.

REFERENCES

1. W. M. Basham and P. H. Mengert. The Effects of the Energy Crisis on Rural Roads in Maine. Public Roads, Vol. 38, No. 3, 1974, pp. 100-106.
2. Effect of the 55 mph Speed Limit. AASHTO, Nov. 1, 1974.
3. L. J. Pignataro. Traffic Engineering Theory and Practice. Prentice-Hall, 1973, pp. 126-131.
4. J. H. Kell and W. Homburger. Traffic Studies. In Traffic Engineering Handbook, Third Ed. (J. E. Baerwald, ed.), Institute of Traffic Engineers, 1965, pp. 275-280.
5. R. P. Shumate and R. F. Crowther. Variability of Fixed-Point Speed Measurements. HRB Bulletin 281, 1961, pp. 87-96.
6. J. C. Oppenlander. Variables Influencing Spot-Speed Characteristics. HRB Special Rept. 89, 1966.
7. F. M. Andrews, J. M. Morgan, and J. A. Sonquist. Multiple Classification Analysis. Survey Research Center, Institute for Social Research, Univ. of Michigan, 1967.

SPONSORSHIP OF THIS RECORD

GROUP 3—OPERATION AND MAINTENANCE OF TRANSPORTATION FACILITIES
Lloyd G. Byrd, Byrd, Tallamy, MacDonald, and Lewis, chairman

Committee on Parking and Terminals
Harry B. Skinner, Federal Highway Administration, chairman
Stephen G. Petersen, Gaithersburg, Maryland, secretary
Frank E. Barker, George K. Benn, Harvey B. Boutwell, Paul C. Box, John Brierley, Robert G. Bundy, John P. Cavallero, Jr., Raymond H. Ellis, William D. Heath, Stedman T. Hitchcock, James M. Hunnicutt, Walter H. King, Herbert S. Levinson, Sven Lindqvist, Brian V. Martin, Norene Martin, Donald M. McNeil, Donald A. Morin, Merritt A. Neale, Harry F. Orr, V. Setty Pendakur, Woodrow W. Rankin, James B. Saag, Lawrence L. Schulman, Steiner M. Silence, E. L. Walker, Jr.

Committee on Traffic Flow Theory and Characteristics
Kenneth W. Crowley, Polytechnic Institute of Brooklyn, chairman
Robert F. Dawson, University of Vermont, vice-chairman
Edmund A. Hodgkins, Federal Highway Administration, secretary
Patrick J. Athol, John L. Barker, Martin J. Beckmann, Martin J. Bouman, Kenneth A. Brewer, Donald E. Cleveland, Lucien Duckstein, Leslie C. Edie, H. M. Edwards, A. V. Gafarian, Denos C. Gazis, Daniel L. Gerlough, John J. Haynes, James H. Kell, John B. Kreer, Leonard Newman, O. J. Reichelderfer, Richard Rothery, August J. Saccoccio, A. D. St. John, William C. Taylor, Joseph Treiterer, William P. Walker, Sidney Weiner, W. W. Wolman

K. B. Johns, Transportation Research Board staff

Sponsorship is indicated by a footnote on the first page of each report. The organizational units and the chairmen and members are as of December 31, 1974.